POLITECNICO
MILANO 1863

SCUOLA DI INGEGNERIA CIVILE,
AMBIENTALE E TERRITORIALE

Bioelectrochemical technologies for simultaneous removal of petroleum hydrocarbons and nitrate from saturated soils

TESI DI LAUREA MAGISTRALE IN
ENVIRONEMNTAL AND LAND PLANNING ENGINEERING
INGEGNERIA PER L'AMBIENTALE E IL TERRITORIO

Author: **Rebecca Dominici**

Student ID: 991204
Advisor: Elena Sezenna
Co-advisor: Gabriele Beretta, Marta Puddu
Academic Year: 2023-2024

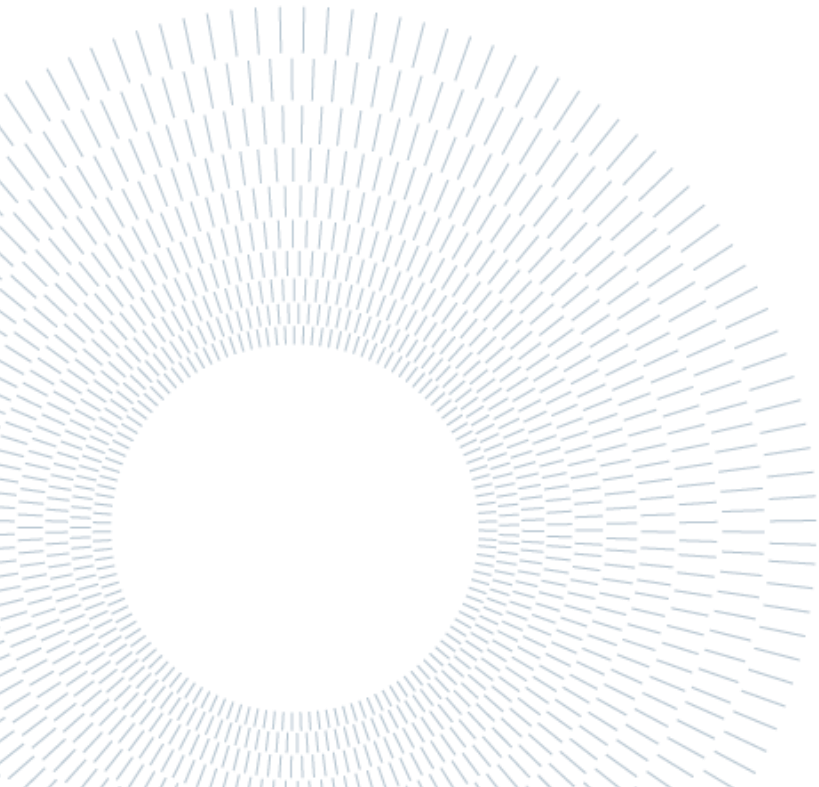

Abstract

Petroleum hydrocarbons and nitrates can contaminate soil, subsoil, and groundwater, encountering humans and harming their health. The Bioelectrochemical system (BES) exploits the potential difference between two locations to transfer electrons from an anodic zone (reducing conditions), where the oxidation of a substance occurs, to a cathodic zone (oxidizing conditions), where they are involved in the reduction of final electron acceptors. This is achieved using a conductive material. In this study, a dual-chamber configuration, inserted into a single reactor, was installed to investigate the removal of hydrocarbons and nitrates from soils under saturated conditions. Two continuous-fed mode BES, namely Microbial Fuel Cell (MFC) and Microbial Electrochemical Snorkel (MES), were constructed alongside an OpenCircuit control system (OC). Nitrate contamination was introduced by adding a KNO_3 solution to the cathode to reach a concentration of 100 mg NO_3^-/L. Their reduction was observed in the MES system with a maximum removal efficiency of 34.53 ± 28.62%. To accelerate microbial growth at the anode, a sodium acetate solution was added. The electrical signal produced by the MFC was detected after each injection. Chemical parameters such as pH, electrical conductivity, and redox potential were monitored, revealing an increase in pH at the cathode and a continuous rise in electrical conductivity throughout the experiment, unaffected by the added solutions. Another batch mode experiment was conducted with OC, MES, and BES at imposed potential, where the greatest nitrate reduction in the aqueous solution at the cathode was observed in the MES (86.76%).

Key-words: Bioelectrochemical systems; microbial fuel cell; snorkel; petroleum hydrocarbons; nitrate.

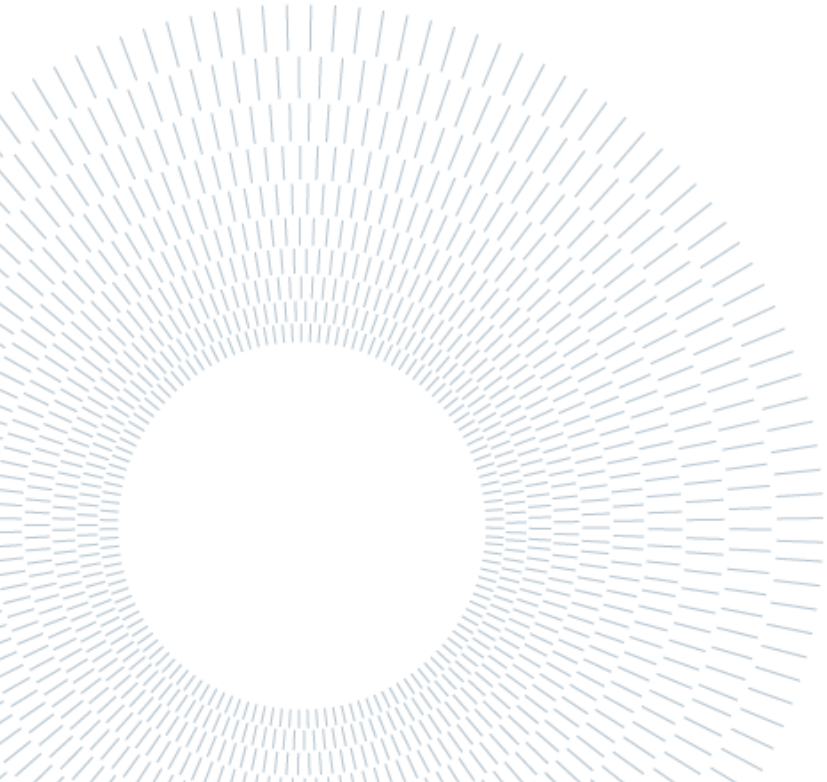

Abstract in italiano

Idrocarburi del petrolio e nitrati possono contaminare suoli, sottosuoli e acque di falda ed entrare a contatto con l'essere umano danneggiandone la salute. Il sistema Bioelettrochimico (BES) sfrutta la differenza di potenziale tra due luoghi per condurre gli elettroni da una zona anodica (condizioni riducenti), in cui avviene l'ossidazione di una sostanza, ad una catodica (condizioni ossidanti), i quali vengono coinvolti nella riduzione di accettori finali di elettroni. Tutto questo grazie un materiale conduttivo. In questo studio, una configurazione a doppia camera, inserita in un unico reattore, è stata installata per investigare la rimozione di idrocarburi e nitrati da suoli in condizioni sature. Due BES a modalità di alimentazione continua, quali Microbial Fuel Cell (MFC) e Microbial Eletrochemical Snorkel (MES) sono stati costruiti in concomitanza con un sistema di controllo a circuito aperto (OC). La contaminazione di nitrati è data dall'inserimento di una soluzione di KNO_3 al catodo per raggiungere una concentrazione di 100 $mgNO_3^-$/L. La loro riduzione è stata rilevata nel sistema MES con una efficienza di rimozione massima di 34.53 ± 28.62 %. Per accelerare la crescita microbica all'anodo è stata inserita una soluzione di acetato di sodio. Da questa è stato rilevato il segnale elettrico prodotto dall'MFC dopo ogni iniezione. Sono stati monitorati parametri chimici quali pH, conducibilità elettrica e potenziale di ossido-riduzione, ottenendo un aumento del pH al catodo e una conducibilità elettrica che crescere durante tutto il periodo di esperimento senza che venga influenzata dalle soluzioni aggiunte. È stato portato avanti un altro esperimento in modalità batch con OC, MES e BES a potenziale imposto in cui la maggiore riduzione di nitrati nella soluzione acquosa al catodo è stata rilevata nel MES (86.76%).

Parole chiave: Sistemi bioelettrochimici; microbial fuel cell; snorkel; idrocarburi; nitrati.

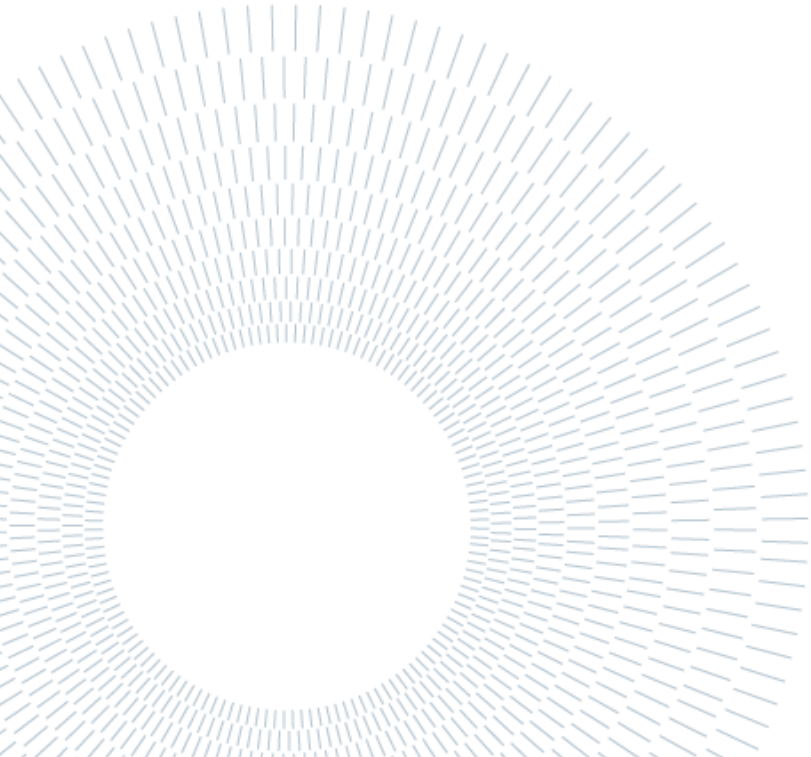

Contents

Introduction

Petroleum hydrocarbons (PHs) are organic contaminants of soil consisted of carbon and hydrogen linked with each other. They have a huge variety of chemical, physical, and biological properties and they interact with the soil based on these characteristics. Indeed, they are dissolved in the aqueous phase, present as vapor in the interstitial gas, sorbed on the solid phase or also be in the liquid form but not dissolved into water (Tucci et al., 2021). Soil characteristics are fundamental to define the interaction with the petroleum hydrocarbons. The origin of the PHs is the intensive use of petroleum oil, a mixture of aliphatic and aromatic hydrocarbons, which became the principal energy source in modern society. Activity such as its exploration, production, and transportation cause environmental PHs contamination (Ossai et al., 2020a). Also, oil tanker incidents can modify terrestrial ecosystems. These compounds can interact directly with the human body by vapor inhalation or also indirectly by soil ingestion and/or dermal contact. Petroleum hydrocarbons contamination consequences are worrying for human health due to their toxicity, but also their persistent in the ambient lead to bioaccumulation in the food chain health (Noori et al., 2022).

Nitrate (NO_3^-) is another pollutant that contaminates groundwater due to intensive N-based fertilizers used in agriculture and due to organic waste derived from intensive feedlots (Bijay-Singh & Craswell, 2021). Based on the European Union (EU) and Word Health Organization (WHO) legislation, the nitrate maximum permissible level in drinking water is 50 mg/L (Gadegaonkar et al., 2023). In fact, it's harmful to human health because it's implicated in diseases like cancer and changing immune systems.

Nowadays the PHs are removed from the soil by different techniques that allow the remediation by the temperature increase of contaminated soil to increase the vapor pressure to allow the pollutants desorption (thermal technologies). Otherwise, physical-chemical technologies have the aim to contain or recover the contaminants thanks to the physicochemical pollutants' properties. While, when contaminants are degraded by microorganisms, it's about bioremediation.

Bioelectrochemical System (BES) is a technology that enables the bioremediation of contaminated soil through a conductive material that acts as an electron acceptor in the anodic part and an electron donor in the cathodic one (Kronenberg et al., 2017). Microorganisms able to interact with electrodes, and thus transfer electrons, are named

electroactive bacteria (EAB), which could cooperate with microorganisms that degrade the pollutants. Microbial fuel cell (MFC) is a bioelectrochemical technology equipped with an external load between anode and cathode to use the electrical energy produced during the treatments. The microbial electrochemical snorkel (MES) is a short-circuited MFC, so it doesn't have any external load, and there's direct contact between the anode and cathode.

The experimental work was carried out at the Environmental Engineering Laboratory – LIA in the Department of Civil and Environmental Engineering. The current case study deals with the simultaneity treatment of petroleum hydrocarbon- and nitrate-contaminated soils in saturated and anaerobic conditions. The treatment was carried on by bioelectrochemical technologies described above, which are compared to usual bioremediation in the same conditions and configuration of microbial fuel cells and snorkel systems. The experiments were carried on in fed-continuous mode and batch mode. The work is structured as briefly outlined below.

Chapter 1 is devoted to a broad introduction to target pollutants that contaminated the soil treated in the experiments and the currently used methods for removing hydrocarbons from contaminated soil. The chapter is useful for understanding the hazardous nature of pollutants, how they can contaminate soil and groundwater, and what are the typical characteristics of remediation methods to highlight their pros and cons.

Chapter 2 encompasses a review of the state of the art in bioelectrochemical systems, with major focus on MFC and MES research about configuration, materials and results.

In chapter 3 are defined and clarified the outline of the thesis topic to underline the context and the objectives of the document.

Chapter 4 is a description of all assumptions made about configurations and materials adopted for the reactors involved in the treatment, as well as all analyses and monitoring conducted during the thesis period.

Chapter 5 provides the results obtained from the various analyses conducted before, during, and after the experiments. These results are discussed and elaborated upon to achieve a critical evaluation of the work.

Finally, chapter 6 consolidates the key research findings from the thesis and offers themes and guidelines for future work continuation.

1 Overview of target pollutants and traditional remediation technologies for hydrocarbons-contaminated soil

1.1. Petroleum Hydrocarbons (PHs) description and classification

Petroleum Hydrocarbons are organic compounds consisting of hydrogen and carbon atoms. These compounds are the principal constituents of petroleum and its refined products such as gasoline, diesel, and jet fuel. They can be aliphatic or aromatic compounds. The aliphatic PHs are classified according to carbon bonds, in alkanes, with single bonds, alkenes, with double bonds, and alkynes, with triple bonds. They can also be in circular structures such as cycloalkanes. The aromatic compounds are characterized by the presence of one or more benzene rings (also known as aromatic rings) in their chemical structure. They are called monoaromatic and polycyclic aromatic hydrocarbons (PAHs). These compounds are highly stable and have distinct properties compared to aliphatic hydrocarbons. They are important in various industries, including the production of plastics, pharmaceuticals, dyes, and solvents.

PHs are also halogenated by adding a fraction of halogens such as Cl, Br, F, and I. They can be aliphatic, as aliphatic chlorinated solvents, or aromatic, as aromatic chlorinated solvents, and are used as refrigerants, pesticides, and herbicides (Noori et al., 2022).
Due to the variety of PHs, they assume different behaviour in the environment depending on their physical-chemical and biological properties, such as density, biodegradability, vapour pressure, etc. In fact, in the interaction with soil, they are subject to (Table 1):

- *volatilization*, the transformation of a chemical from solid or liquid states to the vapour phase;

- *dissolution*, when a chemical species (solute) dissolves in the pore water (solvent);
- *sorption*, chemicals move onto the solid phase;
- *acid-base reactions*, or proton transfer between species;
- *redox reactions* (oxidation-reduction reactions), involve the exchange of electrons between species;
- *biodegradation*, microbial processes that transform the chemical into simpler substances in the presence (aerobic biodegradation) or in the absence of oxygen (anaerobic biodegradation) (Saponaro, 2022a).

PHs can be present in sub-soil as:

- dissolved in the aqueous solution;
- vapor in the interstitial gas;
- sorbed on the solid phase;
- non-aqueous phase liquids (NAPL) when liquid-state organic compounds at ambient temperature are not dissolved into water (Saponaro, 2022a).

The interaction between soil and PHs depends also on soil characteristics, like porosity, density, texture, etc. In general, soluble petroleum hydrocarbons that are not adsorbed into the soil, like monoaromatics hydrocarbons (BTEXs) and aliphatic halogenated hydrocarbons, can move downward through the unsaturated soil until they reach groundwater and spread slowly, but if they have low water solubility, volatility, and biodegradability they persist in the soil and become a continuous source of groundwater pollution (Tucci et al., 2021).

Hydrocarbons	*Mechanisms in subsoil*	*Examples*
Saturated aliphatic hydrocarbons (alkanes)	· Volatilization (from water and NAPL) · Solubilization (from NAPL) · Sorption · Aerobic biodegradation	Methane, propane, butane
Monoaromatic hydrocarbons (BTEXs)	· Volatilization (from water and NAPL) · Solubilization (from NAPL) · Biodegradation	Benzene, toluene, ethylbenzene
Polycyclic aromatic hydrocarbons	· Sorption	Naphtalene, benzo(a)pyrene
Aliphatic chlorinated solvents	· Water solubilization (from NAPL) · Volatilization (from water and NAPL) · Biodegradation	Trichloromethane, vinyl chloride, perchloroethene
Aromatic chlorinated solvents	· Solubilization (from NAPL) · Volatilization (from water and NAPL)	1,2-dichlorobenzene
Polychlorinated biphenyls (PCBs)	· Sorption	Deca-CB

Table 1.1: Type of hydrocarbons and mechanisms that control their behaviour in the subsoil.

Alkanes are less water soluble than BTEXs and are more volatile and biodegradable if the hydrocarbon chain is short; BTEXs are rapidly biodegradable under aerobic conditions but they present a good biodegradability also under anaerobic conditions. Toluene is the faster biodegradable compound, unlike benzene; PAHs are very stable, so highly hydrophobic and poorly volatile compounds as PCBs, especially highly chlorinated compounds; aliphatic chlorinated solvents are very soluble and volatile. They are biodegradable if they have less than five chlorine atoms, while highly chlorinated compounds are anaerobic biodegradable.

The huge and complex problem of hydrocarbon soil contamination is closely linked to the intensive use of petroleum oil, also called *crude oil*. The word petroleum means "rock oil" or "oil from the earth" (Adipah, 2018) because it's produced by the incomplete decomposition of plant and animal biomass over a long time (Ahmed et al., 2018). Crude oil is the principal energy source for heating, manufacturing, and transportation in modern society as well as a raw material in petroleum oil refineries

and petrochemical industries (Varjani & Upasani, 2017). Crude oil is a mixture of alicyclic and paraffinic hydrocarbons, the main types are aliphatic and aromatic hydrocarbons. These last are monocyclic aromatic hydrocarbons, with low molecular weight such as volatile organic compounds (VOCs), and polycyclic aromatic hydrocarbons, which may make up 10% of crude oil (Sammarco et al., 2016). In general, the carbon and hydrogen contents in crude oil are respectively in the range 83-87% and 10-14%, with the presence of small amounts of nitrogen, sulphur, and metals (Ahmed et al., 2018).

The environmental PHs contamination is mainly due to crude oil exploitation, beginning with the anthropogenic release from oil and gas exploration and production, coming to accidental spills in loading and discharge (Ossai et al., 2020a). Moreover, petrochemical industry effluent discharge, fugitive emissions, and oil tanker incidents can influence the terrestrial and marine ecosystems (Ossai et al., 2020a). Based on the 2005 report of Toxic Release Inventory (a United States federal program administered by the Environmental Protection Agency), the crude oil industry is one of ten major sources releasing PHs into the environment (Varjani & Upasani, 2017) and tanker incidents are responsible for the loss of about 5,74 million tonnes of oil from 1970 to 2014 (Ahmed et al., 2018). In Europe, there are over one million petroleum hydrocarbon-contaminated sites (Tucci et al., 2021). Major environmental disasters related to PHs release include marine oil spills, where the marine environment is the largest reservoir and ultimate receiver of pollutants (Ossai et al., 2020a). An example is the Exxon Valdez oil spill in 1989 when an Exxon Shipping Company oil tanker struck a reef in Alaska releasing 11 million gallons of crude oil into the sea and only 10% of the oil was recovered (Lim et al., 2016).

The petroleum hydrocarbons chemical characteristics and composition affect the toxic and lethal nature of these chemical substances (Ossai et al., 2020b). Furthermore, PHs contamination in soil may involve, depending on mode, level, and time of exposure, short- and long-term effects on the environment as well as human and animal health (Noori et al., 2022).

To analyse the sanitary risk associated with PHs is important to define the extent and degree of contamination at the site, so the primary sources, that in this case could be the accident releasing oil, and the secondary sources, meaning the environmental matrices that have been affected, such as soil, subsoil and groundwater. It's fundamental know the type of people exposed to pollutants, because some people spent more time in the proximity of the site and they have different sensibility to the exposure, and the receptors, that may be groundwater and surface water. The

exposure to the PHs contamination can occur through direct exposure to the pollutant secondary source or/and through indirect exposure when the pollutant reaches the receptors from the secondary source. Direct exposure pathways are soil ingestion and dermal contact, while for indirect exposure we considered vapor inhalation. It's possible determinate the chronic daily intake of chemical j through the exposure pathways i, $CDI_{j,i}$ $\left(\frac{mg_{pollutant}}{kg_{bodyweight} \cdot d}\right)$:

$$CDI_{j,i} = \frac{C_{j,i} \cdot CR_i \cdot EF \cdot ED}{BW \cdot AT}$$

where $C_{j,i}$ $\left(\frac{mg_{pollutant}}{d}\right)$ is the chemical j concentration at point of exposure (POE) in the environmental medium of concern (air, soil) for the exposure pathways i and CR_i $\left(\frac{m^3_{air}}{d}, \frac{kg_{soil}}{d}\right)$ the contact rate, that is the assumption rate of the environmental medium for the exposure pathway i (Saponaro, 2022a). EF $\left(\frac{d}{ye}\right)$ and ED (yr) are respectively the exposure frequency and the exposure duration. To the denominator there's the product through BW $(kg_{bodyweight})$, the body weight, and AT (d), the average time (Saponaro, 2022a).

Considering petroleum hydrocarbons, human may be affected to vapor inhalation caused by VOCs, which are easily evaporative and can lead to respiratory irritation and central nervous system depression, for example benzene causes leukaemia and toluene is a teratogen at high dose (Solomon & Janssen, 2010). The short-term effect to the toluene breathing, for several hours, at concentration greater than 100 part per millions (ppm), are fatigue, headache, nausea, and drowsiness (Adipah, 2018). About petroleum aromatic hydrocarbons, in the crude oil, they are toxic and carcinogenic (Sammarco et al., 2016) . Sixteen PAHs are categorized as priority pollutants due to high stability (Varjani & Upasani, 2017), this means that the pollutant persists in the environment, it's absorbed by plant and it's subject to bioaccumulation in the food chain.

Petroleum hydrocarbons are dangerous also for the plant growth because they reduce the water and mineral salt intake and this leads to a lower plant resistance to the pest and diseases (Ossai et al., 2020a).

1.2. Nitrate in the nitrogen cycle and the concern for environment and human health

Nitrate (NO_3^-) is a nitrogen compound and it is involved in the N-cycle enabling the element to return to the atmosphere through different transforming processes mediated by microbes:

- *ammonification*, includes nitrogen (nitrogen fixation) and dissimilatory nitrite reduction to ammonium (DNRA);
- *nitrification*, consists of the oxidation of ammonia to nitrite and the oxidation of nitrite to nitrate;
- *denitrification*, sequential anaerobic reduction of nitrate, nitric oxide, and nitrous oxide to N_2 and it's also defined as biological denitrification;
- *anammox*, described as coupled nitrification-denitrification, is the formation of N_2 started from nitrite and ammonium (NH_4^+) with the intermediates NO and hydrazine (N_2H_4); nitrite-nitrate interconversion (Stein & Klotz, 2016).

The principal issue of nitrate contamination is the N-based fertilizer used in agriculture and it's administered as ammonia (NH_3) and urea (CH_4N_2O), which oxidize to nitrate, the most stable form of N compound (Gadegaonkar et al., 2023). Developing countries in East and South Asia have increased fertilizer N consumption, after the late 1980s, much more than the developed regions, where the consumption has been constant since 1990 (Bijay-Singh & Craswell, 2021). Nitrate can leach from soil into groundwater or surface waters. Approximately 10-30% of N-fertilizer used in agriculture is lost and goes towards several biochemical and bio-physic-chemical processes (Bijay-Singh & Craswell, 2021). Nitrate contamination is worrisome because it can cause side effects in water bodies, soil, and human health and about 25% of N applied to agricultural ecosystems escapes and contaminates water resources as more fertilizer than necessary is used (Bijay-Singh & Craswell, 2021). Moreover, only a fraction is utilized directly by plants (Bijay-Singh & Craswell, 2021). Other important nitrates production sources are the organic waste generated by intensive feedlots and the sewage cities production, but their nitrate-N leaching losses are lower than nitrate-N leaching losses from N fertilizers, except for effluents containing high quantities of mineral N like pig slurry cities (Bijay-Singh & Craswell, 2021). When abundant nutrients such as nitrates reach a water body there's an excessive growth of algae leading to the algae bloom, reducing the sunlight penetration into the water and the

dissolved oxygen, and it can lead to the demise of the aquatic living organisms (Varjani et al., n.d.). This phenomenon is called eutrophication and affects ponds, lakes, reservoirs, and coastal water bodies all over the world and it's now a primary water quality problem (Bijay-Singh & Craswell, 2021).
When groundwater contaminated by nitrate is used for drinking water consumption, it can raise concerns because nitrate is one of the co-factors that play a complex role in causing methemoglobinemia in infants and the first evidence of the link between methemoglobinemia and drinking water dates to the 1940s (Fewtrell, 2004). Methaemoglobin (MetHb) is produced thanks to the nitrite, obtained by the microbial reduction of nitrate in drinking water, that oxidizes the ferrous iron in haemoglobin (Hb) to the ferric form (Fewtrell, 2004). The problem of the presence of Methaemoglobin in the human body is the incapacity to blind oxygen and can cause cyanosis and cerebral anoxia (Fewtrell, 2004). This disease is also called blue baby syndrome because it affects principally bottle-fed or weaned infants who may manifest bluish or brownish gray skin colour (Fewtrell, 2004). Nitrate is implicated also in cancer, hypertension, increased infant mortality, central nervous system birth defects, diabetes, spontaneous abortions, respiratory tract infections, and changes to the immune system (Fewtrell, 2004).
Given the hazardous nature of nitrate contamination in groundwater, the threshold of nitrate and nitrate-nitrogen in drinking water stated by the European Union (EU) and World Health Organization (WHO) regulations are respectively 50 mgNO_3/L (Gadegaonkar et al., 2023) and 10 gNO_3-N/L (Fewtrell, 2004).

1.3. Traditional technique to remove PHs from contaminated soil

The increasing risk of contamination from PHs leads to the research and development of more effective and economical methods for treating the contaminated environmental matrices.Fare clic o toccare qui per immettere il testo.The treatment methods can be applied *in situ* and/or *ex situ*. In the first case, the polluted soil is treated in place, while in ex-situ treatments the contaminated matrix is moved and treated above ground, at the contaminated site in *on-site* remediation, or elsewhere treated or disposed of in *off-site* remediation. Decontamination is also achieved by applying two or more technologies simultaneously or in sequence (the so-called "treatment train") (Saponaro, 2022b). In-situ technologies are generally cost-effective and have low environmental impacts, as no excavation and transportation of the contaminated soil

are required, still, ex-situ treatments are preferable when better control over operating conditions is needed, which often translates into faster degradation rates.

1.3.1. Thermal technologies

Thermal remediation is based on increasing the temperature in unsaturated and/or saturated soil zones to enhance the pollutants' desorption and volatilization, so they can be collected and treated in a Soil Vapor Extraction (SVE) system (Saponaro S, 2022). The advantage of this method is the short treatment time, but the costs are very high due to high energy needs. Thermal treatments typically produce vapours and sometimes liquid waste that requires treatments (Aparicio et al., 2022).

In-situ thermal remediation (ISTR) provides for the application of three methods to heat soil depending on the final target temperature:

- *thermal conductive heating* (TCH, Figure 1.1a) in which heaters placed in wells allow heating of the soil. The wells, with electrically powered resistance heaters, can be vertical (thermal wells) or horizontal (thermal blanket) and achieve 750-800 °C, while contaminated surrounding soil can amount to 300-400 °C due to conduction. Not all pollutants are collected as volatile compounds, because 95-99% of them are destroyed before they arrive at the extraction wells (Saponaro S, 2022);
- *electrical resistivity heating* (ERH, Figure 1.1b) allows reaching the water boiling point (100°C) through the passage of alternating electric current between electrodes, which rapidly heats the most electrically conductive soil and thanks to the water vapor also the less conductive zones (Saponaro S, 2022);
- *steam enhanced extraction* (SEE, Figure 1.1c), where water steam is injected into contaminated soil reaching temperatures of about 170°C (Saponaro S, 2022). Water and pollutant vapors are extracted together.

Other thermal remediation techniques that are both in-situ and ex-situ are:

- *incineration* by combustion or burning at temperatures ranging between 870-1200 °C maintaining oxygen level at 10% for volatile organic compounds (Ossai et al., 2020a);
- *pyrolysis*, involves the thermal heating or thermal cracking of soils contaminated at elevated temperatures, ranging between 400 °C to 1200 °C under pressure, in an anoxic condition or inert atmosphere (Ossai et al., 2020a).

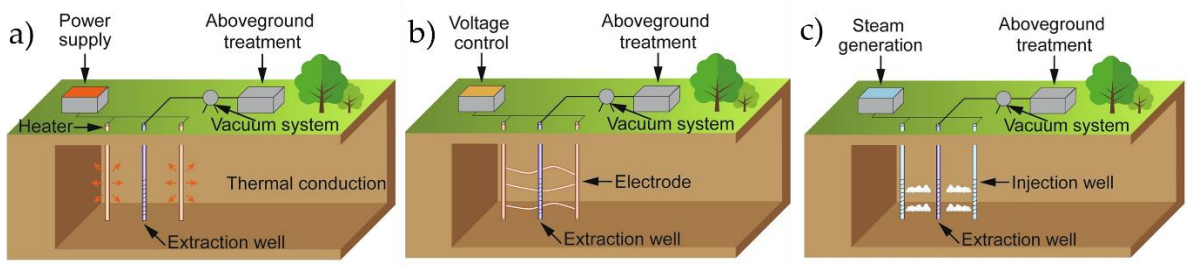

Figure 1.1: In-situ thermal remediation: a) thermal conductive heating; b) electrical resistivity heating; c) steam enhanced extraction.

1.3.2. Physical-chemical technologies

Physical-chemical technologies exploit the physical and/or chemical properties of the pollutants (Aparicio et al., 2022) to recover or contain the contaminants in the soil (Ossai et al., 2020a). These methods are mostly in-situ and/or ex-situ and can achieve the 70-80% of efficiency. These methods need high investment and, after chemical treatments, there's the risk of by-products hazards (Noori et al., 2022) that causes the reduction of soil quality (Tucci et al., 2021). Physical-chemical technologies are:

- *soil washing* (Figure 1.2a), an ex-situ technique to isolate semi-volatile or hydrophobic organic and inorganic pollutants adsorbed onto the fine soil particles, due to their high specific surface. The first soil washing step is the soil pretreatment, to remove large solids (> 50 mm) that may be reused. The process continues with wet separation, in which water is used to separate the smaller soil particles (< X mm) and to reduce the contaminated material volume. This treatment method is indicated to treat soil showing a large amount of coarse particles. So, the water used in the separation isn't immediately contaminated and is exploited more than once making the process less expensive. Later, pollutants may get desorbed from the fine material (< X mm) thanks to an extraction liquid constituted by water and surfactants or water-miscible organic solvents. This solution can affect acid-base reactions or form soluble complex with pollutants (Aparicio et al., 2022). The process is repeated until the concentration is lower than the permissible limit and the liquid is treated, while the solid material < X mm is extracted and reused. The method efficiency depends on the pollutant chemical and physical characteristics but also on the washing solution used (Aparicio et al., 2022);

- *in-situ chemical oxidation* (ISCO, Figure 1.2b) is a groundwater treatment technique involving the injection through wells of an oxidizing agent in a small area with high contaminants concentration (Asghar et al., 2016). The agent accepts electrons released by pollutants to obtain less hazardous compounds (O'Brien et al., 2017). The reduced species choice and the ISCO success depend on the initial soil physiochemical properties, such as permeability, texture, pH, etc (Asghar et al., 2016). Several oxidizing agents are available, whose applicability depends on the speed at which the agent reacts in groundwater and on the electrode potential (E_h), the ability to destroy the pollutants. This capability is linked to the oxidative potential of the substrate and of the substance generated by the oxidizing agent, which can be either reducing substances or other oxidants. The most used oxidizing agents are permanganate (MnO_4^-) and persulfate ($S_2O_8^{2-}$). Both oxidize pollutants through direct electron exchange and persulfate also through the formation of the sulphate radical ($\cdot SO_4^-$) which has a higher persulphate oxidative potential and degrades a wide variety of contaminants (Saponaro S, 2022). The permanganate advantage is the low injection frequency and the reaching long distance due to the slow permanganate reaction in groundwater. While persulfate is more stable than other oxidizing agent, as ozone (O_3) and Fenton's reagent (H_2O_2 and Fe^{2+}) that produce by-products. Ozone is injected in groundwater as gas and this means greater control requirement of gases escaping from the ground, because O_3 is toxic for human, and it can induce the stripping of gases in the unsaturated soil. Instead, Fenton reaction is exothermic and very rapid, so it can treat only the soil near the injection wells. The oxidising agent injection has different involvements on soil properties, for example Fenton's reagent reduced soil pH increasing the solubility of metals, such as Zn and Cu, and their bioavailable to vegetation and soil fauna (O'Brien et al., 2017). In general, hydrogen peroxide shows the higher removal efficiency, followed by permanganate and persulfate (Ossai et al., 2020b);

- *permeable reactive barrier* (PRB, Figure 1.2c) is an in-situ passive treatment system inserted in the subsurface, perpendicular to the plume of contaminated groundwater (Thiruvenkatachari et al., 2008). The most reactive material used is iron (0) thanks to its high purity (Fe(0) > 95%) and affordability (Saponaro S, 2022). Other available materials are zero-valent metals (Zn(0), etc.) and

bimetallic systems (Fe-Pd) but are specific for contaminants such as aliphatic chlorinated solvents (Saponaro S, 2022). However, the reactive material must be environmentally compatible, with a high specific surface, stable over time, cheap, and more permeable than the aquifer, so the water flows through the barrier without altering groundwater hydrogeology (Thiruvenkatachari et al., 2008). The physio-chemical mechanisms that pollutants run into are oxidation-reduction, precipitation, and sorption, but these processes don't reduce the total amount of pollutants (Saponaro S, 2022);

- *soil vapor extraction* (SVE, Figure 1.2d) consists in the contaminated soil washing with fresh air. It moves from the atmosphere to the extraction well, thanks to the pressure gradient applied at the wellhead, passing through the unsaturated soil. The contaminants with low molecular weight and high vapor pressure, such as gasoline, are removed by desorbing from soil particles due to the suction from the surface (Aparicio et al., 2022). The extracted air is treated and released into the atmosphere. This technique is expensive because it requires high energy and it can be applied on large volumes of high permeability soil and deep aquifer (Aparicio et al., 2022);

- *air sparging* (AS, Figure 1.2e) is an in-situ treatment where fresh air is injected through walls into the saturated soil zone to treat dissolved contaminants plume or trapped immiscible contaminants (Leeson et al., 2002). This air is enriched in volatile pollutants and flow towards the unsaturated zone, arriving to the SVE system to collect it (Saponaro S, 2022). It's preferable to treat a sandy or gravelly soil because the low intrinsic permeability of a clay or silty soil restricts the airflow. Moreover, heterogeneous and anisotropy contaminated soil may induce the development of preferential flow paths for the injection air;

- *pump and treat* (Figure 1.2f) method implies contaminated groundwater pumping for above-ground treatments of the pollutants (Ossai et al., 2020a). The treated water is discharged into sewers or a surface water body. This technique is mostly used for highly soluble NAPLs trapped at or below the water table because they represent a continuous source for groundwater pollution (Ossai et al., 2020a). Furthermore, pump and treat is useful to avoid the contaminants sorption into the subsurface solid matric and the same time contaminants

dissolution in the groundwater, due to the water table rising (Ossai et al., 2020a).

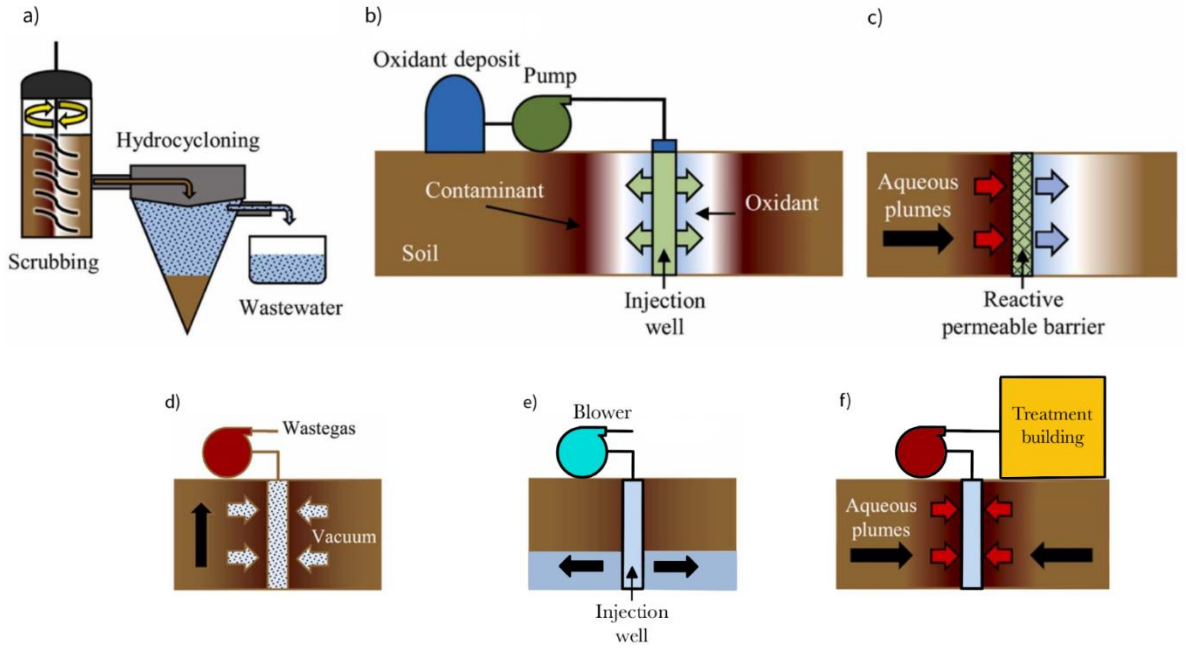

Figure 1.2: Physical-chemical technologies; a) soil washing; b) in-situ chemical oxidation; c) permeable reactive barrier; d) soil vapor extraction; e) air sparging; f) pump and treat. Adapted from (Aparicio et al., 2022).

1.3.3. Biological technologies

Bioremediation allow to accelerate the mineralization of petroleum hydrocarbons thanks to microbial metabolism where PHs are the energy sources with negligible or without hazardous byproduct production (Noori et al., 2022). It can be applied in-situ, with the injection of the right microbial communities (Bioaugmentation), and ex-situ, exploiting controlled environmental conditions (Noori et al., 2022). Pollutants are not always bioavailable to microbial biodegradation, making the treatment ineffective. Other limitations are the low abundance of indigenous microorganisms able to degrade the pollutant and their slow growth rate. As a result, adding chemicals is required to enhance microbial activity, leading to an increase in the cost of a treatment method usually considered less expensive than those described in previous chapters. (Kronenberg et al., 2017). The chemical substances are:

- *macro-nutrients* (NH_4NO_3, NH_4Cl, $CO(NH_2)_2$, $Ca(H_2PO_4)_2$, H_3PO_4, $(NH_4)_2HPO_4$) and micro-nutrients, above all in ex-situ processes, where there's a close contact between the soil and these substances due to the complete mixing;

- *electron acceptors* (O_2, NO_3^-, Fe(III), Mn(IV), SO_4^{2-} or CO_2) because biological processes are based on redox reaction and the pollutants are the electron donors (Saponaro, 2022b). The most used electron acceptor is oxygen because PHs aerobic biodegradation is most favourable than anaerobic biodegradation, but its insertion into the soil is energy-intensive and it leads to the contaminants stripping. While the anaerobic degradation consists in the addition of alternative water-soluble terminal electron acceptors, such as nitrate and sulphate, but it requires high costs of chemicals and there' are stringent regulatory issues related to their use, particularly in-situ (Tucci et al., 2021);
- *co-substrate* to promote the co-metabolism, where biomass degrades substrate and produces enzymes capable of degrading pollutants;
- *specific biomass concentration* to have in the soil specific operative microorganisms that biodegrade contaminants;
- *surfactants*, are organic substances which allow the contaminants hydrophobic remotion since they are strongly bound to the soil matrix (Tucci et al., 2021). They can be degraded before the pollutants and can be adsorbed into the solid phase of the soil.

Many factors can be modified to promote the biodegradation, such as:

- *moisture*, vital for biological processes but in saturated conditions is a problem for aerobic biodegradation due to the low oxygen presence. Moreover, it's difficult to control in in-situ treatment;
- *temperature*. High temperature means a high process rate but increasing soil temperature is expensive;
- *pH*. Biological processes take place within a certain pH range (5-8) and if its modified, the soil can restore the original condition.

Traditional bioremediation techniques are:

- *biostimulation*, in-situ and ex-situ, is the addition of nutrients, bio-surfactants and electron acceptor that are limitation factors to the microbial performance (Ossai et al., 2020a). Organic amendments, such as crop residue and biochar, are useful as biostimulants (Aparicio et al., 2022);

- *bioaugmentation* (Figure 1.3a), both in-situ and ex-situ, involves the supplement of exogenous or pre-enriched autochthonous microbial communities capable of degrading pollutants (Ossai et al., 2020a);
- *bioventing* (Figure 1.3b), like soil vapor extraction technique, is the injection of air into the unsaturated soil zones, by the pressure gradient applied to the injection well head. The air added in the contaminated soil promotes the PHs degradation by microorganisms in aerobic conditions. It's important to define the right air injection rate, because if it's high, it enhances PHs volatilization (Aparicio et al., 2022);

- *biopiling* (Figure 1.3c) is an ex-situ treatment where is enhanced the aerobic biodegradation monitoring key process parameters and operating on:

  - O_2 *concentration*, through blowers and bulking agents (e.g. wood chips) addition to increase porosity and air permeability;
  - *macro-nutrients*, through irrigation/nutrient system, to balance C:N:P ratio at around 100:10:1 in order to don't limit the biomass activity and to increase the microbial density;

  - *acid or base*, to obtain neutral pH (Saponaro, 2022b).

  The contaminated soil mound is extracted and pretreated by sieving (~ 50 mm) and mixing with air, macro-nutrient and acid or base. The biological treatment takes place in two ways:

  - *static piles*, where blowers connected to pipelines in the piles extract air producing a depression, thus atmosphere air enters the soil. Pollutants can volatilize due to the pressure gradient induced and they are collected and treated before the releasing into the atmosphere;

  - *windrow*, is a periodic tilling and turning of piled contaminated soil to allow the atmosphere air to enter the piles (Ossai et al., 2020a). This option in less efficient due to the aeration discontinuity but it's cheaper than static piles.

  Biopiles are between 3 and 4 m high and they have a volume of several hundred m^3 (Aparicio et al., 2022). Moreover, they are placed above linear or waterproof slab to collect pollutants with low vapor pressure and high aqueous solubility (Aparicio et al., 2022). There are also irrigation and heating system to increase

the moisture content and the temperature, because the moisture could be reduced by evapotranspiration and the heating increases microbial activity;

- *biosparging* (BS, Figure 1.3d) is the same process of air sparging but is promote the saturated soil zone aerobic biodegradation by injecting fresh air (oxygen);

- *assisted aerobic biodegradation* (Figure 1.3e) is a passive technology to treat the saturated zone in-situ by applying oxygen releasing compounds (ORC), such as magnesium peroxide and calcium peroxide, which supply the degradation electron acceptor (Saponaro S, 2022). Calcium peroxide is preferable if the site has high pollutants concentration and it's necessary a fast treatment because it's more soluble than magnesium peroxide and it releases 17% by weight of O_2 (Saponaro S, 2022). In general, the treatment lasts 5-6 months;

- *assisted anaerobic biodegradation* (Figure 1.3e), like assisted aerobic biodegradation, is a passive in-situ saturated soil zone treatment. It promotes the anaerobic biodegradation by the organic substrate releasing. The substrate choice depends on the speed releasing into the aquifer. Low molecular weight fatty acids and carbohydrates are typically fast-release, while vegetable oils, whey and ketene are slow-release;

- *phytoremediation* (Figure 1.3f), is an in-situ technique where is exploited the natural process of the green plants and their associated microorganisms by acting as filters or traps in the tissue (Ossai et al., 2020a). Plants and their rhizosphere organisms can remove, stabilize, or detoxify pollutants in different ways:

  - *phytoextraction*, contaminants are accumulated in the aboveground biomass plants (Aparicio et al., 2022);

  - *phytostabilization*, the using of plants to reduce the bioavailability and migration of contaminants in soil thanks to accumulation by roots, adsorption on the root surface or isolation within the root zone using plants as organic pumps (Asghar et al., 2016);

  - *phytovolatilization*, in which contaminants are taken up by plants and thought the evapotranspiration, they are moved into the atmosphere (Asghar et al., 2016);

- *phytodegradation*, the degradation of organic pollutants due to plants and their associated microorganisms (Aparicio et al., 2022).

Phytoremediation is slow and can operate with not very high pollutants concentration since it means slow or absent plants growth. Furthermore, the treatment is confined to the root zone.

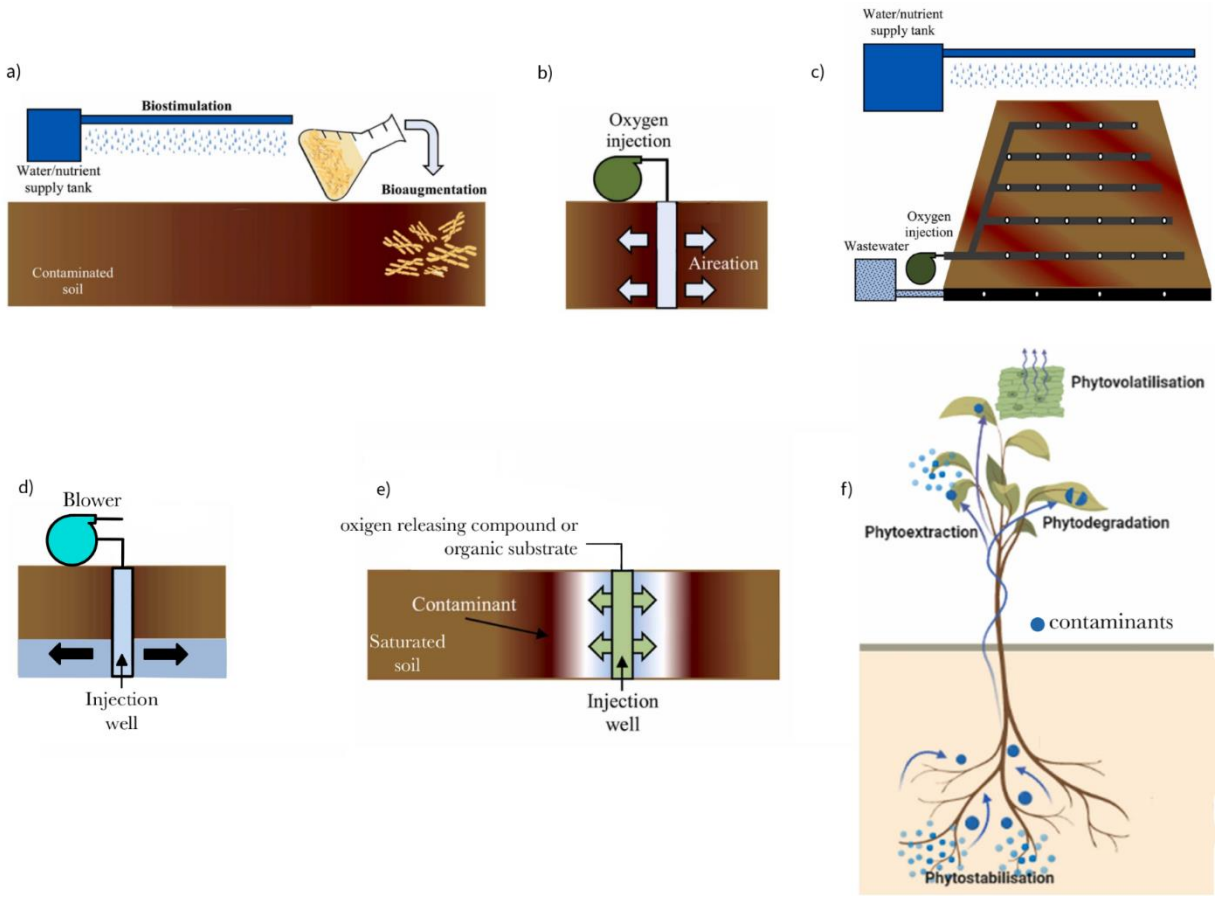

Figure 1.3: biological treatments; a) biostimulation and bioaugmentation; c) bioventing d) biopiling; e) biosparging; f) assisted aerobic/anaerobic biodegradation; g) phytoremediation. Adapted from (Aparicio et al., 2022).

In general, bioremediation technologies are difficult to monitor in real-time microbial activity and process performance (Tucci et al., 2021). An innovative solution is the use of bioelectrochemical systems.

2 State of the art in bioelectrochemical systems (BESs)

2.1. Introduction

Bioelectrochemistry system (BES) is a technology based on the interaction between microorganisms and physical electron conductors (Schröder et al., 2015). Microorganisms oxidize organic substrates, the electron donors, and release electrons to the anode, the electron acceptor; electrons are then transferred to the cathode, another electron donor, via conductive material or wire (Tucci et al., 2021). These electrons are used by other microorganisms in reduction reactions (Kronenberg et al., 2017). At the same time, the generated protons migrate toward the cathode to balance the charge and participate in the cathodic reduction (Tucci et al., 2021). In this way, chemical energy is transformed into electrical energy that can be used to power a load, as happens in a microbial fuel cell (MFC, Figure 2.1) (Tucci et al., 2021). Microorganisms able to interact with the electrode are defined as electroactive microorganisms (electroactive bacteria, EAB), and the biofilm formed by these microorganisms is named electroactive biofilm (Chiranjeevi & Patil, 2020). Microorganisms that release the electrons to the anode are called electrogens, otherwise, they are electrotrophs, that retrieve electrons from a cathode (Yee et al., 2020).

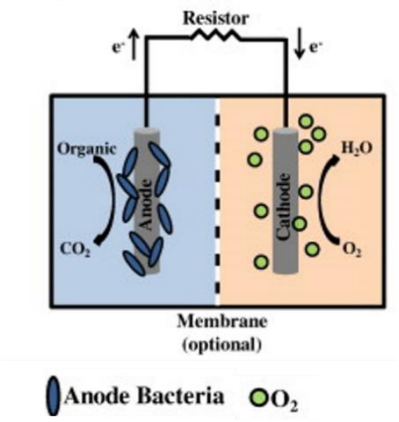

Figure 2.1: Electricity generation in air-cathode microbial fuel cell (Lim et al., 2016).

Electroactive microorganisms can interchange electrons with insoluble conductive materials via extracellular electron transfer (EET) (Kronenberg et al., 2017).

EET occurs through:

- *Direct EET*, cells establish direct physical contact with the electrode, thanks to microbial cell redox-active components. This type of mechanism is possible thanks to proteins, such as outer-membrane multiheme c-type cytochromes (MHC) and other heme proteins, and thanks to protrusions from cells (pili), that increase the electron transfer mainly under anaerobic conditions (Tiquia-Arashiro & Pant, 2019). Moreover, cells may also present nanowires, conductive pili employed to transfer electrons, without physical whole-cell contact. They are electrically conductive bacterial appendages that allow the microorganism to achieve. Direct electron transfer was discovered for the first time in sediment bacteria, like *Geobacteria* species (Tucci et al., 2021).
- *Facilitate or mediated EET*, electrons are carried inside and outside the cell through molecular redox compounds, released by the cell itself, that are soluble electron-shuttling compounds (Yee et al., 2020). The mediator remains stable, capable of being oxidized and reduced repeatedly: they are reduced by the cell, migrate to the electrode and release electrons to the anode; later on, they are oxidized and accept electrons from the cathode.Fare clic o toccare qui per immettere il testo.

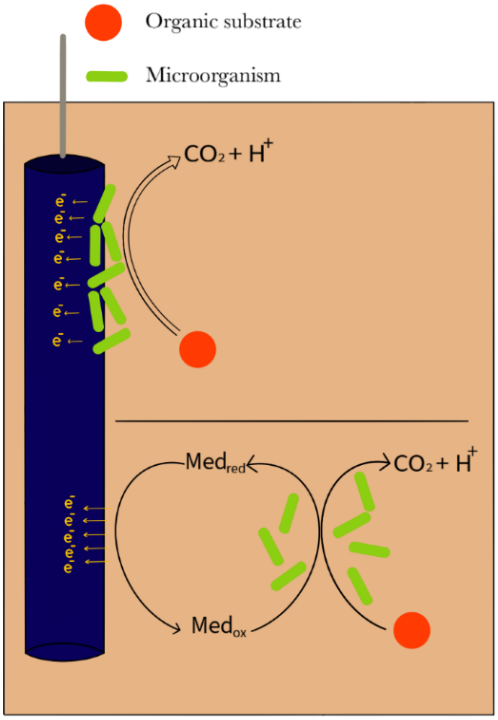

Figure 2.2: The extracellular electrons transfer from microorganisms to a conductive material. On the upper part is described the direct EET, while on the lower part the facilitate or mediated EET.

Electroactive and not electroactive microorganisms can also collaborate in a complex syntrophic and/or cooperative interaction (Noori et al., 2022). A microbial community (non-electroactive bacteria) oxidizes PHs to obtain simpler molecules, like acetate, a fermentation product, Fare clic o toccare qui per immettere il testo.that are mineralized by electroactive bacteria, to CO_2 using electrodes as an electron sink (Noori et al., 2022).

Other mechanisms that take place in the removal of contaminants in a BES system, in addition to the direct anodic oxidation, cathodic reduction, or cooperative oxidation driven by syntrophic communities, are:

- the adsorption of contaminants onto the surface of the electrodes or within the biofilm colonizing the electrodesFare clic o toccare qui per immettere il testo.;
- electrokinetic removal, whereby the chemical speciation and distribution of soil contaminants is influenced by the applied electric current (Tucci et al., 2021).

Depending on the type of contaminants, various removal mechanisms can occur.

Bioelectrochemical systems are less energy-expensive compared to other chemical or physical treatments. Moreover, microbial fuel cells allow Fare clic o toccare qui per immettere il testo.electricity generation, which can supply small electronic devices, such as monitoring systems, or be used to charge batteries.Fare clic o toccare qui per immettere il testo.

2.2. Soil Microbial Fuel Cell (MFC)

Microbial fuel cell technology exploits the redox gradient between two compartments to allow the electron flow from the anode to the cathode: an electrode present in the anode zone acts as an electron acceptor due to the compound's oxidation by anaerobic bacteria, whereas the cathode is the electron donor that enables the reduction of the compound. In this way, electrical power is generated. In general, MFC performance is evaluated in terms of power density, i.e. the power output obtained from MFC system monitoring, normalized to some reactor characteristics, such as the cathode-specific area, to ease the comparison of different systems. The observation of frog legs twitching in response to electrical discharge by Luigi Galvani in 1790 marks the beginning of the field of bioelectricity. After, Michael Cresse Potter discovered the electron transfer between platinum electrodes and suspension of yeast and Escherichia coli in 1910, the research on BES systems began. In 1960 the National Aeronautics and Space Administration (NASA) paid attention to MFCs to produce current from organic wastes in its long-haul space flights. With the oil crisis and the greenhouse gas emissions increasing, the MFC system seemed a clean energy-generating technology possibility, even though the interest wasn't constant due to the absence of

enduring stability (Gupta et al., 2023). Since the early 2000s, thanks to the research and studies on MFC materials and design, the literature on MFC systems has rapidly begun growing.

Soil microbial fuel cell (SMFC) provides the remediation of hydrocarbons, heavy metals, pesticides, and antibiotics (T. Li et al., 2021). According to Kumar et al., degradation of volatile organic compounds (VOCs) such as benzene, ethylbenzene, toluene, and xylene in the MFC occurs through three steps: mass transfer of compounds from gaseous phase to liquid phase, compounds diffusion into the biofilm, and their degradation by microbes present in the biofilm (Kumar et al., 2019). In the literature, most soil MFCs employ oxygen as the terminal electron acceptor in the cathodic chamber, that is why it's called "air-cathode", and it's often in direct contact with atmospheric air. Besides, the protons flowing from the anode to the cathode through an ion-exchange membrane (IEM), are reduced into water. Another electron acceptor that is removed from groundwater by MFC systems is nitrate, where most of the time acetate (CH_3COO^-) is the electron donor in the anode chamber (Wu et al., 2020).

Bioelectrochemical systems have limited impact on the microbes and the environment, so they are considered eco-friendly candidate technology for removing PHs (Fatehbasharzad et al., 2022).

2.2.1. Construction materials

Electrodes are the backbone of BES systems; they influence both the microbial activity and the electron transmission rate. Electrodes generally must be:

- electrically conductive, to accelerate the electron transfer;
- biocompatible, because electrode materials affect the release of products during the biodegradation;
- chemically stable in the reactor solution;
- with a large surface area to enhance the sorption effect and the transfer capacity system;
- cost-effective.

Electrodes can be in metal, such as noncorrosive stainless-steel mesh (Figure 2.3b) and copper, even if this latter isn't employed due to copper toxicity to the bacteria (Logan et al., 2006). *Carbon-based electrode*s possess the characteristics listed above, making them the most common choice for an MFC reactor. Figure 2.3 shows the most widely used carbon-based materials, they have 2D architecture and a defined surface area, such as *carbon cloth* (CC),

carbon felt (CF), *carbon mesh* (CM), *graphite brush* (CB), *granular graphite* (GG), *graphite felt* (GF), *graphite sheet* (GS) and *graphite rod* (GR). Electrodes in microfiber carbon brushes have 3D architecture and enhance biodegradation rates thanks to the additional surface area, but are used in benthic environments, such as marine sediments (Noori et al., 2022). Graphite felt is an optimum choice due to its larger surface area and greater adsorption potential (Fatehbasharzad et al., 2022). Indeed, in a laboratory experiment with soil microbial fuel cell graphite felt, carbon cloth, activated carbon fiber felt (ACFF), graphite paper, and aluminum sheet electrodes are tested for petroleum degradation during 115 days of operation (Table 2.2) (Yu et al., 2021). The best removal efficiency is attributed to the graphite felt (59.14%). Another material widely used in laboratory-scale MFCs is *biochar*, the solid product of waste biomass pyrolysis (> 400°C) already known as a soil amendment to improve fertility and sequestrate carbon (Weber & Quicker, 2018). Biochar can exchange electrons with microbes despite its low electrical conductivity (< 500 mS/cm). Redox-active functional groups on biochar surface allow it to operate as an electron conduit during the microbe-to-microbe interspecies electron transfer process (Figure 2.9) (Tucci et al., 2021). This phenomenon allows for increasing the radius of influence (ROI) of the pollutant removal, as reported by Cai et al. who observed ROI increases up to ~16 cm with biochar compared to 4 cm without biochar (Cai et al., 2020).

Both anode and cathode structures can be modified with *catalysts* to accelerate the biodegradation. Petroleum hydrocarbon removal from polluted saline soil using carbon mesh as anode and carbon mesh with 0.1 mg/cm^2 Pt catalyst as cathode was studied, allowing 15.2 ± 0.6% removal efficiency of in 25 days (X. Wang et al., 2012). In general, the use of Pt loading is expensive. Activated carbon (AC) catalyst is a good alternative, as MFC with AC catalyst produced a maximum power density of 1220 mW/m^2 compared to 1060 mW/m^2 obtained by Pt catalyst (F. Zhang et al., 2009). Moreover, metals such as $Mn^{2+/3+}$ are also used as catalysts. Indeed, a MnO_2-coated anode showed higher alkane removal, thanks to the increased microorganism adhesion on the anode, in comparison to the pristine carbon anode (Nandy et al., 2020). A strategy to improve the extracellular transfer rate, the power output, and the pollutant removal is the modification of carbon electrode surface with functional groups and conductive nanocomposites materials (*surface functionalization*), such as carbon nanotubes (CNT), nanoparticles (CNP), and reduced graphene oxide (rGO) that enhance the electrical conductivity, the surface area, and biomass content (Noori et al., 2022).

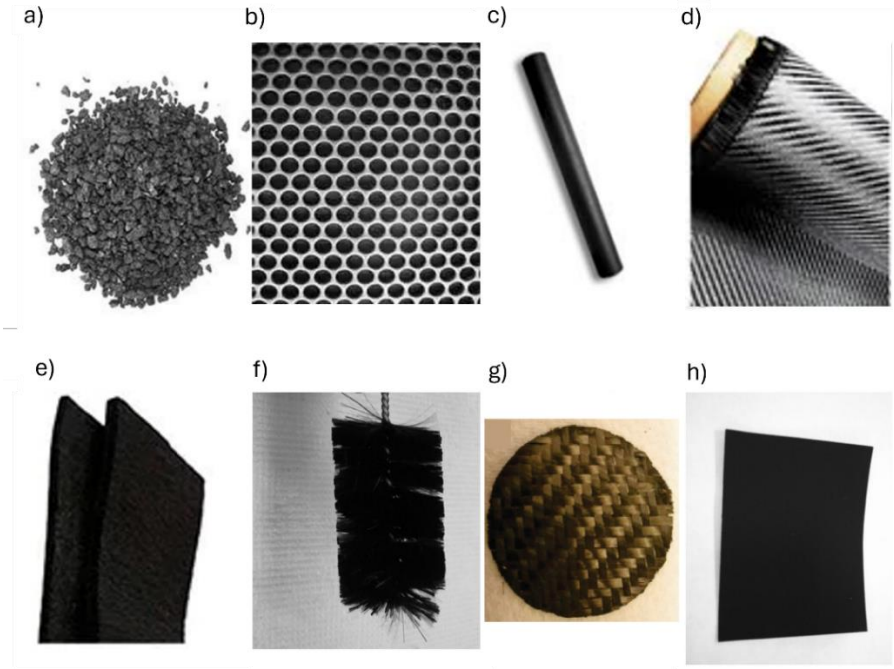

Figure 2.3: Electrodes material for MFC system: a) granular graphite; b) stainless-steel mesh; c) graphite rod; d) carbon cloth; e) graphite felt; f) graphite brush; g) carbon mesh; h) carbon felt. Adapted from (Noori et al., 2022; Rusli et al., 2019; X. Wang et al., 2009).

Generally, between the anodic and cathodic compartment there is an *ion-exchange membrane* (IEM), which most of the time is a *proton exchange membrane* (PEM), also known as *cation exchange membrane* (CEM), allows the protons flow, produced during the biodegradation in the anodic chamber, towards the cathode chamber. It is made by the linking of negatively charged functional groups to a backbone and it has high conductivity to cation and low internal resistance (Rahimnejad et al., 2014). The membrane prevents the mixing of the two chambers' solutions: when the anode solution reaches the cathodic side, biofouling is induced on the cathode; when oxygen from the cathode arrives at the anodic zone, anaerobic pollutants degradation gets inhibited (T. Li et al., 2021).
Nafion membranes are widely used in MFC systems, and they consist of "*perfluorosulfonic acid membrane composed of hydrophobic fluorocarbon backbone (–CF_2–CF_2–) to which hydrophilic sulfonate groups (SO_3^-) are linked*" (Fatehbasharzad et al., 2022). These membranes have high proton conductivity and enough ion exchange capacity, but under neutral pH, they allow the flowing of K^+, Na^+, NH_4^+, Ca^{2+}, and Mg^{2+} respect H^+ with subsequent pH increasing and salt precipitation (Fatehbasharzad et al., 2022).
Other membranes have been developed:

- anion exchange membrane (AEM), with positively charged functional groups linked to the backbone, is rarely applied in MFC;

- bipolar membrane (BMP), combines both anion and cation exchange layers and dissociates water molecules to H^+ and OH^-, it reduces the pH imbalance between the cells (T. Li et al., 2021).

Natural materials membranes, such as terracotta, earthenware, and clayware membranes, are cost-effective alternatives to commercial membranes. Ceramic membranes can be modified in raw material, including oxides such as alumina, and in the kilning process, improving permeability, porosity, water absorption, and porosity (Fatehbasharzad et al., 2022). A ceramic membrane is comparable to conventional IEM in terms of voltage generation, power, and current density, but it has lower production cost and higher structural strength (Patel et al., 2022). Today, the use of ceramic membranes in MFC systems for pH control is still limited.

Co-substrates, such as glucose ($C_6H_{12}O_6$) and acetate (CH_3OO^-) promote bacterial growth and enhance the co-metabolism, reducing the internal resistance. They lead to a beneficial synergism in the medium and accelerate the degradation. The oxidation reactions and the electron production of glucose and acetate are:

$$C_6H_{12}O_6 + 6H_2O \rightarrow 6CO_2 + 24H^+ + 24e^-$$

$$CH_3COO^- + 2H_2O \rightarrow 2CO_2 + 7H^+ + 8e^-$$

For example, contaminated PHs soil was mixed with 0.1% and 0.5% (w/v) of glucose solutions and treated with MFCs producing maximum power densities of 43 mW/m² and 35 mW/m², respectively, and PHs degradation rates up to three times higher than that of the open circuit (Table 2.2) (X. Li, Wang, Wan, et al., 2016). Furthermore, a study investigated the effects of different sodium acetate concentrations as the carbon source on the output of a soil microbial fuel cell (Kilinc & Catal, 2023). The results are shown in Table 2.1. Dosing acetate in MFC systems is also widely used to treat nitrate-contaminated groundwater.

CH_3COONa concentration (mg/L)	***Power density (mW/m^2)***
3281.2	48.04
4921.8	98.79
6562.4	125.36
8203	208.32
9843.6	227.43

Table 2.1: MFCs performance for different sodium acetate concentrations (Kilinc & Catal, 2023).

2.2.2. Reactor design and geometry

The typical arrangement for MFCs with air-exposed cathode is a two-chamber MFC including *H-type* MFC, consisting of two bottles connected by a tube containing a membrane separator, usually a cation exchange membrane, secured in the middle of the tube. Anyway, the connection tube isn't strictly necessary, and the chambers are pressed up onto both the membrane sides (Figure 2.1). This system usually produces low power density, which depends on the cathode, anode, and membrane surface area (Logan et al., 2006). Another configuration is the *U-type* microbial fuel cells (Figure 2.4). An example is reported by Wang et al., with a hollow membrane electrode assembly (MEA) into a rectangle box, as represented in Figure 2.4C (X. Wang et al., 2012). They have shown PH degradation rate increases by 120%, from 6.9 ± 2.5% (open circuit control) to 15.2 ± 0.6%, with a power density of 0.85 ± 0.05 mW/m^2 during 25 days of the experiment (X. Wang et al., 2012). In this configuration, the MFC performance decreases as the distance among the electrodes is increased; a *column-type* design (Figure 2.4B) in a pilot-scale reactor allowed the remediation right up to the reactor edge, reaching about 90-300 cm of ROI (Lu et al., 2014). This column-type reactor consists of an anode and a cathode wrapped around a porous pipe and separated by a glass fiber. This study confirmed the increase in PHs biodegradation by an SMFC, with a 241% performance increase compared to the baseline control reactor. Besides, the maximum power density of this reactor with biochar as anode (BCA) is lower than the maximum power density with graphite granule anode (GGA). A similar configuration is the *insertion-type* MFC, which is based on a simple cylinder configuration (Figure 2.4A). For example, this design was used to remove phenol, an aromatic organic compound, with hydroxyl group (-OH) bonded to a benzene ring, from waterlogged soil with 90.1% removal, efficiency, compared to 27.6% and 12.3% of the open-circuit and non-MFC reactors, (X. Li, Wang, Zhao, et al., 2016). *Multi-anode* systems consisting of *horizontal* or *vertical* anodes (Figure 2.4D) can improve PHs biodegradation. Zhang et al. tried both systems to determine which of them gives better PH degradation (Y. Zhang et al., 2015). They used three parallel anode layers (HA = horizontal anode; VA = vertical anode), 2 cm distant from each other, and an air-exposed cathode at the bottom of the reactor. After 135 days of experiment, HA has shown 12.5% PHs removal, compared to 8.3% of VA configuration, this means that the THPs degradation in HA system was 50.6% higher than in VA. Another laboratory experiment, with a horizontal multi-anode design, tested the presence of sand in the soil, proving better performance with a sand-rich soil (X. Li et al., 2015). A simplified soil MFC used a *graphite rod* as the anode (Figure 2.4E). A laboratory experiment studied the influence of conductive carbon fiber mixed with PHs contaminated soil on its treatment, showing enhanced PH degradation rates by 329% and 100% in comparison to open and closed-circuit without carbon fiber (Huang et al., 2011).

Another configuration is used especially when materials such as graphite felt and carbon cloth are used: anode and cathode are placed horizontally, with the anode at the bottom of the reactor and the cathode in the upper part directly in contact with water. It's an example of the laboratory scale test operated by Yu et al. (Figure 2.4F).

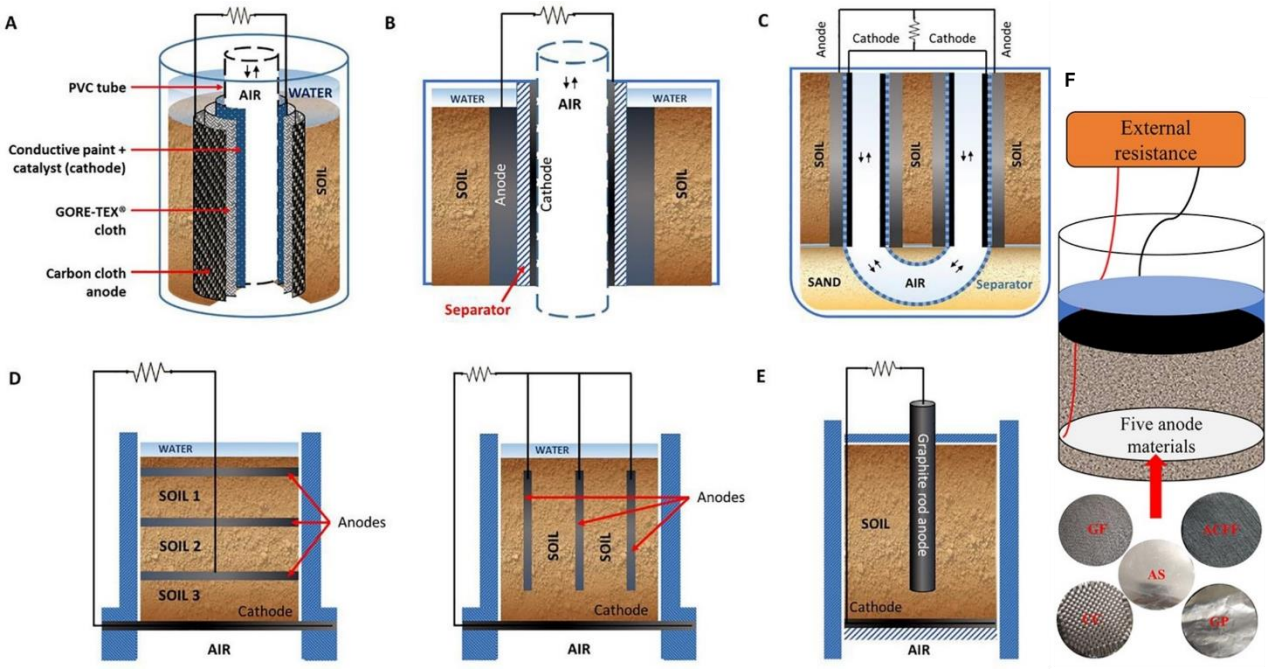

Figure 2.4: Different types of MFC reactor design for petroleum hydrocarbons removal: A) insertion-type; B) column-type; C) U-type; D) multi-anode; E) graphite rod; F) horizontal anode and cathode. Adapted from (Tucci et al., 2021) and (Yu et al., 2021).

2.2.3. Soil characteristics relevant to MFC

The soil electrical conductivity (EC), measured in mS/cm, is essential in the interaction between electrodes and biomass. It's the ionic mobility measure inside the soil matrix: high EC means low internal electron transport resistance, so best PHs biodegradation performance.

Electrical conductivity can be manipulated through:

- *water content;* according to Wang et al., a water content increase leads to a decrease in soil internal resistance, for instance from 42.6 Ω, with 23% water content, to 7.4 Ω, with 33% and electrical conductivity increases from 8.36 ± 0.59 mS/cm to 13.4 ± 2.3 mS/cm respectively (X. Wang et al., 2012). These results are directly linked with the petroleum hydrocarbon degradation rate;
- *soil texture*, coarse soil generally shows better PH degradation performance than fine soil. Indeed, at the same water saturation, sandy soil is preferable to clay soil, due to the superior mass transport process through the soil pores (Noori et al., 2022). A

laboratory scale study assessed PH removal in sandy and clay soil at the same water saturation, obtaining a degradation of 48-59% and 42-45% respectively (Table 2.2) (H. Wang et al., 2019). Furthermore, a larger radius of influence was obtained in the sandy soil compared to clayey soil, due to the higher sandy soil hydraulic conductivity (Tucci et al., 2021). Also, X. Li et al. observed better performance in sand-rich soil than sand-poor soil, with removal TPHs efficiency of 22 ± 0.5%, compared with 15 ± 0.1% respectively (Table 2.2) (X. Li et al., 2015).

- *salinity*, which can have dual effects on the biodegradation. Sodium chloride added to sediment improved its electrical conductivity (Hong, Chang, Choi, & Chung, 2009), but high salinity may inhibit microorganisms, thus 30% increase in PH degradation rate was observed in soil with limited soluble salt content (X. Qin et al., 2012).

Design	Soil type	Pollutant	Anode material	Cathode material	External load (Ω)	Days	Maximum power density (mW/m²) / voltage (V)	Removal efficiency (%)	Reference
Horizontal anode and cathode	Aged soil	Gasoline and diesel mixture	Graphite felt (GF) carbon cloth (CC) ACEF Graphite paper (GP) Aluminium sheet (AS)	Graphite felt	1000	115	GF → 346 ± 5 CC → 192 ± 5 ACEF → 255 ± 5 GP → 130 ± 5 AS → 300 ± 5	GF → 59.14	(Yu et al., 2021)
U-type	Saturated saline soil	PHs	Carbon mesh	Carbon mesh + Pt catalyst	1000	25	0.85 ± 0.05 mW/m²	15.2 ± 0.6	(X. Wang et al., 2012)
Column-type	Saturated soil	Diesel	Graphite granule anode (GGA) biochar anode (BCA)	Stainless steel mesh + Pt/C catalyst	100	120	GGA → 3.4 ± 0.1 mW/m² BCA → 8.8 ± 0.3 mW/m²	82.1-89.7	(Lu et al., 2014)
Insertion-type	Saturated soil	Phenol	Carbon felt	Carbon cloth + Pt/C catalyst	100	10	29.45 mW/m²	90.1	(Huang et al., 2011)
Multi-anode	Saturated soil	PHs	Carbon mesh HA = horizontal anode VA = vertical anode	Stainless steel mesh + activated carbon catalyst	1000	135	HA → 0.282 ± 0.015 V VA → 0.285 ± 0.025 V	HA → 12.5 VA → 8.3	(Y. Zhang et al., 2015)
Horizontal multi-anode	Aged soil LS = low sand soil HS = high sand soil	PHs	Carbon mesh	Activated carbon	1000	135	LS → 870.4 ± 10.2 mW/ m² HS → 938.4 ± 44.2 mW/ m²	LS → 15 ± 0.1 HS → 22 ± 0.5	(X. Li et al., 2015)
Graphite rod	Saturated soil	PHs	Graphite rod	Activated carbon	100	144	17.3 mW/ m²	30 ± 0.1	(X. Li, Wang, Zhao, et al., 2016)

Design	Soil type	Pollutant	Anode material	Cathode material	External load (Ω)	Days	Maximum power density (mW/m²) / voltage (V)	Removal efficiency (%)	Reference
Column-type	Saturated/unsaturated sandy soil (SS and USS) Saturated/unsaturated clay soil (SC and USC)	diesel	Carbon felt	Carbon cloth + activated carbon catalyst	1000 before 100 after	248	SS → 120 mW/m²	SS → 48-59 CS → 42-45	(H. Wang et al., 2019)
Horizontal multi-anode	Saturated aged soil HG → high glucose LG → low glucose	PHs	Carbon mesh	Activated carbon	1000	135	HG → 43 mW/m² LG → 35 mW/m²	LG → 21%	(X. Li, Wang, Wan, et al., 2016)

Table 2.2: Summary of studies on soil MFC.

2.2.4. Nitrate removal by MFC systems

Bioelectrochemical methods, such as microbial fuel cells, are a promising prospect for nitrate (NO_3^-) contaminated water remediation, and they are known as denitrifying bioelectrochemical systems (D-BES) (Figure 2.5). In these systems, heterotrophic bacteria oxidize organic matter in the anode chamber to produce electrons that flow, from a conductive electrode to a cathode chamber, where denitrifying bacteria reduce NO_3^- to nitrous oxide (N_2O) and nitrogen gas (N_2):

$$NO_3^- + 5e^- + 5H^+ \rightarrow 0.5N_2 + 2H_2O + OH^-$$

Nitrate removal with MFC is mainly studied in wastewater treatment, but some laboratory-scale experiments were also carried out with groundwater, indeed there aren't studies on the treatment of nitrate-contaminated saturated soil. Afsham et al. (2015) investigated nitrate removal from a sediment microbial fuel cell (SMFC), where an insertion-type soil MFC have the cathode filled by groundwater (Figure 2.6). They studied the nitrate reduction by two SMFC for testing the anaerobic, trough N_2 insufflation, and aerobic conditions in the cathode compartment. While in the waterlogged anode chamber is present a graphite bars as anode. After ten days, nitrate-nitrogen was reduced with a removal rate of 12.4 $mgNO_3^-$-N/L/d (55 $mgNO_3^-$/L/d), and a removal efficiency of 63%, in the anaerobic conditions, compared with 8.5 $mgNO_3^-$-N/L/d (37.5 $mgNO_3^-$/L/d), the removal rate in aerobic conditions (Afsham et al., 2015).

Regarding groundwater microbial fuel cell, the nitrate reduction isn't always proved on groundwater extracted directly from the subsoil, but sometimes *synthetic groundwater* is reproduced in laboratory. It is design to resemble the natural groundwater chemical composition. Its use is cost-effective but is also safe, especially if there are hazardous contaminants to manage. Despite these advantages, the site-specific conditions, such as microorganisms and chemical species and physical-chemical conditions, are lost. According to C. Wang et al., the nitrate reduction is obtained in a synthetic groundwater after seven days of experiment with a reduction rate of 10.44 ± 0.22 $mgNO_3^-$-N/L/d and a removal efficiency more than 99% (Table 2.3) (C. Wang et al., 2021).

In the study mentioned before, both anode and cathode were inoculated with influent on a sewage treatment plant and after one-month synthetic wastewater was inserted in the anode for the experiments. This means that the high removal efficiency and rate aren't obtained with the same microorganisms present in the groundwater and the experiment doesn't last long thanks to the previous microorganisms' acclimatization in the new environment, before the effective experiment duration. Other studies have shown the nitrate removal from synthetic groundwater but using other inoculum, such as activated sludge, obtaining a removal efficiency of 77.6 ± 6.3 (Tabel 2.3) (Vidotto et al., 2020) and digestate sludge, with a reduction rate of 154.2 ± 24.4 $mgNO_3^-$-N/L/d (Table 2.3)(Tong & He, 2013). Otherwise, MFC

can be inoculated with effluents from other MFC reactors, as is described in the Pous et al. research, where was used the effluent of MFC to treat acetate (anode) and nitrite (cathode)-enriched wastewaters (Table 2.3) (Pous et al., 2013).

In all these studies the principal used co-substrate is acetate that fed the anode chamber mainly as sodium acetate (Table 2.3).

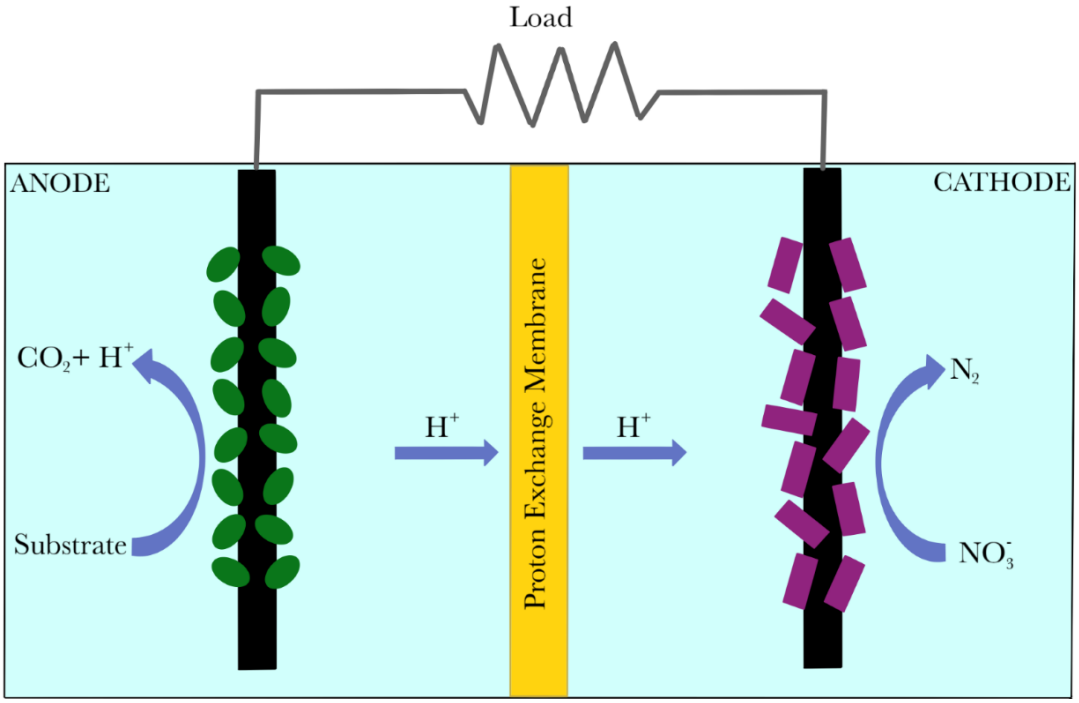

Figure 2.5: Nitrate reduction from water matrix scheme diagram.

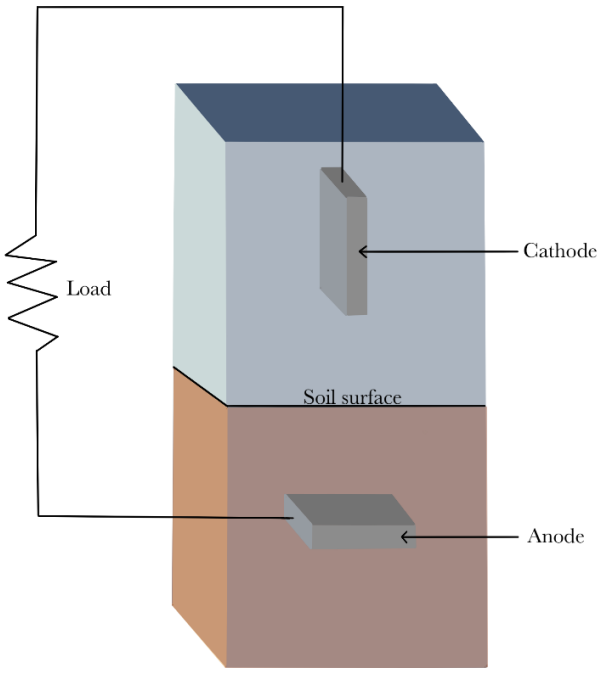

Figure 2.6: Sediment microbial fuel cell scheme about Afsham et al. study.

Groundwater type	Inoculum	Volume (mL)	Load (Ω)	Days	Co-substrate (mg/L)	Initial concentration ($mgNO_3^-$/L)	Removal efficiency (%)	Reduction rate ($mgNO_3^-$-N/L/d)	Reference
Synthetic	Activated sludge	200	100	20	0.5 $mgCH_3COONa$/L (0.39 mgCOD/L)	26.3 ± 0.3	77.6 ± 6.3	0.9	(Vidotto et al., 2020)
Natural	Effluent wastewater MFC	600	25	97	Acetate (283 ± 75 mCOD/L)	125.42 ± 27.24	64	12.14 ± 3.59	(Pous et al., 2013)
Synthetic	Sewage	234	1000	7	1 gCH_3COONa/L (0.78 gCOD/L)	221.43 ($NaNO_3$)	> 99	10.44 ± 0.22	(C. Wang et al., 2021)
Not specified	Other MFCs	50	1000	5	Sodium acetate	3011 (KNO_3)	96	130	(Vijay et al., 2020)
Synthetic	Digested sludge	160	10	14	0.5 $mgCH_3COONa$/L (0.39 mgCOD/L)	($NaNO_3$)	Not specified	154.2 ± 24.4	(Tong & He, 2013)
Natural (SMFC)	-	1000	500	10	-	Not specified	63	12.4	(Afsham et al., 2015)

Table 2.3: Literature mentioned for nitrate reduction from groundwater and soil.

2.3. Microbial Electrochemical Snorkel (MES) for hydrocarbons and nitrate removal from soil and sediment

Microbial electrochemical snorkel (MES) is a short-circuited microbial fuel cell that has aim to maximize the organic substrates oxidation. In this technology anode and cathode are made of a single piece of conductive material that crosses zones with different chemical compositions, such as an anaerobic zone and the upper part exposed to aerobic water. From this example take place the "snorkel" name, because microorganisms in the anaerobic part can "respire" thanks to the snorkel that link the anaerobic condition with the oxygen contained in the aerobic upper layer.
MES is a recent developed technology studied in laboratory scale, with its first application in 2011 for maximizing the chemical oxygen demand removal from wastewater (Table 2.5). In this research was demonstrated the major COD removal efficiency (57%) by MES compared to an MFC (Erable et al., 2011). Over the years, the research on MES application focused on petroleum hydrocarbons removal from marine sediments but there are also studies on hydrocarbons contaminated soil and denitrification from sediment.

It's important to underline that sediment and soil are two different matrices with different bio-chemical characteristics. In anaerobic sediment conditions, the main terminal electron acceptor is sulphate (SO_4^{2-}), because oxygen (O_2) and nitrate (NO_3) are not available in the deep marine system due to the mass transport of solutes governed by slow molecular diffusion (Marzocchi et al., 2020). Besides, in sediment SO_4^{2-} can be regenerated via the re-oxidation of sulphide (H_2S), in the oxic-anaerobic interface, where insoluble iron (Fe) and manganese (Mn) oxides are the electron acceptors. It's possible that during the PHs oxidation, the sulphate demand from the PHs degrading microorganisms is higher than the sulphate supply derived from the H_2S oxidation (Marzocchi et al., 2020). Then, petroleum hydrocarbons can persist in the sediment, but with the conductive electrode there's a no-exhaustible electron acceptor that enhance the sulphate availability.

Cable bacteria are microorganisms present in the sediment that have the same snorkel role: thanks to their centimetre-long filaments can reach O_2 after the sulphide oxidation in the sediment to regenerate sulphate (Matturro et al., 2017).

2.3.1. Construction materials

The *electrode*, as in other bioelectrochemical systems, is the core of the reactor which allows the electron passage, produced from substrates oxidation, from the anode to the cathode, where electron acceptors are present. It can be made of iron that is used, for example, to remediate nitrate contaminated water present above the sediment (Yang et

al., 2015). In this research 2 mg/mL $NaNO_3$ was added in the system to simulate the water nitrate contamination (Table 2.5). The initial concentration in the system is higher than 2 mg/L thanks to the NO_3^- diffused from the sediment. The reactor with only iron rode (Fe-MES) showed in the experiments firsts days a slightly decreasing of nitrate concentration (from 2.09 mg/L to 2.03 mg/L) due to the low amount of denitrifying bacteria. While, the removal efficiency reaches 98% in 16 days, with a nitrate concentration of 0.04 mg/L. The reactor with iron rod and a carbon felt (Figure 2.7) on the anode zone didn't show any significant nitrate reduction.

The carbon-based materials are the preferable for MES, thanks the previous studies on the materials performance for other BESs that demonstrate good removal efficiency due to the relevant carbon-based electrodes electrical conductivity, chemical stability, large surface area, biocompatibility and economical access. Indeed, carbon fiber brush is used for soil remediation (Figure 2.7) and the most electrode material tested in the MES systems for contaminated oil marine sediment is graphite. In this case, the MES is also named "Oil spill Snorkel" used for the first time in Italy (2015) thank to Viggi et al. that monitored for 417 days the petroleum hydrocarbons biodegradation in two microcosms with one and three graphite rods respectively (Viggi et al., 2015). They found a significant reduction of TPH in both snorkel with one and three snorkel (12 ± 1% and 21 ± 1%) after 200 days, but with prolonged experiment time, in all the treatments, also in the control systems, the removal efficiency exceeding 80% (Table 2.5).

Other studies on sediment matrix have focused on petroleum hydrocarbons removal using graphite electrode, but also, they investigated on the impact of cable bacteria and snorkel on the bioremediation. For example, Marzocchi et al. prepared four microcosms: 1) control; 2) snorkel; 3) cable bacteria; 4) snorkel and cable bacteria (Marzocchi et al., 2020). The major alkane degradation occurs in the firth system, confirming the snorkel role as electron acceptor and the cable bacteria support for PHs oxidation by reducing the accumulation of a toxic product (H_2S) (Table 2.5).

Otherwise, was studied the alkane biodegradation of two crude oils at increased or ambient hydrostatic pressure (HP) using two graphite rods (Figure 2.7). Snorkels enhanced alkanes biodegradation at both 10 and 0.1 MPa within only seven weeks (Table 2.5) (Aulenta et al., 2021).

Catalyst, such as in microbial fuel cell, is an option to enhance the organic substrates biodegradation. Activated carbon is widely used in oil contaminated sediments treatments, such as the oil-contaminated River Tyne sediments, in the UK (Viggi et al., 2017). It was demonstrated that the organic contaminants oxidation with the MES use, accelerate the sulphate reduction processes (Table 2.5).

In none of microbial electrochemical snorkel research were planned the *membrane* use application between anode and cathode, which are defined by oxygen concentration

gradient with depth. Besides, is not studied any *co-substrate* insertion for removal PHs or nitrate from sediment and soil.

2.3.2. Reactor design and geometry

The most common reactor design consists of one or more electrode rods or wire that connect the anaerobic compartment with the upper water zone (Figure 2.7).
Rogińska et al. have studied how the configuration and the material condition the mixed potential of MES systems. Every experiment is conducted in cylindrical reactor with 5 cm of sediment and 25 cm of water. The study carried on three different experiments:

- Preliminary experiments: four iron wires and four stainless steel wires were inserted in two reactors, one for stainless steel anode for iron, with different electrode parts exposed to water and sediment (water-sediment ratio 0:1, 1:1, 5:1 and 1:0) (Figure 2.8);
- First experiment: stainless steel grid as electrodes both in water and sediment to evaluate the MES with different anode and cathode ratios. In one reactor the anode and cathode grids had the same sizes (8 x 4 cm) and in another reactor two anode grids (8 x 4 cm) were four times bigger than the cathode grid (4 x 4 cm) (Figure 2.8);
- Second experiment: one graphite felt electrode in sediment (8 x 4 cm) was connected with another graphite felt electrode (3.5 x 1 cm) thanks the stainless steel wire; graphite felt electrode (8 x 4 cm) connected with only the stainless steel wire (Figure 2.8). This experiment was useful to know the electrode material importance on microbial electrochemical snorkel performance (Rogińska et al., 2021).

For each experiment were measured the potentials versus the Standard Hydrogen Electrode (SHE), the electrode reference which potential is defined as zero volts at all temperatures. The potentials suitable to nitrate reduction range from -300 to -100 mV vs. SHE. The preliminary experiments results are shown in Table 2.4. They demonstrate that stainless steel and iron had different behaviours, because iron wires reached very negative potential, making the material unsuitable due to corrosion, while stainless steel wire only in water had the greatest potential versus the stainless steel wire only in sediment. Indeed, with the same or different portions of the wires in water and sediment, the potential did not change.

Material	*Water:sediment ratio*	*Potential (mV) vs. SHE*
Stainless steel	1:0	Between +450 and + 650
Stainless steel	0:1	-250
Stainless steel	1:1	Between -140 and -150
Stainless steel	1:5	Between -140 and -150
Iron	1:0	Below -400
Iron	0:1	Below -400
Iron	1:1	Below -400
Iron	1:5	Below -400

Table 2.4: Metallic wires redox potentials given from sediment and water different ratios.

About the second experiment, a more negative potential (-160 mV vs. SHE) was reached when anode electrode surface was higher than the cathode surface. This confirm the possibility to use stainless steel meshes as electrodes for MES system, considering that major is the electrode surface, major is the electrochemical denitrification efficiency. While the graphite felt electrode only in the cathode zone made possible a more negative potential (-240 mV vs. SHE). Regarding the presence of the graphite felt electrode in the anode part, was obtained high potential values after two months (+400 mV vs. SHE).

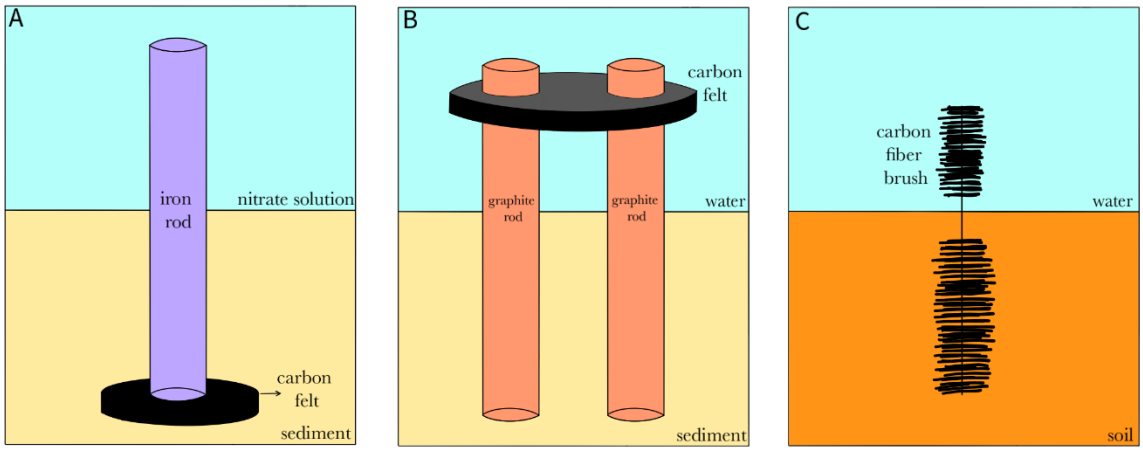

Figure 2.7: Design scheme examples of microbial electrochemical snorkel: A) single iron rod with carbon felt in the anode zone (Yang et al., 2015); B) two graphite rods with carbon felt in the cathode compartment (Aulenta et al., 2021); C) single carbon fiber brush as snorkel (Viggi et al., 2022).

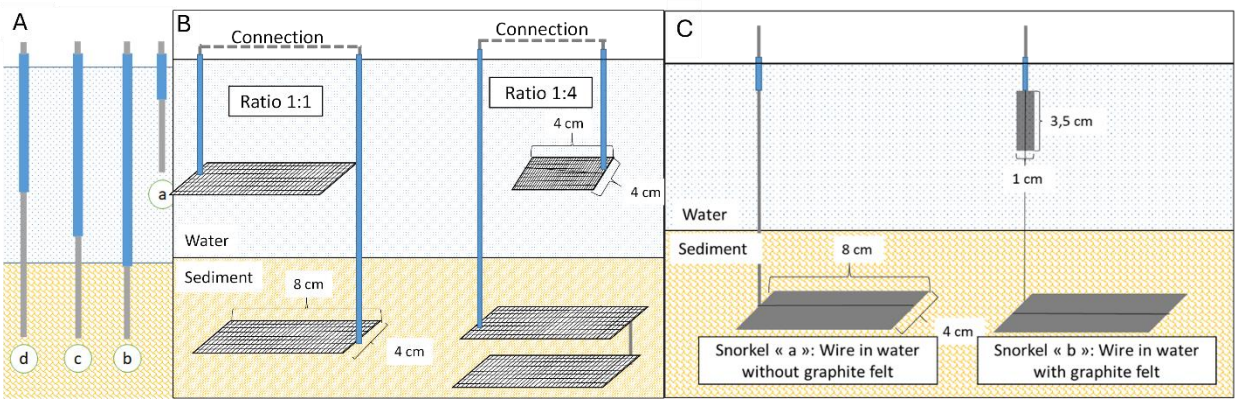

Figure 2.8: Experimental design and geometry schemes: A) stainless steel wires with different portions inserted in water and sediment; B) stainless steel meshes as anode and cathode with same and different sizes; C) Graphite felt electrodes as anode and stainless steel wire «a» and graphite felt «b» as anode. Figure adapted from (Rogińska et al., 2021).

2.3.3. Soil characteristics relevance to MES

The ions mobility into the soil and sediment matrices, so the electrical conductivity (EC), allow electrons to flow from the oxidative organic matter to the anode and from the cathode to the soluble electron acceptors (O_2, NO_3^- and SO_4^{2-}). Regarding the microbial electrochemical snorkel, are verified the observations made about soil characteristics relevance to MFC in some MES research.

For example, Viggi et al. have exploited pine wood biochar to increase the snorkel radius of influence, for PHs removal, because of the conductive network construction with microbes (Figure 2.9) (Viggi et al., 2022). In this study were set up four reactors: 1) snorkel; 2) open circuit control; 3) snorkel with biochar; 4) open circuit control with biochar. In every reactor was reached, at the end of the 450 days, a removal efficiency of 82-85% (Table 2.5). Hence, neither the snorkel nor the biochar have had an impact on petroleum hydrocarbons removal.

Differently, the Oil-Spill Snorkel made by Viggi et al. have taken advantage of the sand addition in the sediment, because elevated particle size sediment shows major biodegradation performance (Table 2.5) (Viggi et al., 2015).

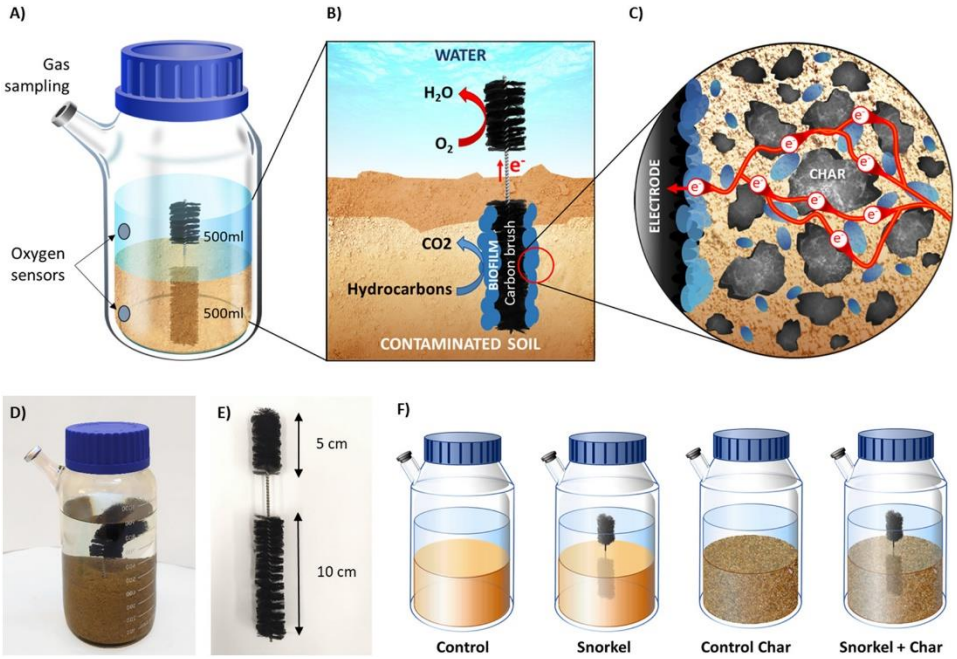

Figure 2.9: Biochar influence on electron transfer process in soil. Taken from (Viggi et al., 2022).

Matrix	Design	Pollutant	Snorkel material	Days	Initial concentration	Removal efficiency (%)	Reference
Sediment	1 rod + graphite felt anode and platinum cathode	Nitrate	Iron	16	2.09 mgNO_3^-/L	98	(Yang et al., 2015)
Sediment	1 and 3 rods	PHs	Graphite + granular activated carbon S^3 → 3 rods S → 1 rod	417	S^3 → 11.9 ± 0.12 mg/g_dry S → 11.8 ± 1.01 mg/g_dry	S^3 → 21 ± 1 S → 12 ± 1 (day 200)	(Viggi et al., 2015)
Sediment	1 rod + carbon felt cathode	PHs	Graphite + top carbon felt	49	Not specified	Alkanes: Snorkel → 24 Cable bacteria → 25 Snorkel + cable bacteria → 54%	(Marzocchi et al., 2020)
Sediment	2 rods + carbon felt disk cathode	Alkanes	Graphite	49	Not specified	Not specified	(Aulenta et al., 2021)
Sediment	3 rods	PHs	Graphite rod + granular activated carbon	466	12 mg/g	Day 175 → 15 Dat 286 → 32	(Viggi et al., 2017)
Soil	1 brush	PHs	Carbon fiber brush + biochar	450	212 ± 10 mg/kg	82-85	(Viggi et al., 2022)

Table 2.5: Microbial electrochemical snorkel studies on nitrate and petroleum hydrocarbons removal from sediment and soil.

3 Aims of the thesis work

The bioelectrochemical systems have attracted significant attention from the scientific community for potential in-situ remediation. Starting with the Microbial Fuel Cell, which enable the production of electricity energy through the biodegradation and biotransformation of organic and inorganic substances, respectively. Such as in other bioremediation methods, described in Chapter 1, the core of this technology is the provision of electron acceptor and/or electron donor that that supports contaminated soil bioremediation processes. So, the MFC technology resolves the lack of the acceptor/donor electrons thanks to the electrode presence, that is an inexhaustible electrons acceptor/donor. Microbial Electrochemical Snorkel (MES) system was employed to simply the system used by the MFC and make the technology more economically accessible for the full-scale application. In this context, scientific research is focusing on carbon-based electrode and natural membrane materials, also to make the technology as eco-friendly as possible.

How is shown in Chapter 2, microbial fuel cell research applied to soil treatment deals separately with the contaminated saturated soil by hydrocarbons and the groundwater contaminated by nitrates. While the Snorkel technology literature is focused especially on marine sediment. This thesis project aims to install and monitor the same configuration both as a microbial fuel cell and as a snorkel, to treat saturated soil contaminated by hydrocarbons in the anodic chamber and saturated soil contaminated by nitrates in the cathodic one. This was done for fed-continuous mode, while in batch mode, the snorkel and the bioelectrochemical system with applied voltage were set up. Both continuous and batch reactors were compared to open circuit reactor. The behaviour of the systems subjects to these technologies has been evaluated thought electrical and chemical parameters monitoring and analysis.

4 Materials and methods

4.1. Soil characterization

Three different soils from sites in northern Italy were used during the laboratory experiment:

- gasoline contaminated soil (GCS);
- not-contaminated soil for the batch tests (NCS-B);
- ot-contaminated soil for the continuous flow experiment (NCS-C).

Soils were kept in containers in a cool and shaded location up to their use. These samples were placed in aluminum containers and then under laboratory hoods to air dry. The soils were mixed several times to expedite the drying process, ensuring that even the most humid areas were exposed to the air, and then sieved to ensure more homogenous conditions for the tests and to carry out soil characterization. As described by (Carter & Gregorich, 2007), soil characterization was performed on the soil fraction < 2 mm, whereas for the set-up of the reactors the following fractions were considered:

- <6 mm for the NSC-B;
- <4 mm for the GCS inserted in the batch reactors;
- <2 mm for the GCS and NCS-C for the continuous flow systems.

Soils were characterized through chemical and physical analysis. Chemical analyses included:

- pH;
- organic carbon;

- carbonate content;
- nitrate and ammonium;
- electrical conductivity.

The soil physical analysis included:

- particle size distribution;
- water content;
- field capacity.

4.1.1. pH

The pH is the solution acidity or alkaline indication and it's obtained from the following formula:

$$pH = -\log[H^+]$$

where $[H^+]$ is the hydrogen ion concentration.
If the pH is 7 the solution is neutral, otherwise it's acid (pH<7) or alkaline (or basic), for pH >7. Soil pH influences lots of biochemical and physical properties of the soil. For example, the dissolved organic carbon (organic carbon passing through a filter with a 0.45 μm diameter), increases with pH; or microbial activity is typically favoured in the 5.5 - 8.8 pH range. The soil pH is also influenced by base cations associated with bicarbonates and carbonates in water. Figure 4.1 indicates typical pH values for different soils.
Soil pH was measured in 0.01 M $CaCl_2$ solution, applying a 1:10 soil-to-solution ratio, using 2 g of soil and 20 mL of salt solution. The soil slurry is shaken for 30 minutes and let stand for one hour. The pH is detected through a pH probe.

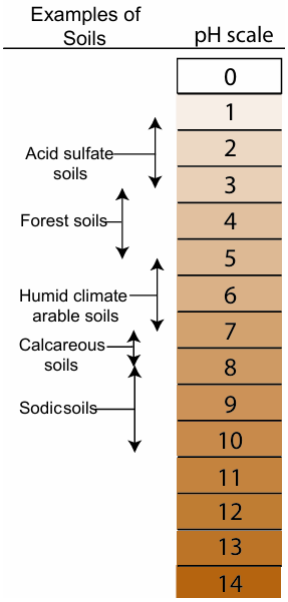

Figure 4.1: Examples of pH values for different soils. Taken from (Mccauley, 2009).

4.1.2. Organic carbon content

Soil organic matter (SOM) is commonly defined as the organic fraction of the soil exclusive of undecayed plant and animal residues, their partially decomposed products, and the living soil biomass (Carter & Gregorich, 2007). So, it includes the non-living portion of the organic fraction present in the solid phase of the soil.
SOM was estimated as loss-on-ignition (LOI) by burning about 5 g of soil (dried at 105°C to constant weight for 24 hours) in a muffle furnace at 550°C for 30 minutes to allow complete organic carbon oxidation and volatilization to CO_2.

4.1.3. Carbonates

Carbonates are natural soil constituents, such as calcite ($CaCO_3$) or dolomite. Carbonate influences the pH, the amount of exchangeable cations, the redox potential, the easily soluble salt presence, and the CO_2 partial pressure in the soil air (Tatzber et al., 2007).
An approximate gravimetric method is used to estimate the carbonate content in a soil sample, thanks to the CO_2 produced during the reaction of carbonate and acid. An air-dried soil sample (< 2 mm) is inserted into 10 mL of HCl-$FeCl_2$ reagent solution, to have a 1:5 soil-to-solution ratio. The reaction takes place with the carbonate decomposition into CO_2. From the difference between the initial weight of the sample and the final weight, after the reaction is complete, which usually takes about two hours, the amount of CO_2 produced is obtained. The percentage of equivalent $CaCO_3$ is computed as:

$$CaCO_3eq\ (\%) = \frac{g\_CO_2\ lost}{g\_soil} \cdot 227.3$$

The equation is referred to only calcite because, in general, this method allows measuring the calcium carbonate content. However, dolomite is present when the weight still decreases significantly after 30 minutes, due to lower dolomite reactivity to the HCl (Carter & Gregorich, 2007).

4.1.4. Nitrate and ammonium

Ammonium (NH_4^+) is present in soil as an exchangeable cation, but the fixed and non-exchangeable forms contribute to the total nitrogen content in the soil. Nitrate (NO_3^-) instead is soluble in water. A 2.0 M KCl solution allows extracting the exchangeable NH_4^+, as it can be replaced by K^+ of the salt solution, and NO_3^- present in the soil. Nitrite (NO_2^-) is usually present in negligible amounts.
After mixing air-dried soil and the extractive solution, in a 1:10 ratio, into a flask, the slurry is shaken for 30 minutes. The solution is filtered through a Whatman No. 42 filter paper and nitrate and ammonium concentrations are determined. The measures are then referred to the dry soil.

4.1.5. Electrical conductivity

Electrical conductivity (EC) is an index of the soil salinity and indicates the abundance and mobility of ions in the matrix. It's affected by the cation presence such as Na^+, Ca^+, and Mg^+, and by the anions SO_4^{2-} and Cl^-. Less important, due to the minor amount in the soil, are potassium, bicarbonate, carbonate, and nitrate. A saline soil has an electrical conductivity greater than 4 dS/m at 25°C (Carter & Gregorich, 2007).
EC in soil is measured by creating a soil slurry with 0.01 M KCl and air-dried soil, 1:5 solid-to-liquid ratio. The sample is shaken for 30 minutes, let stand for 30 minutes, and then measured thanks to an EC probe.

4.1.6. Particle size distribution

The particle size distribution analysis allows for determining the texture of soil used in the experiment. According to the Italian Geotechnical Association (AGI) system the particle size can be defined in five classes (Table 4.1).

Particle size	*Diameter range*
Clay	< 2 μm
Silt	2 – 60 μm
Sand	60 – 2000 μm
Gravel	2 – 20 mm
Cobbles	> 20 mm

Table 4.1: Soil classification according to the Italian Geotechnical Association.

The particle size distribution curve is obtained by soil sieving where the percentage by weight of particles that have been retained or passed through sieves of certain sizes is determined.
Soil texture is attributed based on weight ratios of particle size fractions, according to, for instance, the Italian Geotechnical Association classification system.

4.1.7. Water content

Water in soil takes part in the hydrologic cycle, with continuous exchange with atmosphere, thanks to the evapotranspiration, and groundwater, due to the percolation. Moreover, soil is the water reservoir for the vegetation. Soil water content can change due to the precipitation. From a chemical perspective, water acts as the medium for transporting dissolved substances and suspended biological particles that contribute to soil formation and degradation.
The thermogravimetric method is used to determine the soil water content. The sample is first weighed and then placed in an oven at 105°C for 24h. The sample is reweighed, and the difference between the initial and final weights corresponds to the water evaporated during the process, and thus to the water content in the soil, typically referred to the weight of the dry soil.

4.1.8. Field capacity

The field capacity is the water retained in soil against gravity and corresponds to the water available for plants. To estimate soil field capacity, a wet soil sample (added with a known amount of water) is placed above a filter paper (12-25 μm pore diameter) and let draining for 24 hours to allow complete water drainage. The residual moisture in the soil at the end of drainage, normalized to dry soil, is the soil field capacity.

4.2. Materials and reactors design

4.2.1. Continuously fed systems

Transparent plastic tubes (3.5 cm in diameter, 20 cm in length) were used for the microcosms setup. The lower half portion of the tube was filled with saturated gasoline-contaminated soil, GCS, whereas saturated NCS-C was added in the upper part. A layer of saturated kaolin, a clay type, was used as a natural membrane for the protons flowing from the reducing to the oxidizing compartment. Before its use, kaolin was mixed with water in a solid-to-water ratio of 1:1.2. Water added to the systems was purged with nitrogen to ensure anaerobic conditions. Both anode and cathode electrodes were made of two circular graphite felts, 3.5 cm diameter and 0.5 cm thick. A steel mesh was inserted between the two felts and joined with plastic wire. Whatman filter papers (pores diameter of 0.45 μm) were placed between each soil type and kaolin. The electrodes were horizontally inserted at the top and bottom of the tubes, with one side in direct contact with the soil. The other electrode's side was buried in granular graphite to increase the electron transfer rate and radius of influence. The granular graphite at the anode was preliminary treated to enhance biofilm development. Microorganisms were subjected to acclimation through a slurry-type process, in which a semi-liquid mixture of contaminated soil and water (1:10 w/v) was kept in agitation to prepare microorganisms to better degrade the contaminants. This solution was introduced through a recirculation system into a reactor, the same used for continuously-fed systems, filled with granular graphite. The acclimation lasted for 21 days in a dark room, maintaining a temperature of 18°C. Three different systems, each one in duplicate, were set up:

- Microbial Fuel Cell (MFC);
- Snorkel (S);
- Open Circuit Control (OC).

Water and soil quantities in the systems are shown in Table 4.2.

The MFC and snorkel electrodes were connected to titanium wires (1 mm x 8 cm, diam. x length, 99,6% purity) with one end coming out of the reactor. The portion of wire lying inside the reactor was isolated with heat-shrinking sheaths (diameters ranging between 0.5 mm to 1.5 mm). Electrodes in the snorkel reactors were short-circuited; a 50 Ω external load (R_1) was attached to each MFC. The anode and cathode compartments were named "_A" and "_C", respectively. The reactors were incubated

in a dark and temperature-controlled room at 18°C. In Figure 4.2 materials and design reactors are reported.

Each reactor worked in continuous flow mode, with water recirculation in each chamber, thanks to peristaltic pumps, to keep water flowing in the soil and avoid dead-end zones (Figure 4.3). Table 4.3 summarizes the volumes of the recirculation piping.

System	*Water (mL)*	*GCS (g)*	*NCS-C (g)*
OC	81.50 ± 13.09	96.40 ± 13.09	73.33 ± 14.69
S	79.50 ± 4.19	99.18 ± 4.19	112.03 ± 39.64
MFC	95.00 ± 7.02	89.68 ± 7.02	85.54 ± 2.58

Table 4.2: Water and soil quantities inserted in each type of reactor in continuous fed mode.

System	*Tube volume (mL)*
OC1_A	55
OC1_C	55
OC2_A	55.5
OC2_C	59
S1_A	62
S1_C	68
S2_A	71
S2_C	74
MFC1_A	63
MFC1_C	65
MFC2_A	62
MFC2_C	57

Table 4.3: Recirculating piping volumes for each compartment in each system.

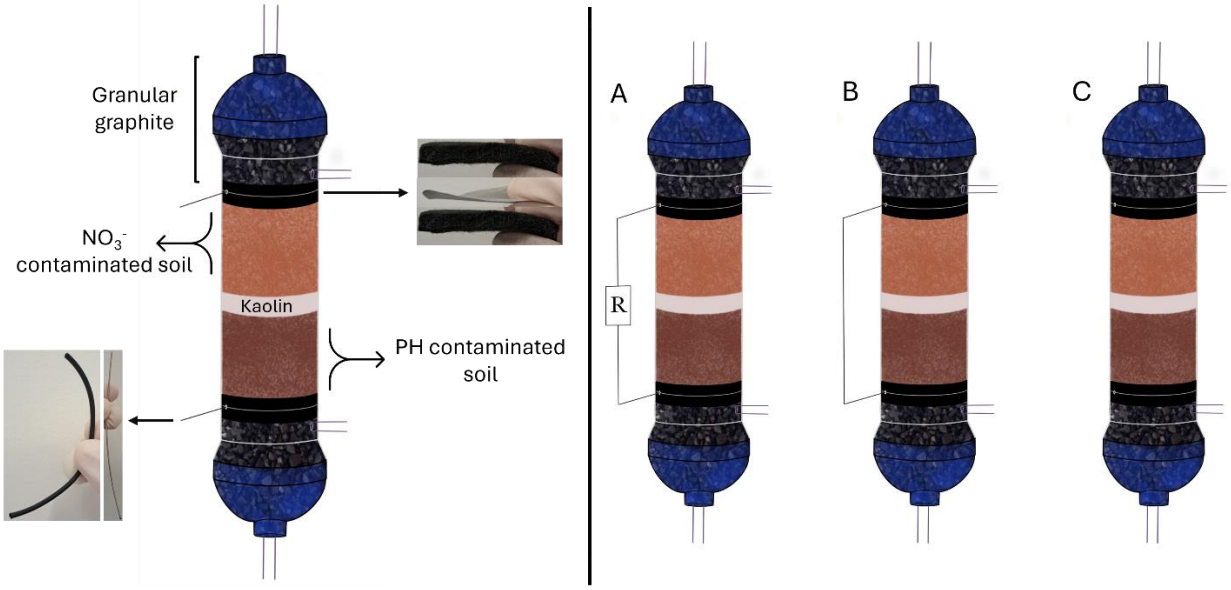

Figure 4.2: On the left: configuration and materials of reactors in continuous fed mode; on the right the systems: A) Microbial Fuel Cell; B) Snorkel; C) Open Circuit Control.

4.2.2. Batch systems

The same contaminated soil (GCS), or better its fraction with particle size < 4 mm, was used for the batch system reactors; the non-contaminated soil NCT-B, instead, is different from the one in the continuous systems; it is the fraction < 6 mm collected from up to 1.5 m below ground surface at a site in the Milan metropolitan area.

The batch reactors were prepared in glass jars (20 cm length x 11.5 cm diameter). The configurations, shown in Figure 4.3, were the same as the continuous reactors, with larger electrodes and titanium wires to adapt to the jar size (electrodes 9 cm in diameter and 0.5 cm of thickness; anodic Ti wires 1 mm diameter x 30 cm long; cathode Ti wires 1 mm in diameter x 15 cm long). The anode and cathode compartments were named respectively "_A" and "_C". The setup was the same as the continuous systems, except in batches no granular graphite was used, and it was substituted with saturated clean sand in the cathodic compartment in the upper part of the jars (Figure 4.3). A few centimetres of free water (1 – 3 cm) above the sand assured soil complete saturation. Three treatments, with two replicates, were prepared:

- BioElectrochemical treatment with 500 mV externally applied voltage (BET);
- Snorkel (S);
- Open Circuit Control (OC).

The water, soil, and sand amounts added to each reactor are presented in Table 4.4. The titanium wires extended from the jar lid, insulated with adhesive tape, to allow the cathode and anode of the BET systems to connect to an external power supply and a 10 Ω external load (R_2). The wires of the snorkel reactors were directly connected to create a short circuit. The systems were placed under the hood at room temperature (22 - 27 °C).

System	*Water (mL)*	*GCS (g)*	*NCS-B (g)*	*Sand (g)*
OC	458.33 ± 10.41	756.37 ± 107.46	576.54 ± 99.97	255.87 ± 32.18
S	326.67 ± 37.54	705.50 ± 3.30	552.16 ± 2.91	304.14 ± 0.36
BET	353.33 ± 75.06	742.98 ± 151.21	549.77 ± 84.32	243.26 ± 130.69

Table 4.4: Water and soil quantities inserted in each type of reactor in batch mode.

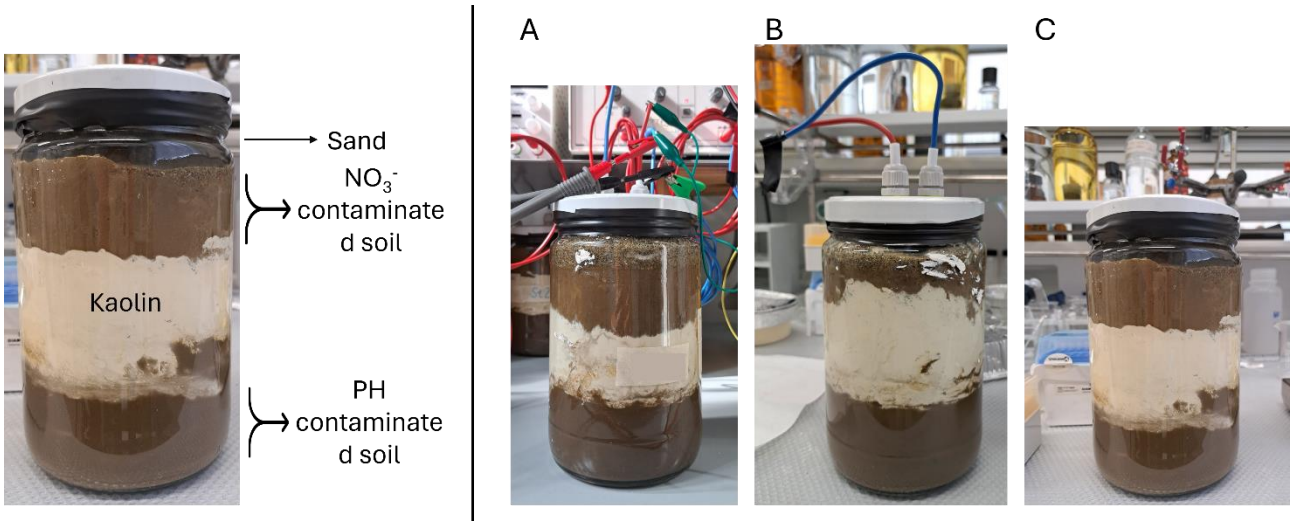

Figure 4.3: On the left: materials and configuration reactor of batch systems. The electrodes aren't visible because they have a diameter lower than the jar; on the right the systems: A) Bioelectrochemical Treatment with applied voltage; B) Snorkel; C) Open Circuit Control.

4.3. Conducing and monitoring experiments

4.3.1. Continuously fed systems

Operation

The microbial fuel cell, snorkel, and open control circuit reactors were nominated as MFC1, MFC2, S1, S2, OC1, and OC2. Knowing the total volume of the recirculation zone, considering the volume of the recirculating tubes, and assuming a porosity of 40% for the area occupied by granular graphite, the concentrations of sodium acetate

to be included in a volume of 5 ml have been determined, to obtain a final concentration of 0.5 gCH_3COONa/L (in term of COD is 0.39 gO_2/L) (Table 4.5). While potassium nitrate (KNO_3) solution was added in the cathode compartments in a volume of 5 mL to obtain a final nitrate concentration of 100 mgNO_3^-/L (Table 4.5). The experiment lasted 80 days, with the solutions injection once a week for 5 weeks (on days 20, 33, 39, 47, and 55).

System	*Volume recirculation zone (mL)*	*CH_3COONa concentration (g/L)*	*KNO_3 concentration (g/L)*
OC1_A	80	8	-
OC1_C	80	-	2.75
OC2_A	81	8	-
OC2_C	84	-	2.75
S1_A	87	8.75	-
S1_C	93	-	3.05
S2_A	96	9.5	-
S2_C	99	-	3.05
MFC1_A	88	8.75	-
MFC1_C	90	-	3.05
MFC2_A	87	8.75	-
MFC2_C	82	-	2.75

Table 4.5: Sodium acetate and potassium nitrate concentrations of solution added in anode and cathode recirculation zone respectively.

Continuous monitoring: electrochemical and chemical analyses

The voltage (V) across the 50 Ω external load (R_1) was recorded every 15 minutes by a data acquisition system (PicoLog data logging Technology) connected to a computer (Figure 4.4).

The recirculation water in the anode and cathode compartments allowed us to monitor pH, electrical conductivity (EC, µS/cm), and oxidation-reduction potential (ORP, mV) through pH, EC, and ORP probes. They were connected to transducers and an Arduino-based data logger, recording data every minute (Figure 4.4).

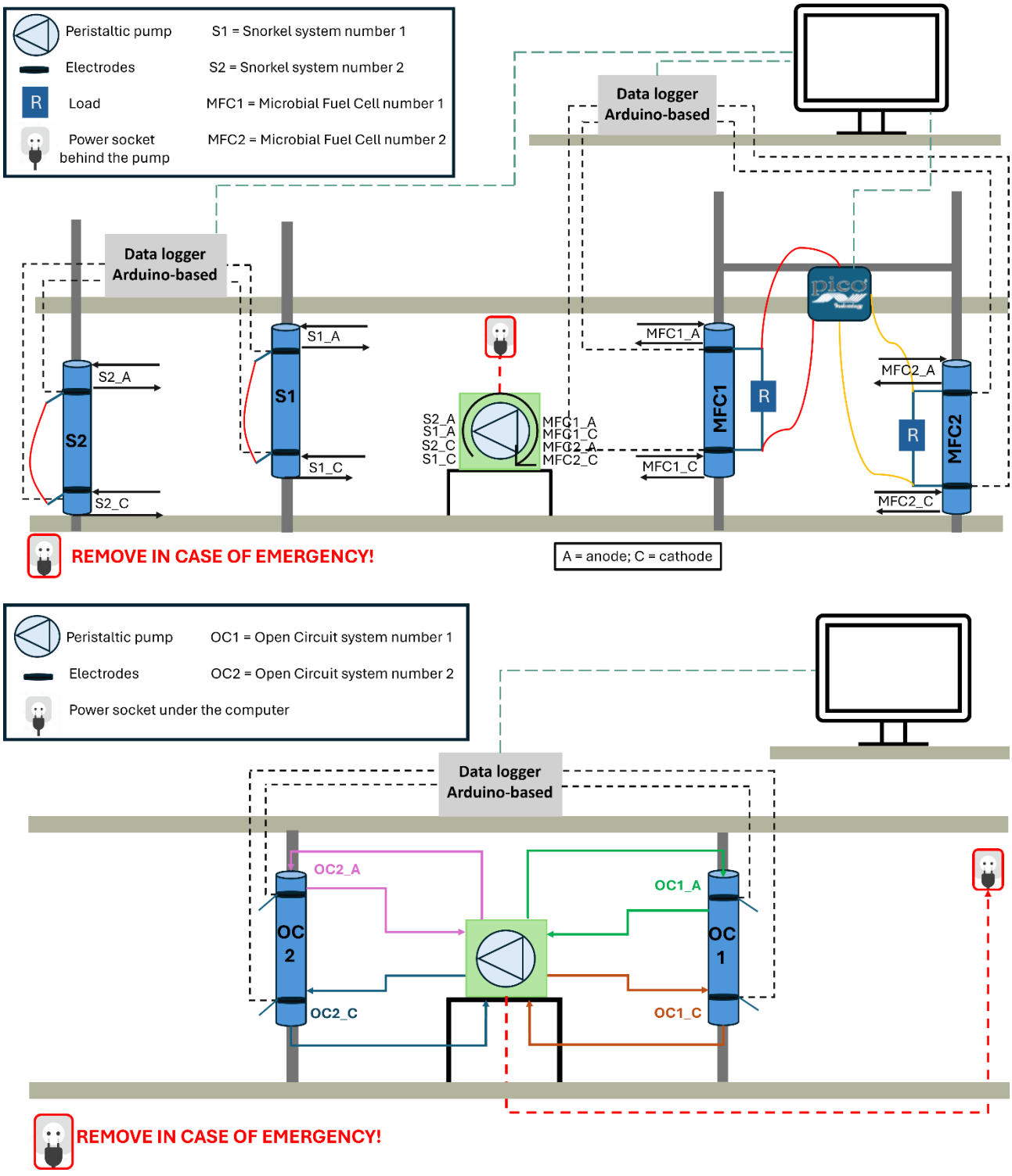

Figure 4.4: Set up of the entire continuous bioelectrochemical systems.

Spot monitoring: chemical analyses

Chemical Oxygen Demand (COD, mgO_2/L) and nitric nitrogen ($mgNO_3^-$-N/L) concentrations from the anode and cathode zones were periodically analysed in water samples from the recirculating piping using Hach Lange Cuvettes. Sampling and

analysis took place once or twice a week for 13 weeks. In the weeks when acetate and nitrate injections were scheduled, monitoring was performed before and after the injection. The analyses were performed on days 5, 19, 20, 33, 38, 39, 46, 47, 53, 55, 60, 66, 73, 80. On days 19 and 66, ammonium nitrogen (mgNH_4^+-N/L) and total nitrogen (mgN/L) were determined. Water samples were also tested for pH and electrical conductivity (µS/cm).
After 80 days of monitoring, the number 2 systems were dismantled, and soil samples were collected to determine pH, EC, organic matter, and total petroleum hydrocarbon (TPH) concentration. While pH, EC and dissolved oxygen (DO) were monitored from the water samples containing in the recirculating pipes.

Calculations

In the MFC systems, the *current* (I, mA) through Ohm's law and the *power* output (p_1, mW) with time were monitored:

$$I = \frac{V}{R}; \qquad p = I \cdot V \rightarrow p = \frac{V^2}{R}$$

V (mV) is the *voltage* measured and recorded with the PicoLog Technology.

The power is normalized to the reactor characteristics to make systems operating under different conditions and configurations comparable and obtain the *power density* (P, mW/m^2). Normalization can be performed with the projected anode surface area (Park & Zeikus, 2003) or also considering the cathode as a reference (Huang et al., 2011). In this case, the normalizing was carried out with the *projected anode surface area* (A = 30.24 cm^2). The power density is obtained from the following formula:

$$P = \frac{V^2}{A \cdot R}$$

It was possible to determine the *Coulombic Efficiency* (CE, %) which is defined as "*the ratio of total electrons (in Coulombs) transferred to the anode from the substrate oxidation to the maximum electrons (Coulombs) if the entire substrate oxidation produced current*" (Logan et al., 2006).

$$CE = \frac{PM_a \cdot \int_0^{t_c} I\, dt}{F \cdot b_a \cdot V_{an} \cdot \Delta COD}$$

The electrons derived from the acetate oxidation and used for the current production are obtained by the product between the CH_3COO^- molecular weight (PM_a, g/mol) and the integration over time of the current (I) produced during a complete substrate oxidation cycle t_c (s). The maximum number of electrons that could be generated by

acetate oxidation is calculated as the product of the Faraday constant (F, 96485 C/mol); the conversion factor (b_a) i.e. the number of electrons exchanged per mole of acetate in its oxidation; the anode chamber volume (V_{an}, L); the COD variation in the time cycle t_c (ΔCOD, g/L). The conversion factor (b_a = 8) was obtained by the conversion reaction from bicarbonate to acetate (Logan et al., 2006):

$$2HCO_3^- + 9H^+ + \mathbf{8}\boldsymbol{e}^- \rightarrow CH_3COO^- + 4H_2O$$

The *removal efficiency*, obtained for COD (r_{COD}, %) and nitrate ($r_{nitrate}$, %) concentrations, was calculated as:

$$r = \frac{x_i - x_f}{x_i} \cdot 100$$

where x_i and x_f are the initial and final concentrations respectively.

4.3.2. Batch systems

Operation

The experiment with batch reactors was set up during the continuous reactors experiment and it lasted 21 days. The reactors named are: OCt1, OCt2, OCt3, BESt1, BESt2, BESt3, St1, St2, and St3, where the "t" specifies the time at which each system was dismantled to collect samples:

- t1 → day 7;
- t2 → day 14;
- t3 → day 21;

Continuous monitoring: electrochemical analyses

In the BET systems, the electric voltage was applied by power supplies in direct current, while the produced voltages were measured by multimeters (Figure 4.5).

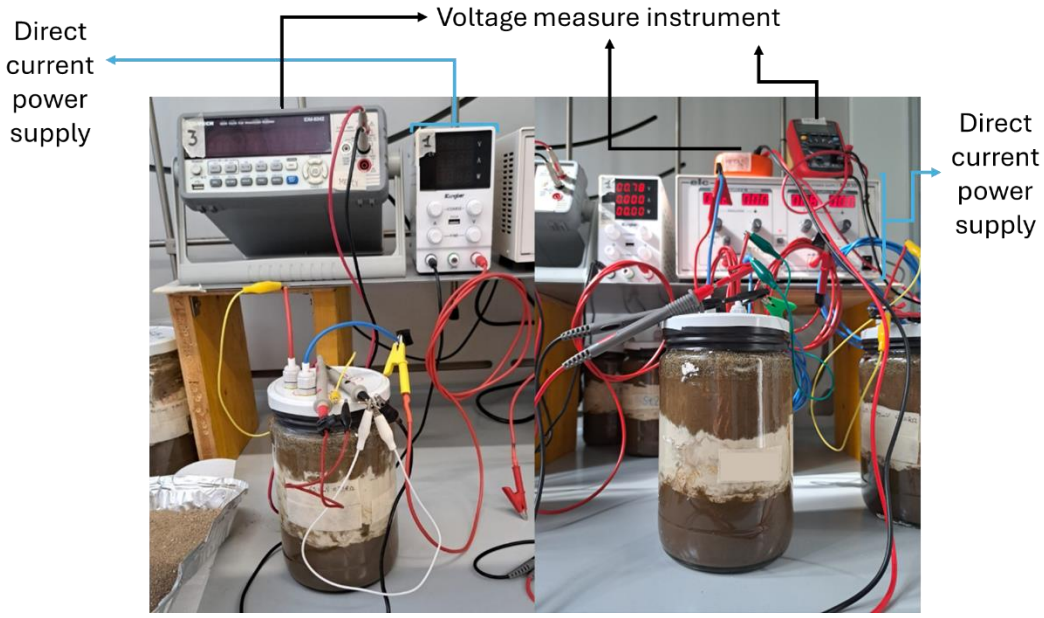

Figure 4.5: Two BET reactors in batch mode, power supplies, and measuring instruments.

Spot monitoring: samples collected and parameters analysed

For reactors dismantled at time t3, some chemical parameters, such as pH, EC, and organic carbon. pH, EC, dissolved oxygen (mgO_2/L), nitrate and nitrogen content, were analysed in the water phase of each reactor.

5 Results and discussion

5.1. Soil characterization

The methods described in Chapter 4, paragraph 4.1, were applied to soil characterization. Table 5.1 summarizes the initial characteristics of the soils used in the tests.

Parameter	*GCS*	*NCS-B*	*NCS-C*
pH (-)	7.41 ± 0.10	4.66 ± 0.19	7.32 ± 0.03
Organic carbon (%)	3.17 ± 0.03	4.46 ± 0.42	4.26 ± 0.34
Carbonates (%)	8.83 ± 2.97	4.47 ± 0.68	4.27 ± 0.52
NO_3^- (mg/kg_DS)	5.61 ± 0.75	*	*
NH_4^+ (mg/kg_DS)	6.00 ± 0.07	2.24 ± 0.17	*
Electrical conductivity (µS/cm)	1436.00 ± 36.5	1371.33 ± 2.08	1364.00 ± 1.00
Water content (%)	1.08 ± 0.31	1.08 ± 0.12	1.43 ± 1.11
Field capacity (%)	38.50 ± 0.70	41.12 ± 0.07	45.89 ± 2.22
Sand (%)	86.69	96.25	83.91
Silt and clay (%)	13.32	3.75	16.09

Table 5.1: baseline soil characterization of gasoline-contaminated soil (GCS), not-contaminated soil used in batch systems (NCS-B), and not-contaminated soil used in fed-continuous systems (NCS-C). The acronym DS stands for "Dry Soil". The asterisk (*) refers to nitrate and ammonium concentrations below the lower limit of detection of the Lange Kit (0.22 mg/kg_DS and 0.025 mg/kg_DS, respectively).

From soil sieving, starting with soil previously sieved to 2 mm, it was possible to obtain the granulometric curve for each soil (Figure 5.1).

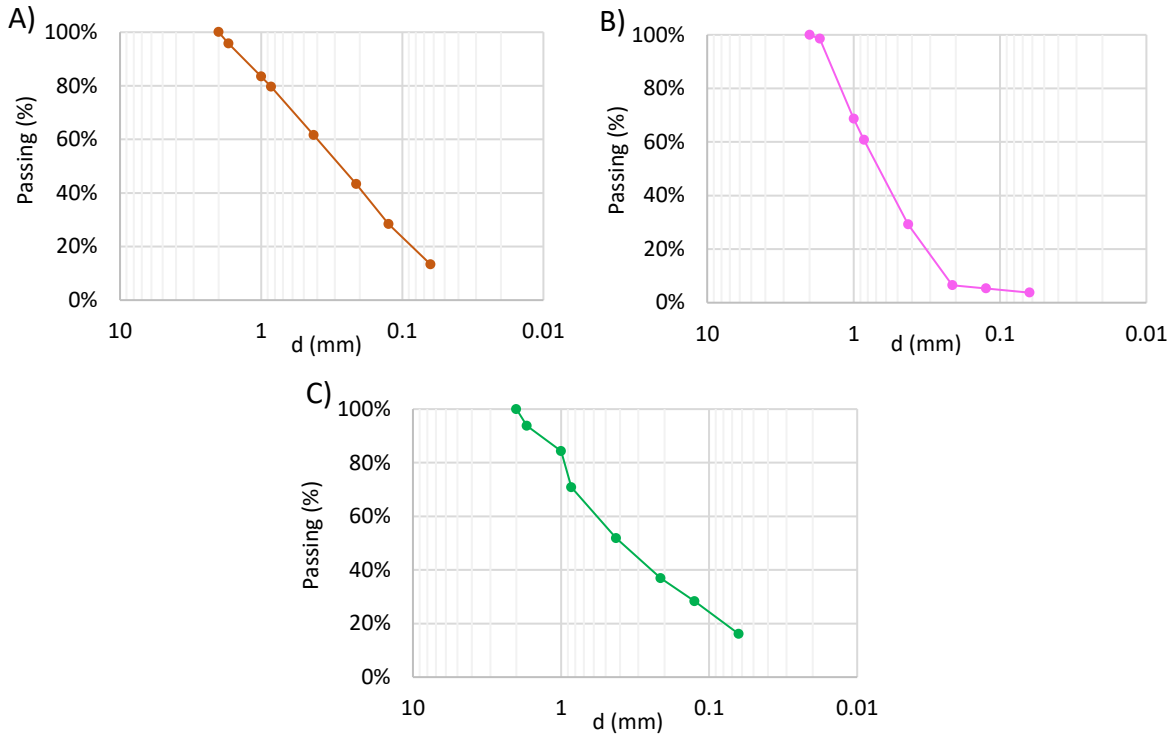

Figure 5.1: Granulometric curves of: A) GCS; B) NCS-B; C) NCS-C.

Particle size distribution curves of all the soils are similar with relevance to particles ranging between 60 and 2000 μm in diameter, as described in Table 5.1. From these results the soils used in the experiments are named *silty sand soil* for both gasoline-contaminated soil and not-contaminated soil in fed-continuous mode reactors, and *sand soil* for not-contaminated soil in the batch systems.
The soil capacity to retain the water is larger in the NCS-C, followed by NCS-C and GCS. It is the opposite for carbonate content, probably just calcium carbonate since the samples quickly reacted to the HCl-$FeCl_2$ solution, and negligible weight decrease was observed except in the initial 30 minutes of contact.

5.2. Continuously fed systems

Continuous monitoring: electrochemical and chemical analyses

The voltage curves were obtained thanks to the electrochemical monitoring of MFC1 and MFC2 during the 80 days of experimentation (Figure 5.2).

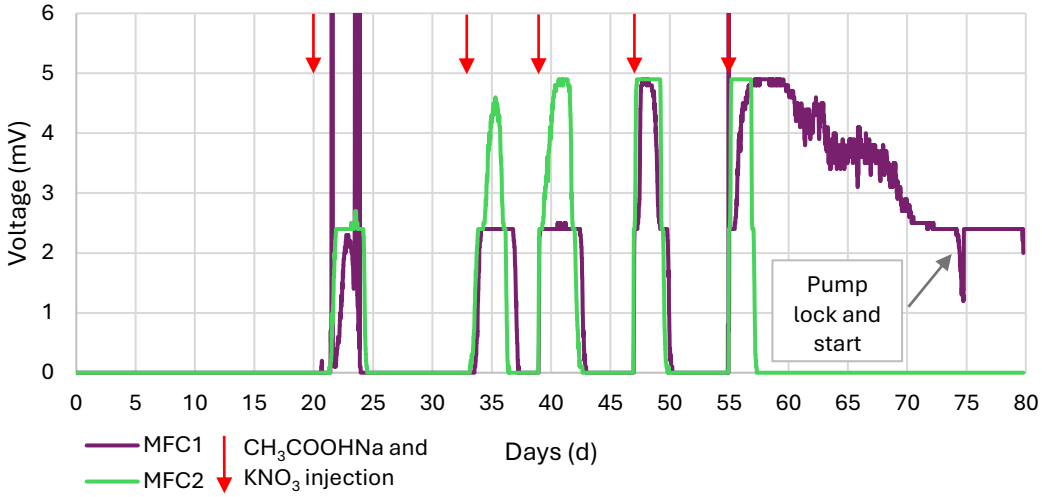

Figure 5.2: Voltage curves of Microbial Fuel Cell reactors.

The voltage curves show five picks, with the initial MFC1 maximum voltage value of 279.9 mV, due to the high concentration of acetate introduced into an environment with microorganisms unaccustomed to that type of organic substrate (Mao et al., 2016). Following this the values stabilized on 2.45 ± 0.05 mV (maximum power density 3.97 ± 0.23 mW/m^2) in the second and third cycles, reaching the maximum stable value of 4.9 ± 0.1 mV (maximum power density 17.94 ± 2.92 mW/m^2) in the fourth and fifth cycles. On the last day of the experiment, the latter cycle was still ongoing, reaching 2.4 mV. MFC2 showed a gradual growth from a pick of 2.7 mV in the first cycle, up to the maximum voltage of 4.9 ± 0.1 mV (maximum power density 162.04 ± 0.10 mW/m^2) in the fourth and last cycles. So, MFC2 demonstrates more stable and comparable voltages than MFC1. No voltage was registered in any MFC when acetate and KNO_3 solution weren't injected, only the MFC1 at the end of the test showed a long-lasting signal after acetate spike, decreasing more slowly over time. On the 74th day, the recirculation pump was turned off and switched on again the following day. This caused a sudden decrease in the signal, followed by recovery upon restarting the recirculation system.

Regarding the chemical parameters monitoring, several graphs demonstrate their temporal trend (Figure 5.3).

A)

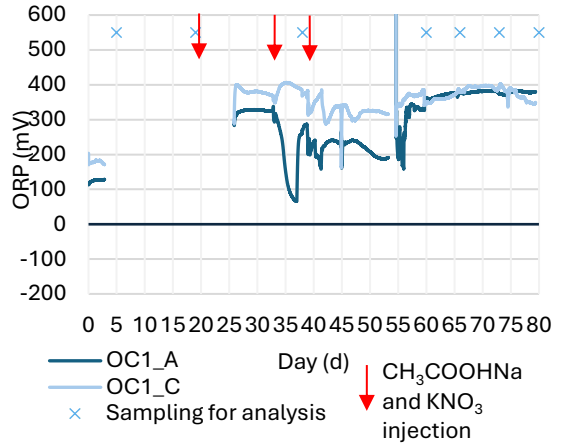
ORP (mV)
600
500
400
300
200
100
0
-100
-200
0 5 10 15 20 25 30 35 40 45 50 55 60 65 70 75 80
OC1_A
OC1_C
Sampling for analysis
Day (d)
CH3COOHNa and KNO3 injection

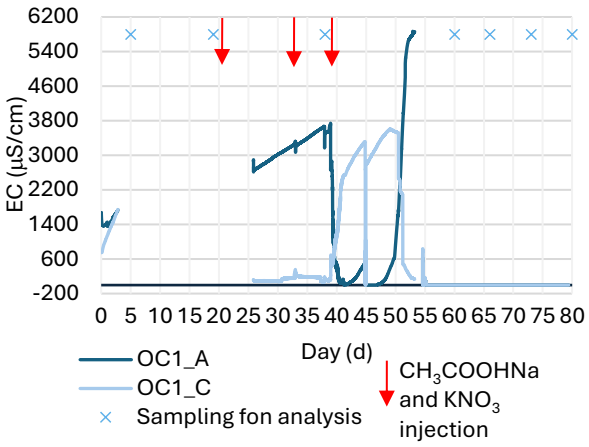
EC (µS/cm)
6200
5400
4600
3800
3000
2200
1400
600
-200
0 5 10 15 20 25 30 35 40 45 50 55 60 65 70 75 80
OC1_A
OC1_C
Sampling fon analysis
Day (d)
CH3COOHNa and KNO3 injection

B)

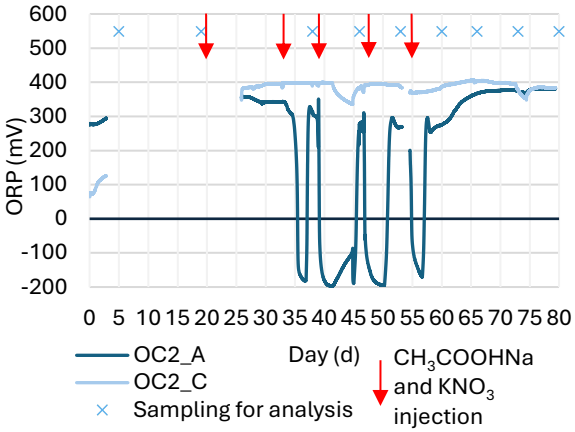
ORP (mV)
600
500
400
300
200
100
0
-100
-200
0 5 10 15 20 25 30 35 40 45 50 55 60 65 70 75 80
OC2_A
OC2_C
Sampling for analysis
Day (d)
CH3COOHNa and KNO3 injection

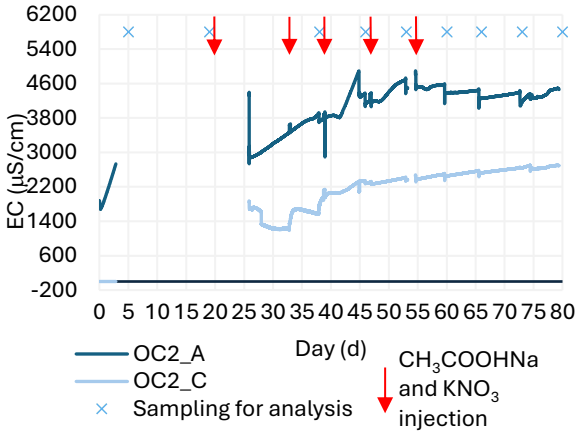
EC (µS/cm)
6200
5400
4600
3800
3000
2200
1400
600
-200
0 5 10 15 20 25 30 35 40 45 50 55 60 65 70 75 80
OC2_A
OC2_C
Sampling for analysis
Day (d)
CH3COOHNa and KNO3 injection

C)

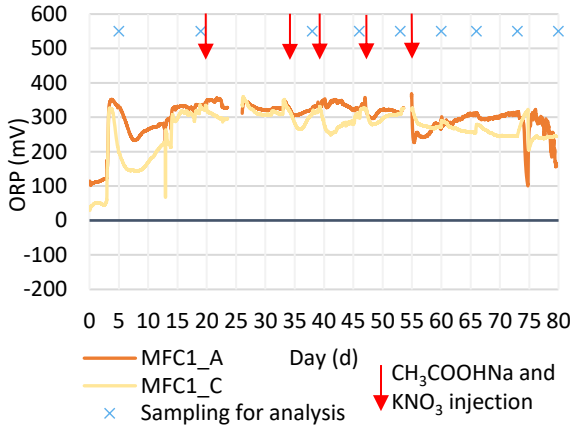
ORP (mV)
600
500
400
300
200
100
0
-100
-200
0 5 10 15 20 25 30 35 40 45 50 55 60 65 70 75 80
MFC1_A
MFC1_C
Sampling for analysis
Day (d)
CH3COOHNa and KNO3 injection

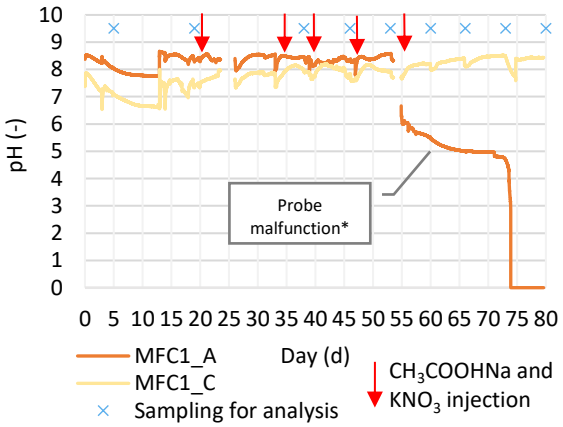
pH (-)
10
9
8
7
6
5
4
3
2
1
0
Probe malfunction*
0 5 10 15 20 25 30 35 40 45 50 55 60 65 70 75 80
MFC1_A
MFC1_C
Sampling for analysis
Day (d)
CH3COOHNa and KNO3 injection

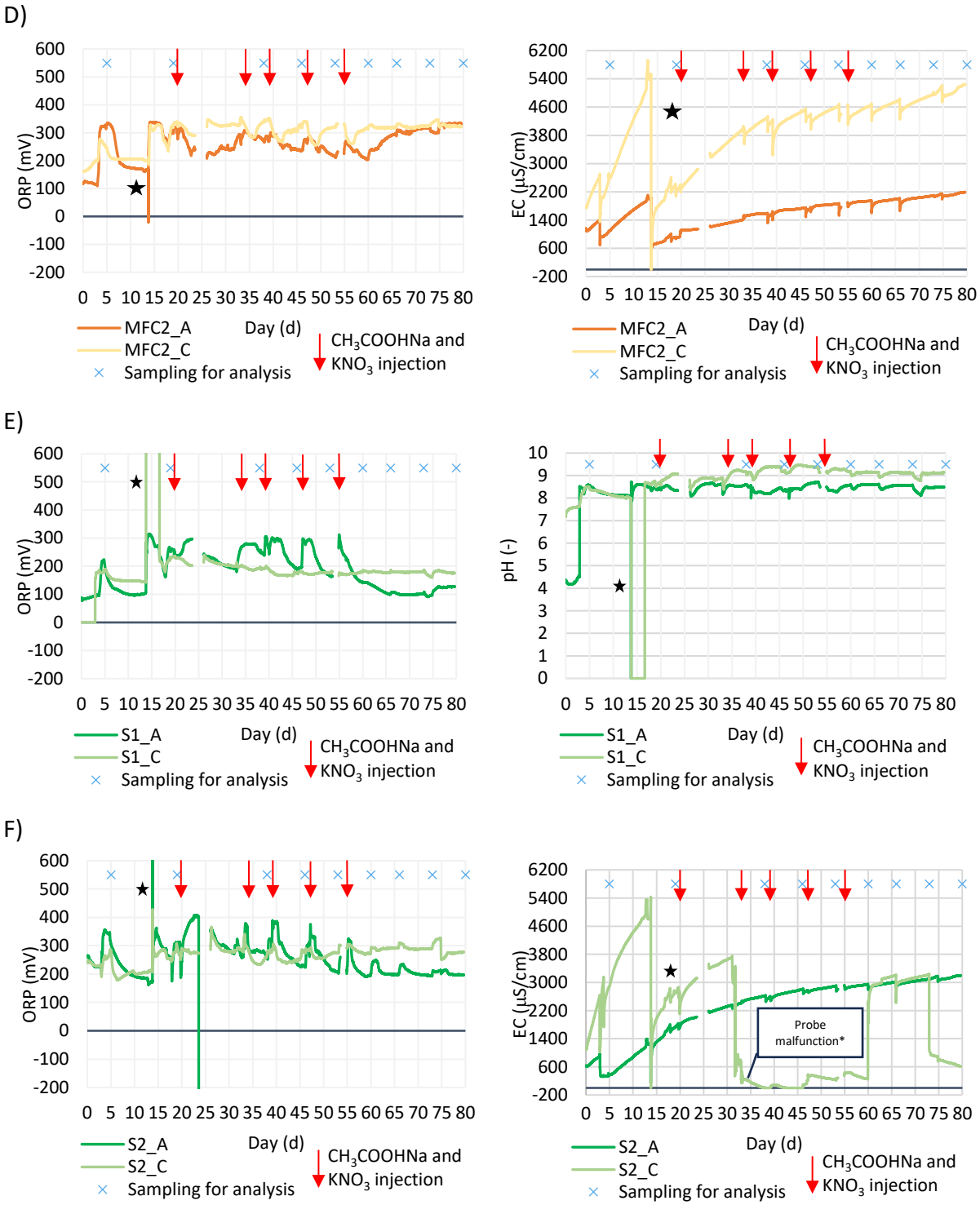

Figure 5.3: Chemical parameters of fed-continuous systems monitored in continuous: A) ORP and EC for OC1; B) ORP and EC for OC2; C) ORP and pH for MFC1; D) ORP and EC for MFC2; E) ORP and pH for S1; F) ORP and EC for S2. Sometimes the probes didn't work properly (*) and in some graphs the signal was influenced by the recirculation pipe arrangement on days 13 and 14 (★). The interruption of the lines indicates a temporary power outage.

The electrical conductivity of all the systems tends to grow during the experiment period. Generally, the EC increase is due to the rise in mobile ions concentration produced during acetate degradation. In this case, the EC trend doesn't seem to be influenced by the injection of CH_3COONa and KNO_3 solutions. The growth can be observed from the beginning of the experiment. Moreover, a slight decrease of the signal followed by its increase at the spikes, is caused by the temporary recirculation switch-off to allow dosing. The electrical conductivity increase trend is especially evident in the last 20 days of the test when only sampling for chemical analysis was performed. The OC1 on day 45 was temporarily suspended due to the clogging of a valve in the recirculating tubes that caused gas accumulation between the cathode felt and soil.
The pH was monitored only in MFC1 and S1. Considering the period, from day 19 to day 53.5, when it's possible to compare data between the two systems (anomalies in the signal from the MFC1_A pH probe and maintenance of the recirculating pipe makes it impossible to compare pH data in the remaining periods) the recorded pH values were:

- 8.39 ± 0.13 for MFC1_A;
- 7.86 ± 0.21 for MFC1_C;
- 8.45 ± 0.15 for S1_A;
- 9.09 ± 0.27 for S1_C;

The cathodic pH showed a slight increase with time due to the injection of nitrate solution, reaching in the last 10 days, when just sampling was carried out, a constant value of 8.36 ± 0.2 in MFC1 and 9.07 ± 0.1 in S1. Moreover, pH slight increase at the cathode is confirmed by the values on days 19^{th} and 80^{th}: 7.42 ± 0.04 and 8.43 ± 0.10 for MFC1; 8.62 ± 0.04 and 9.12 ± 0.01 for S1. This is probably caused by proton consumption as demonstrated by another study, while no pH reduction occurred in anode chambers caused by proton accumulation (X. Wang et al., 2012).
Concerning the ORP monitoring, it's possible to notice the different behaviour of the open circuit control compared to the other reactors: the ORP recorded in the anode chamber decreased after the acetate injection, differently, it increased in MFC and S systems (Figure 5.4). Likely due to the presence of dissolved oxygen in the samples analysed after the treatment (Table 5.3), the relevant decrease in ORP for OC2_A can be attributed to the partial organic degradation by aerobic metabolism, causing the oxygen removal and thus the oxidation-reduction potential decreasing. Indeed, the organic substrate in the anode compartment, sodium acetate in this case, is the electron donor for microbial respiration, and oxygen is the preferred electron acceptor as long as it is sufficiently present. When oxygen is insufficient for microbial metabolism,

alternative electron acceptors are used, such as nitrate. Nitrate concentration in the anode chamber on the 5th and 66th days was measured. On the 66th day, the levels were lower than those observed on the 5th day, and the detection method, too. Therefore, nitrate could get reduced in the anode chamber. Generally, in natural soil systems, ORP ranges from -1 V to +1 V; under aerobic conditions, ORP is above +300 mV, so lower ORP values indicate nitrate and other alternative electron acceptors are reduced (Fiedler et al., 2007).

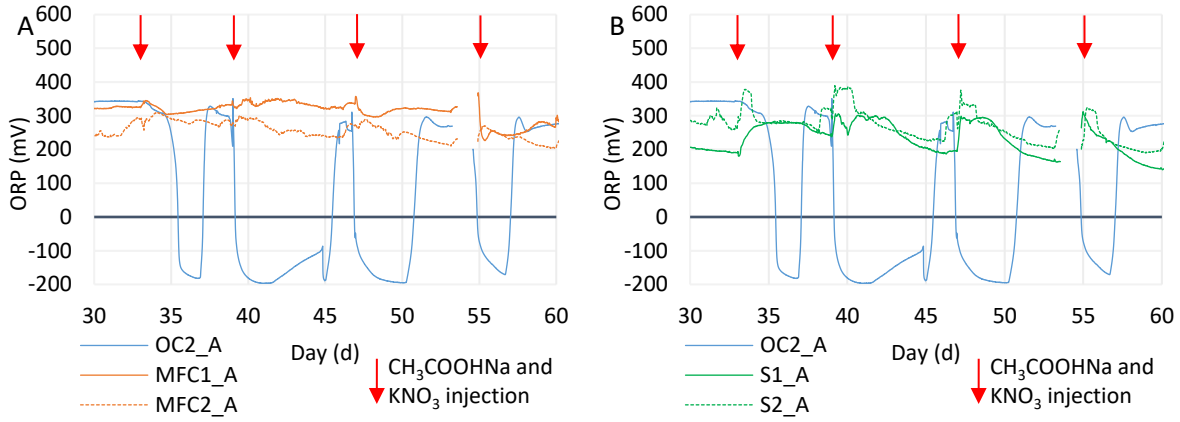

Figure 5.4: Comparison between anode ORP: A) OC2, MFC1, and MFC2; B) OC2, S1, and S2. Lines interruption indicates a temporary power outage.

The ORP behaviour in MFC_A and S_A systems is quite different from that observed in the OC2_A reactor. While the latter showed ORP sudden decreases upon sodium acetate dosing in the anode chamber and rose again several days later, the other systems, especially the snorkels, initially showed an increase in the ORP, reaching a plateau before decreasing as in OC2_A. Given that acetate oxidation is linked to current production, it is possible that there was a modification of the organic matter content in the soil, from its reduced to oxidated form. (Hong, Chang, Choi, Kim, et al., 2009). Probably the resistance participating in the microbial fuel cell technology makes the electron transfer harder, so the system's response to the ORP change is less obvious than the snorkel system. Additionally, during the electrochemical signal, the ORP decreases until the voltage come back to zero (Figure 5.5). Typically, the reduction in ORP is due to the decreasing of oxygen and other electron acceptors that influence the oxidative-reduction potential in positive mode.

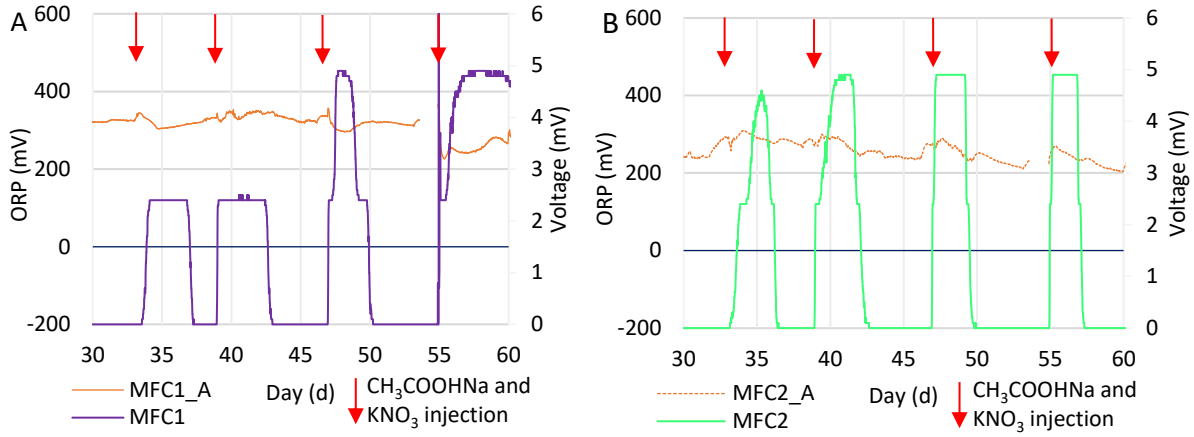

Figure 5.5: Recorded anode ORP and MFC voltage from test days 30 to 60: A) MFC1; B) MFC2. Line interruption in the ORP indicates a temporary power outage.

Spot monitoring: chemical analyses

During the 80 days of the experiment, specific monitoring of pH, EC, COD, and nitrate concentrations were conducted. pH and EC values were measured on days 19, 33, 38, 46, 47, 53, 55, 60, 66, 73 and 80. The results are shown respectively in Figure 5.6 and Table 5.2.

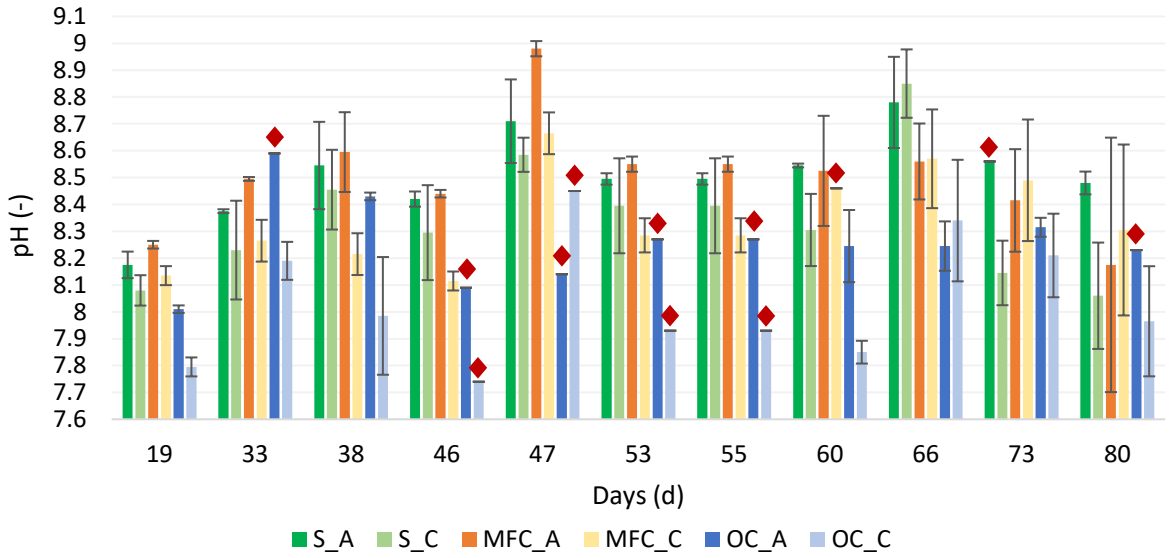

Figure 5.6: pH average values and standard deviation in the anodic and cathodic compartments of each type of reactor. The red diamonds indicate values obtained by measurements of just one of the replicates.

Spot pH measures were conducted in all the systems, both in anodic and cathodic chambers. These results confirmed the pH trend obtained by the continuous monitoring for MFC1 and S. The pH values in the anode compartment of the MFC1

system help to understand its pH trend from day 53.5 on when we experienced probe malfunction. The result showed a pH decrease from day 19, pH = 8.24, to day 80, with 7.85.

System	*Electrical conductivity (µS/cm) on sampling days*										
	19	**33**	**38**	**46**	**47**	**53**	**55**	**60**	**66**	**73**	**80**
S1_A	1.53	2.79	3.05	3.35	3.24	3.51	3.51	3.62	3.92	> 4.0	> 4.0
S1_C	> 4.0	> 4.0	> 4.0	> 4.0	> 4.0	> 4.0	> 4.0	> 4.0	> 4.0	-	3.09
S2_A	1.18	2.01	2.17	2.46	2.45	2.6	2.6	2.7	2.83	2.76	3.13
S2_C	1.63	2.3	2.25	2.1	1.98	1.94	1.94	2.03	-	>4	1.97
MFC1_A	1.14	2.27	2.44	2.78	2.76	3.05	3.05	3.33	3.66	3.66	> 4.0
MFC1_C	1.19	1.83	1.95	2.08	1.98	2.12	2.12	2.2	2.27	-	2.33
MFC2_A	0.54	1.01	1.06	1.22	1.28	1.33	1.33	1.44	1.53	1.65	1.66
MFC2_C	1.36	2.36	2.52	2.67	2.53	2.75	2.75	2.87	2.85	2.75	3.16
OC1_A	1.05	1.13	1.91	-	-	-	-	1.45	1.27	1.34	1.51
OC1_C	0.99	1.49	1.54	-	-	-	-	0.66	0.58	0.76	0.58
OC2_A	1.01	1.79	1.92	2.27	2.08	2.25	2.25	2.1	2.08	2.35	2.17
OC2_C	1.04	1.62	1.74	1.88	1.89	1.98	1.98	2.12	1.88	1.96	2.31

Table 5.2: Electrical conductivity data for each system/compartment at sampling.

Electrical conductivity, as discussed previously, increased both in the anode and cathode compartments.

The values of pH, EC and DO obtanined by the monitored after 80 days of OC2. MFC2 and S2 work are shown in Table 5.3.

Systems	*pH (-)*	*EC (mS/cm)*	*DO (mgO_2/L)*
OC2_A	7.68	4190	5.52
OC2_C	7.19	4550	8.25
S2_A	8	6050	5.01
S2_C	7.79	3550	4.84
MFC2_A	8.03	3170	8.17
MFC2_C	7.56	6090	8.23

Table 5.3: Monitoring of chemical parameters after 80 days of experiment.

On the sampling days, nitrate concentration and COD were measured at the anode and cathode, respectively (Figure 5.7 and Figure 5.9).

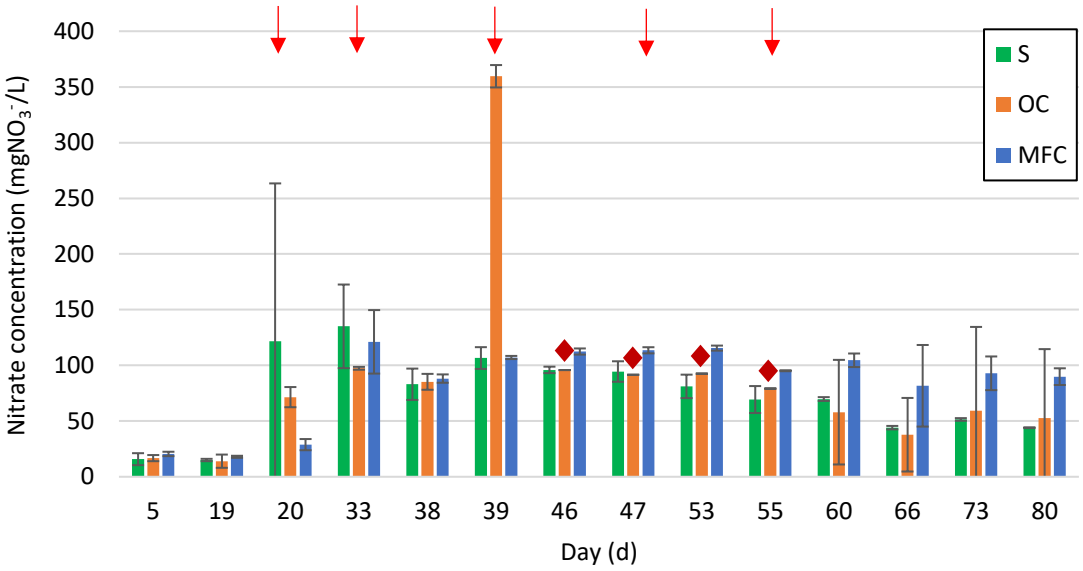

Figure 5.7: Nitrate concentrations obtained in water samples from S, OC, and MFC systems, as mean value and standard deviation of the replicates. The arrows mark the CH_3COONa and KNO_3 injection days. The red diamonds are referred to the values obtained by the analysis of a single reactor.

Initially, at the beginning of the tests, all the systems showed low NO_3 concentrations (up to about 20 mg/l); after KNO_3 injection, nitrate increased, especially in the reactors with snorkel technology. In some systems, especially in microbial fuel cells, NO_3 levels remained stable throughout the test; otherwise, nitrate reduction with time was observed in the snorkel reactors, as summarized in Table 5.4.

Cycle	$r_{nitrate}$ *(%)*
2	34.53 ± 28.62
3	9.49 ± 11.01
4	14.26 ± 2.81
5	Increasing concentration

Table 5.4: Nitrate removal efficiency obtained by the snorkel technology.

While the levels of ammonium nitrogen, nitrous nitrogen, and total nitrogen were verified at the cathode on day 19, nitrous nitrogen was considered negligible, as in each sample it was below its limit of quantification (0.6 $mgNO_2^-$-N/L). Thus, ammonium nitrogen is derived from the difference between total nitrogen and nitrate

nitrogen. On day 66, the total nitrogen was verified in the systems. Figure 5.8 shows the concentrations of total nitrogen measured on days 19 and 66, considering the mean values and standard deviation of the replicate reactors for each technology.

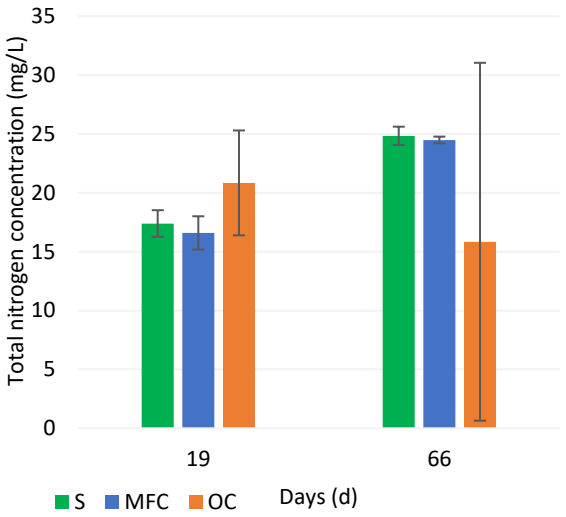

Figure 5.8: Total nitrogen of the systems on day 19 and 66.

The large value in the standard deviation for OC on day 66 is Associated with OC1 maintenance on day 55, following a valve clogging on day 45 causing the detachment of the felt and soil in the anode chamber.

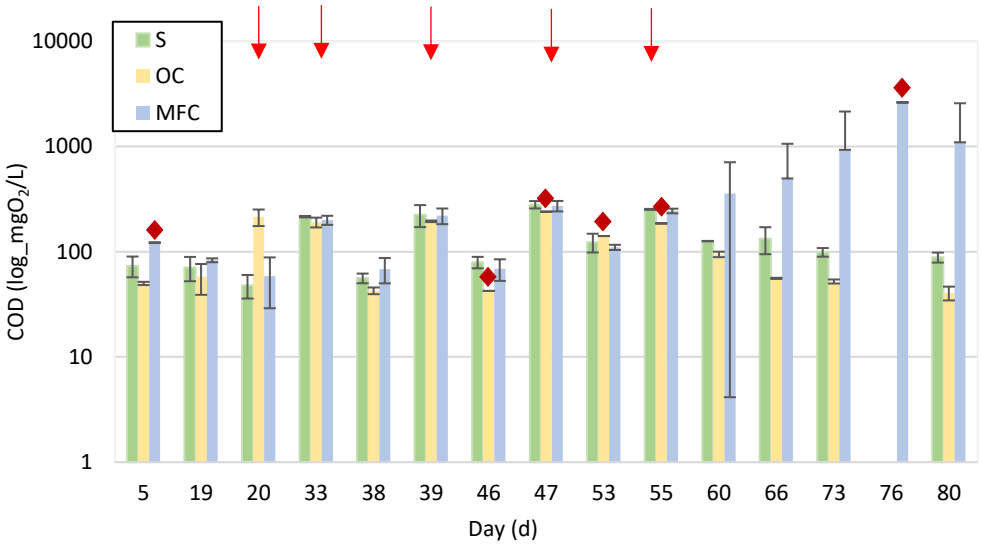

Figure 5.9: COD in water samples from Snorkel (S), Open Circuit Control (OC), and Microbial Fuel Cell (MFC) systems. The arrows indicate the injection days of CH_3COONa and KNO_3. The red diamonds mark the values obtained by only one reactor.

COD variation is much more pronounced compared to the variation in nitrate concentration. At the first spike of acetate, open circuit controls showed a higher COD

in comparison to the snorkels and MFCs, likely due to a major volume of solution recirculated in time, considering the 30 minutes between injection and sampling. Because of this, on subsequent injection days, more time was allowed between the injection and the sampling. Nevertheless, all systems consistently showed a more immediate response over time to the presence of acetate in the systems. Additionally, the COD rarely reached the initially considered threshold limit of 290 mgO_2/L. This phenomenon may be attributed to substance adsorption on the electrode. Furthermore, it's evident that the MFC systems, especially the MFC1, exhibited a high COD after the last acetate injection. It is necessary to specify that the analyses conducted on the solutions extracted for COD analysis on days 60, 66, and 73 always exceeded the Lange Kit upper limit (150 mgO_2/L), yet they still show an increasing trend. This trend continues until reaching the data on day 76 (2620 mgO_2/L) and 80 (2140 mgO_2/L).

To better understand the role of the acetate solution inserted in the anode chamber and the potassium nitrate solution in the cathode chamber, the correlation with the electrochemical signal provided by the microbial fuel cells was evaluated (Figure 5.10). COD concentration, as discussed previously, showed a more pronounced variation during the cycles compared to nitrate; nitrate levels after the end of the cycle are somewhat higher than at the beginning. This confirms that acetate, and thus the organic substance supplied to the system, is directly linked to the production of electrical energy (Kilinc & Catal, 2023).
Moreover, COD levels identified from day 60 onwards are higher than the maximum achievable with the addition of the sodium acetate solution (290 mgO_2/L). It is important to consider that hydrocarbons are poorly soluble in water, and therefore their bioavailability, especially in soils, is limited, making their biodegradability challenging (He et al., 2022). So, high concentrations could be attributed to the desorption of the pollutants from the soil, supporting a more prolonged energy production compared to other electrochemical cycles. To check this assumption, hydrocarbon concentrations before and after the treatment should be analyzed.

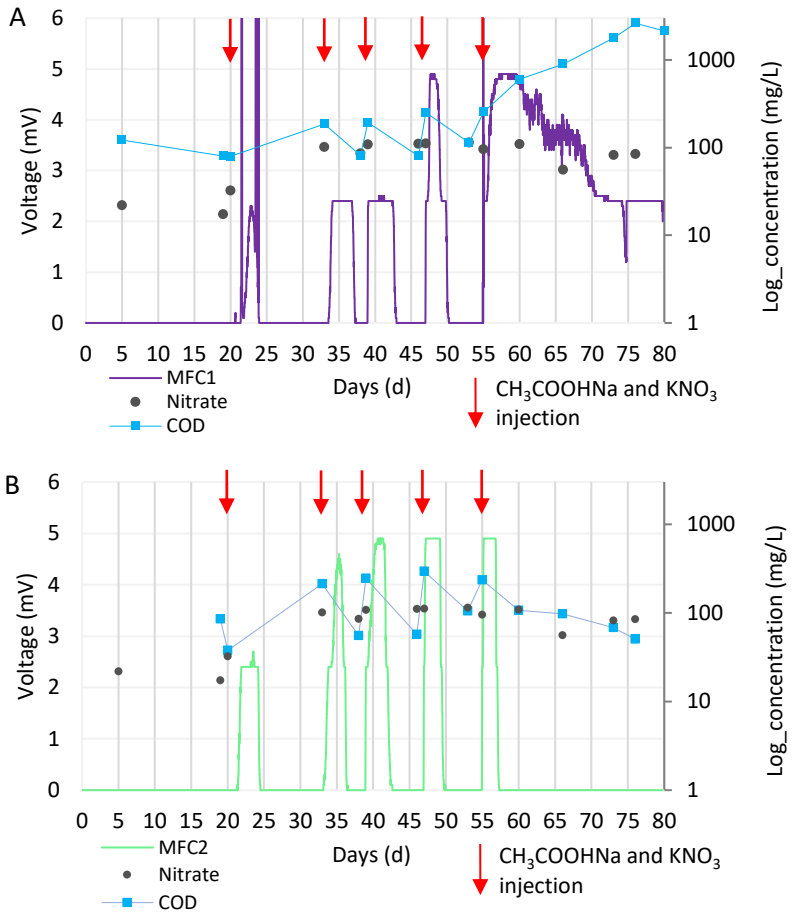

Figure 5.10: Voltage, nitrate, and COD concentrations in the cathode and anode compartments, respectively in A) MFC1; B) MFC2.

COD removal (%) in each of the four cycles, considering both replicates, was higher than 50%. Table 5.5 summarises the COD removals for each technology, considering COD concentrations at the beginning and the end of cycles. It's possible to observe how the removal efficiency decreased with the cycles and how the OC system presented the highest removals in the first cycles, but the lowest in the last.

System	*r_{COD} (%) Cycle 2*	*r_{COD} (%) Cycle 3*	*r_{COD} (%) Cycle 4*	*r_{COD} (%) Cycle 5*
S	73.98 ± 2.35	64.11 ± 4.05	56.22 ± 5.35	50. 08 ± 0.34
MFC	65.04 ± 12.74	67.68 ± 12.74	59.22 ± 6.94	54.42
OC	77.59 ± 0.76	78.46	41.33	46.98

Table 5.5: COD removal efficiency for each technology type during the bioelectrochemical cycles. In case no standard deviation is provided data is based on a single reactor. The removal rate value pertains to a single system.

Especially for the microbial fuel cells, the duration of each cycle was assumed as the period between an acetate spike and the COD monitoring event, several days after the decline of the circulating current, that would actually identify the true closure of the cycle. To evaluate the error that this assumption entails, the COD variation in MFC1 and MFC2 in cycle 2 was chosen as a reference, as in such cycle the COD analysis (day 38.6) was performed only a couple of days after the current signal turned to zero (day 37.3 for MFC1 and day 36.5 for MFC2). The COD variation was assumed to be a straight line, as there were no intermediate values between the beginning and end of a voltage cycle. In the other cycles, COD levels were obtained up to 4 days after the actual end of the cycle. So, their variations were compared to the reference variation to define the error made when deciding to use a COD concentration not related to the actual end of the cycle. Thus, the slopes of the lines identified by the initial concentration and the hypothesized final concentration of COD for the MFC1 and MFC2 systems were defined, considering the reference variation slope to be -20.80 and -31.63 for MFC1 and MFC2, respectively (Table 5.6). In every case, except for the line of cycle 4 in MFC1, there is an overestimation of the concentration with a larger error referred to the lines of MFC1 cycle 3 (21.98 %) and MFC2 cycle 5 (19.07 %). The least significant variation is that of cycle 4 for MFC1, with an error of 0.52 %.

Cycle	*MFC1 slope error (%)*	*MFC2 slope error (%)*
3	21.98	14.66
4	-8.97	0.52
5	-	19.07

Table 5.6: Errors attributed to COD variation measured in MFC systems taking into account the ΔCOD reference defined by cycle 2 in MFC1 and MFC2.

The COD variation was also useful to estimate the Coulombic efficiency (CE,%) for each cycle, except for the last cycle of MFC1, since after 80 days of the experiment, a voltage signal was still detected, and for cycle 1, because the concentration measurement is not available at the end of the cycle (Figure 5.11).

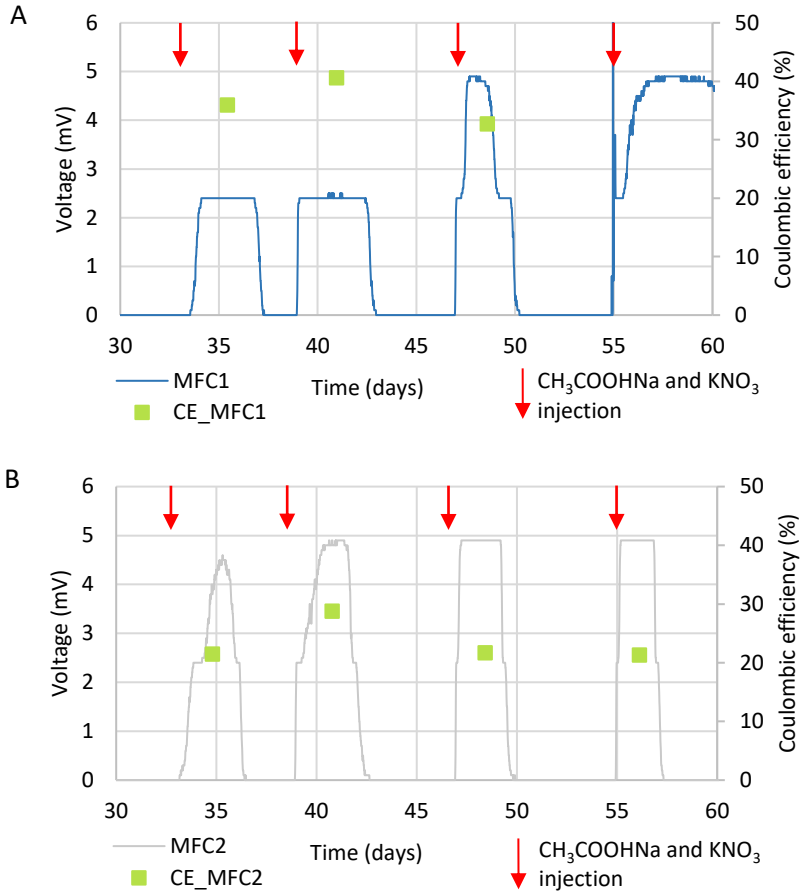

Figure 5.11: Voltage and Coulombic efficiency for MFC1 (A) and MFC2 (2).

The results in terms of Coulombic efficiency suggest that the electric signal is only due to a portion of the acetate introduced into the systems.

5.3. Batch systems

Continuous monitoring: electrochemical analyses

The continuous monitoring of the bioelectrochemical systems in batch mode resulted in the voltage recording over time, as shown in Figure 5.8. The recorded voltage at the ends of the load, is part of the voltage applied between the anode and cathode that is used to drive the current through the external load.

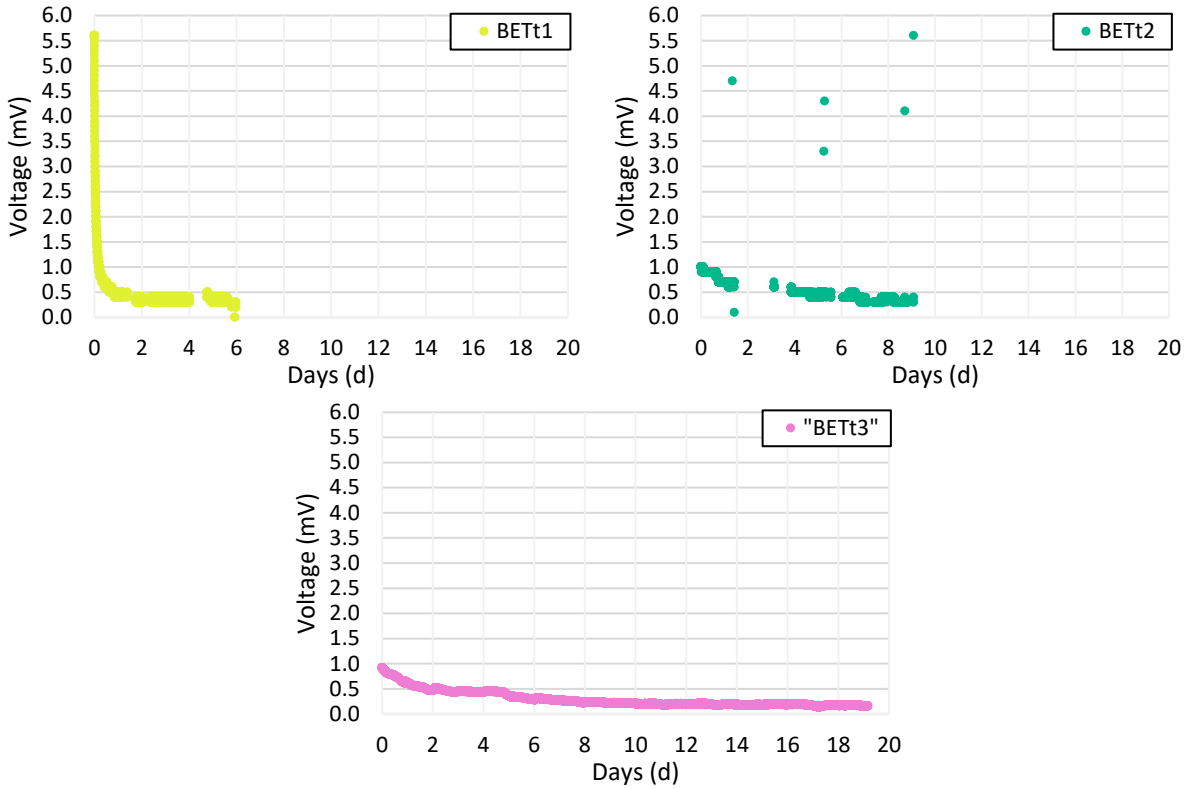

Figure 5.12: Voltage monitoring over time in BETt1, BETt2 and BETt3. The interruption of the lines indicates a temporary power outage.

Due to the limits of the monitoring devices, the voltage recording lasted 6 days for BETt1, 9 days for BETt2, and 19 days for BETt3. In any way, the curves show a decreasing trend with time, approaching zero.

Spot monitoring: collected samples and analyzed parameters

At the end of batch tests (t3), reactors were dismantled and pH, electrical conductivity, and organic content in soil were analyzed. Considering also the initial soil characteristics (Table 5.1), Figure 5.13 and Figure 5.14 show the organic carbon contents at the beginning (t0) and the end (t3) of the tests. EC and pH data are reported in Table 5.7.

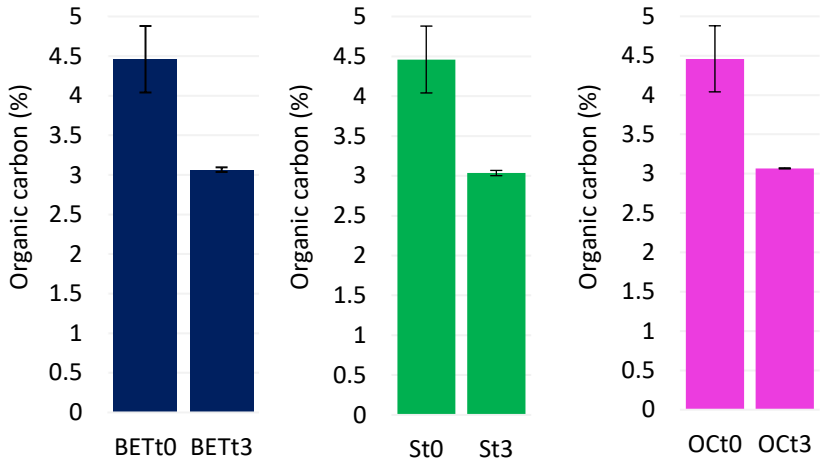

Figure 5.13: Comparison of NCS-B organic carbon content at the beginning (0) and the end (3) of batch tests for each technology.

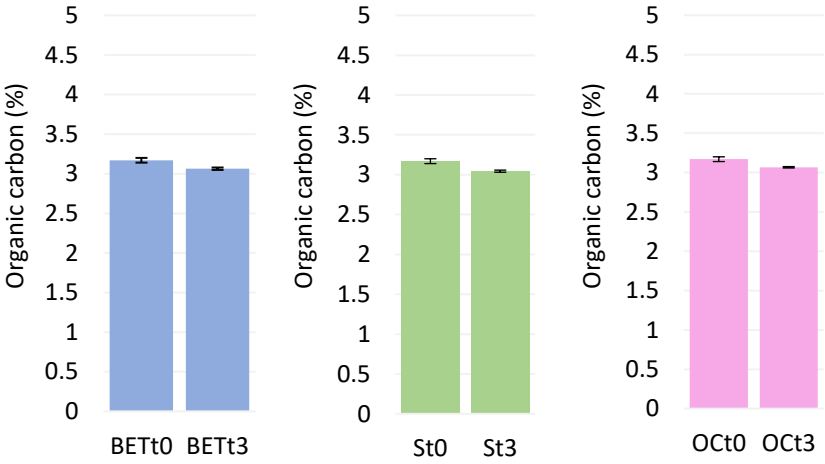

Figure 5.14: GCS organic carbon content at the beginning (0) and the end (3) of batch tests for each technology.

Parameters	*System*	*GCS*	*NCS-B*
pH (-)	METt3	7.13 ± 0.09	7.04 ± 0.06
EC (µS/cm)	METt3	1632 ± 27	1381 ± 76
pH (-)	St3	7.09 ± 0.07	6.99 ± 0.04
EC (µS/cm)	St3	1571 ± 48	1369 ± 45
pH (-)	OCt3	7.35 ± 0.03	6.94 ± 0.05
EC (µS/cm)	OCt3	1429 ± 69	1361 ± 82

Table 5.7: pH and electrical conductivity of GCS and NCS-B in time 3.

Despite the lower organic carbon content of contaminated soil GCS than the uncontaminated soil NCS-B, at the end of the test, similar residual values were achieved in all the reactors.
Soil pH is a fundamental parameter to define the physiochemical and biological properties of the soil. Based on the pH levels, pollutant removal and microbial community change. The pH of the uncontaminated soil, initially below neutrality, presents a pH between 6 and 7 at the end of the treatment. Microorganisms' activity, such as for electroactive bacteria, is supported in neutral environments. Meanwhile, the GCS maintained a neutral pH from start to finish.
The electrical conductivity in the cathode compartments remained very close to the EC measured before the treatment began, whereas at the anodes, GCS electrical conductivity is higher in BET, followed by the snorkel, and then the OC. In one research study, the electrical conductivity variations in the anode compartment are related to diesel degradation, as diesel degradation products could increase EC, despite diesel being electrically insulating (Mao et al., 2016). The lack of EC variation in OC might confirm that, unlike in bioelectrochemical systems, there was no significant degradation of hydrocarbons.

pH, electrical conductivity (EC), dissolved oxygen and nitrate concentrations in the overlaying water were monitored on day 7, for BETt1, St1 and OCt1, on day 14, for BETt2, St2 and OCt2, and on day 21, for BETt3, St3 and OCt3 (Figure 5.15). At time 0 (systems setup day), the nitrate concentration was defined as 100 mgNO_3^-/L by adding KNO_3 to the water. Regarding dissolved oxygen, it's hypothesized that the data obtained on day 21 are the most accurate, given that the water samples were transferred to a baker before using probe on days 7 and 14. This could have led to an increase in dissolved oxygen on the samples. However, the reduction in dissolved oxygen over time may be due to the microorganism's respiratory activity, which is confirmed in the OCt system, as happened in a study investigating the removal of hydrocarbons from marine sediment using snorkel technology (Viggi et al., 2015). Therefore, it would be necessary to investigate in the BETt and St systems whether this decrease is also or solely related to the activity on electroactive microorganisms that use the cathode's electrons to reduce oxygen.
Also nitrate concentration reduction was present in the OCt system, but with a lower consumption over time compared to the BETt systems. St reactors showed a gradual increase in the nitrate concentration until reaching 112.93 mgNO_3^-/L on day 14, and a rapid decease until day 21. Considering day 0 and 21, BETt and St systems had the grater removal efficiency (85.54 % and 86.76 %) compared to the OCt systems (65.59 %).

It's possible to observe how the electrical conductivity in the St systems decreased from day 14 to day 21, which corresponded to the same period of nitrate reduction. Likewise, the increase in nitrates from day 7 to day 14 is accompanied by an increase in EC. This can be explained by the fact that electrical conductivity increases with the rise of ions in the solution. If those ions are subsequently consumed, as might be the case with nitrates (and hydrogen), the conductivity tends to decrease. The opposite behaviour is observed in the EC of BETt and OCt systems.

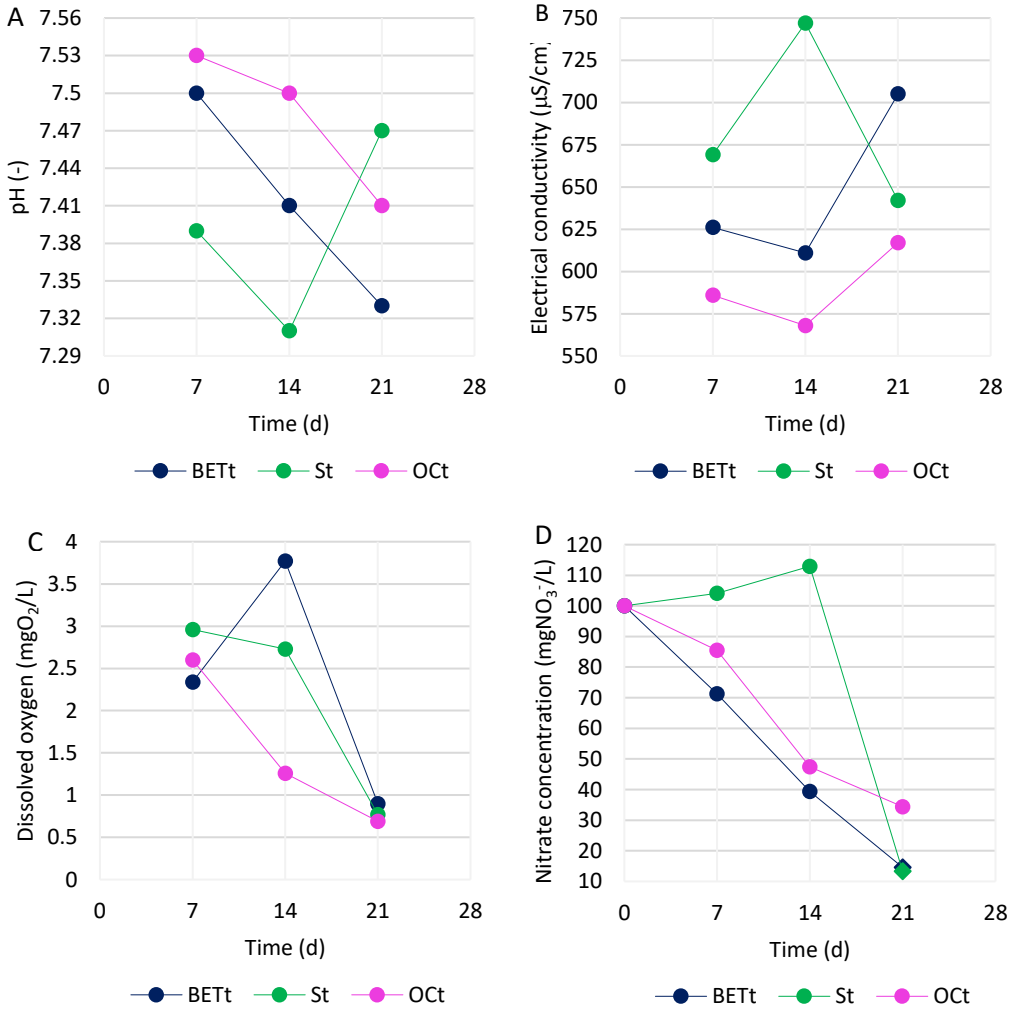

Figure 5.15: pH (A), EC (B), DO (C) and nitrate concentration (D), for the different treatments, on day 7, 14 and 21. The concentration measures on day 21 of nitrate are below the lower limit of detection of the Lange Kit (22 mgNO_3^-/L).

6 Conclusions and future developments

The thesis work explored the application of two bioelectrochemical systems, the microbial fuel cell (MFC) and the microbial electrochemical snorkel (MES), in comparison to open-circuit control (OC) systems, for the remediation of contaminated soil. These systems were installed both in continuous-fed and batch-mode reactors. To allow for a better comparison, the same reactor configuration was used for all three technologies, utilizing graphite felt as the electrodes and kaolin as a semipermeable layer dividing the anodic compartment from the cathodic one.

Regarding continuous flow systems, sodium acetate was added to the anodic system, while a potassium nitrate solution, up to about 100 mgNO_3^-/L, was dosed at the cathode to simulate nitrate-contaminated groundwater. The oxidation of the non-fermentable organic substance at the anode produced an electrical signal, identifying an electrical cycle for each phase of CH_3COONa solution injection in the MFCs. Initially, the MFC2 system was adapted, reaching a maximum power density of 162.01 mW/m². The reproducibility of the cycles was less evident in the MFC1 system, which reached the same power density as MFC2 but without closing the cycle before the end of the experiment. Therefore, it was possible to define a coulombic efficiency, which is generally higher for MFC1 (36.39 ± 3.96 %) compared to MFC2 (23.29 ± 3.64 %). This means that only part of the electrons produced by the acetate oxidation were transferred from the anode to the cathode, producing an electric current. Additionally, the COD removal rate decreased over time, identifying the MFC as having the best removal rate both after the fourth (59.22 ± 6.94 %) and fifth injection (54.42 %).
Regarding the removal of petroleum hydrocarbons, relevant soil analyses after treatment are not available, while for nitrates in the MFC and OC systems, a slight increase in concentrations was observed. The snorkel system reacted the best, obtaining the highest removal rate of 34.53 ± 28.62 %. The injection and oxidation of the organic substance at the anode led to a general increase in pH at the cathode comparing values at days 19 and 80 of the tests (from 7.42 ± 0.04 to 8.43 ± 0.00 for MFC1; from 8.62 ± 0.04 to 9.12 ± 0.01 for S1). Electrical conductivity increased throughout the experiment and was not influenced by the added solutions. As for the ORP, it showed opposite behaviors in the OC and the bioelectrochemical systems.

About batch systems, the reduction of organic matter in NCS-B is much more pronounced than in GCS, due to a higher initial content, eventually reaching the same levels as GCS. So, further analyses are needed to verify if the removal of PHs has occurred. Moreover, nitrate analyses of the water present at the cathode have shown that an MES technology and a BET with imposed potential allow for a greater reduction of nitrate at the cathode compared to the control system, with a removal efficiency of 86.76% and 85.54%, respectively.

To improve the performance of the bioelectrochemical systems and the analysis of their outputs, it would be necessary to:

- characterize the microbial community involved in the oxidation/reduction of the pollutants and try to enlighten the metabolic and electron transfer mechanisms to identify which microbial strains can improve the technology's efficiency;
- define the degradation kinetics of the organic substances to correlate biodegradation to the electricity production in the microbial fuel cells;
- investigate the long-term stability of the bioelectrochemical treatment;
- scale up the system to make it as similar as possible to in situ applications;
- explore possible combinations with other technologies to compensate for the limitations of a single technology and broaden the spectrum of applications;
- conduct economic evaluations concerning the type of materials considered, the possibility of inserting catalysts, and the type of membrane, to make the application of the bioelectrochemical system the basis of sustainable development;
- define an energy harvesting system that makes the use of a microbial fuel cell technology advantageous;
- identify and improve the influence radius for pollutant removal within the contaminated matrix.

7 Bibliography

Adipah, S. (2018). Introduction of Petroleum Hydrocarbons Contaminants and its Human Effects. *Journal of Environmental Science and Public Health*, *03*(01). https://doi.org/10.26502/jesph.96120043

Afsham, N., Roshandel, R., Yaghmaei, S., Vajihinejad, V., & Sherafatmand, M. (2015). Bioelectricity Generation in a Soil Microbial Fuel Cell with Biocathode Denitrification. *Energy Sources, Part A: Recovery, Utilization and Environmental Effects*, *37*(19), 2092–2098. https://doi.org/10.1080/15567036.2012.671900

Ahmed, F., Fakhruddin, A. N. M., & Fakhruddin, A. (2018). *A Review on Environmental Contamination of Petroleum Hydrocarbons and its Biodegradation*. https://doi.org/10.19080/IJESNR.2018.11.555811

Aparicio, J. D., Raimondo, E. E., Saez, J. M., Costa-Gutierrez, S. B., Álvarez, A., Benimeli, C. S., & Polti, M. A. (2022). The current approach to soil remediation: A review of physicochemical and biological technologies, and the potential of their strategic combination. In *Journal of Environmental Chemical Engineering* (Vol. 10, Issue 2). Elsevier Ltd. https://doi.org/10.1016/j.jece.2022.107141

Asghar, H. N., Rafique, H. M., Zahir, Z. A., Khan, M. Y., Akhtar, M. J., Naveed, M., & Saleem, M. (2016). Petroleum hydrocarbons-contaminated soils: Remediation approaches. In *Soil Science: Agricultural and Environmental Prospectives* (pp. 105–129). Springer International Publishing. https://doi.org/10.1007/978-3-319-34451-5_5

Aulenta, F., Palma, E., Marzocchi, U., Viggi, C. C., Rossetti, S., & Scoma, A. (2021). Enhanced hydrocarbons biodegradation at deep-sea hydrostatic pressure with microbial electrochemical snorkels. *Catalysts*, *11*(2), 1–11. https://doi.org/10.3390/catal11020263

Bijay-Singh, & Craswell, E. (2021). Fertilizers and nitrate pollution of surface and ground water: an increasingly pervasive global problem. In *SN Applied*

Sciences (Vol. 3, Issue 4). Springer Nature. https://doi.org/10.1007/s42452-021-04521-8

Cai, X., Yuan, Y., Yu, L., Zhang, B., Li, J., Liu, T., Yu, Z., & Zhou, S. (2020). Biochar enhances bioelectrochemical remediation of pentachlorophenol-contaminated soils via long-distance electron transfer. *Journal of Hazardous Materials*, *391*. https://doi.org/10.1016/j.jhazmat.2020.122213

Carter, M. R., & Gregorich, E. G. (2007). *Soil Sampling and Methods of Analysis Second Edition Edited by*.

Chiranjeevi, P., & Patil, S. A. (2020). Strategies for improving the electroactivity and specific metabolic functionality of microorganisms for various microbial electrochemical technologies. In *Biotechnology Advances* (Vol. 39). Elsevier Inc. https://doi.org/10.1016/j.biotechadv.2019.107468

Erable, B., Etcheverry, L., & Bergel, A. (2011). From microbial fuel cell (MFC) to microbial electrochemical snorkel (MES): maximizing chemical oxygen demand (COD) removal from wastewater. *Biofouling*, *27*(3), 319–326. https://doi.org/10.1080/08927014.2011.564615

Fatehbasharzad, P., Aliasghari, S., Shaterzadeh Tabrizi, I., Khan, J. A., & Boczkaj, G. (2022). Microbial fuel cell applications for removal of petroleum hydrocarbon pollutants: A review. *Water Resources and Industry*, *28*. https://doi.org/10.1016/j.wri.2022.100178

Fewtrell, L. (2004). Drinking-water nitrate, methemoglobinemia, and global burden of disease: A discussion. In *Environmental Health Perspectives* (Vol. 112, Issue 14, pp. 1371–1374). https://doi.org/10.1289/ehp.7216

Fiedler, S., Vepraskas, M. J., & Richardson, J. L. (2007). Soil Redox Potential: Importance, Field Measurements, and Observations. In *Advances in Agronomy* (Vol. 94, pp. 1–54). https://doi.org/10.1016/S0065-2113(06)94001-2

Gadegaonkar, S. S., Mander, Ü., & Espenberg, M. (2023). A state-of-the-art review and guidelines for enhancing nitrate removal in bio-electrochemical systems (BES). *Journal of Water Process Engineering*, *53*. https://doi.org/10.1016/j.jwpe.2023.103788

Gupta, S., Patro, A., Mittal, Y., Dwivedi, S., Saket, P., Panja, R., Saeed, T., Martínez, F., & Yadav, A. K. (2023). The race between classical microbial fuel cells, sediment-microbial fuel cells, plant-microbial fuel cells, and constructed wetlands-microbial fuel cells: Applications and technology

readiness level. In *Science of the Total Environment* (Vol. 879). Elsevier B.V. https://doi.org/10.1016/j.scitotenv.2023.162757

He, Y., Zhou, Q., Mo, F., Li, T., & Liu, J. (2022). Bioelectrochemical degradation of petroleum hydrocarbons: A critical review and future perspectives. In *Environmental Pollution* (Vol. 306). Elsevier Ltd. https://doi.org/10.1016/j.envpol.2022.119344

Hong, S. W., Chang, I. S., Choi, Y. S., & Chung, T. H. (2009). Experimental evaluation of influential factors for electricity harvesting from sediment using microbial fuel cell. *Bioresource Technology*, *100*(12), 3029–3035. https://doi.org/10.1016/j.biortech.2009.01.030

Hong, S. W., Chang, I. S., Choi, Y. S., Kim, B. H., & Chung, T. H. (2009). Responses from freshwater sediment during electricity generation using microbial fuel cells. *Bioprocess and Biosystems Engineering*, *32*(3), 389–395. https://doi.org/10.1007/s00449-008-0258-9

Huang, D. Y., Zhou, S. G., Chen, Q., Zhao, B., Yuan, Y., & Zhuang, L. (2011). Enhanced anaerobic degradation of organic pollutants in a soil microbial fuel cell. *Chemical Engineering Journal*, *172*(2–3), 647–653. https://doi.org/10.1016/j.cej.2011.06.024

Kilinc, B., & Catal, T. (2023). A Novel Microbial Fuel Cell for the Sensing of Sodium Acetate in Soil. *Polish Journal of Environmental Studies*, *32*(5), 4931–4936. https://doi.org/10.15244/pjoes/168804

Kronenberg, M., Trably, E., Bernet, N., & Patureau, D. (2017). Biodegradation of polycyclic aromatic hydrocarbons: Using microbial bioelectrochemical systems to overcome an impasse. *Environmental Pollution*, *231*, 509–523. https://doi.org/10.1016/j.envpol.2017.08.048

Kumar, S. S., Kumar, V., Malyan, S. K., Sharma, J., Mathimani, T., Maskarenj, M. S., Ghosh, P. C., & Pugazhendhi, A. (2019). Microbial fuel cells (MFCs) for bioelectrochemical treatment of different wastewater streams. *Fuel*, *254*. https://doi.org/10.1016/j.fuel.2019.05.109

Leeson, A., Johnson, P. C., Johnson, R. L., Vogel, C. M., Hinchee, R. E., Marley, M., Peargin, T., Bruce, C. L., Amerson, I. L., Coonfare, C. T., Gillespie, R. D., & Mcwhorter, D. B. (2002). *AIR SPARGING DESIGN PARADIGM*.

Li, T., Li, R., & Zhou, Q. (2021). The application and progress of bioelectrochemical systems (BESs) in soil remediation: A review. In *Green*

Energy and Environment (Vol. 6, Issue 1, pp. 50–65). KeAi Publishing Communications Ltd. https://doi.org/10.1016/j.gee.2020.06.026

Li, X., Wang, X., Ren, Z. J., Zhang, Y., Li, N., & Zhou, Q. (2015). Sand amendment enhances bioelectrochemical remediation of petroleum hydrocarbon contaminated soil. *Chemosphere*, *141*, 62–70. https://doi.org/10.1016/j.chemosphere.2015.06.025

Li, X., Wang, X., Wan, L., Zhang, Y., Li, N., Li, D., & Zhou, Q. (2016). Enhanced biodegradation of aged petroleum hydrocarbons in soils by glucose addition in microbial fuel cells. *Journal of Chemical Technology and Biotechnology*, *91*(1), 267–275. https://doi.org/10.1002/jctb.4660

Li, X., Wang, X., Zhao, Q., Wan, L., Li, Y., & Zhou, Q. (2016). Carbon fiber enhanced bioelectricity generation in soil microbial fuel cells. *Biosensors and Bioelectronics*, *85*, 135–141. https://doi.org/10.1016/j.bios.2016.05.001

Lim, M. W., Lau, E. Von, & Poh, P. E. (2016). A comprehensive guide of remediation technologies for oil contaminated soil — Present works and future directions. In *Marine Pollution Bulletin* (Vol. 109, Issue 1, pp. 14–45). Elsevier Inc. https://doi.org/10.1016/j.marpolbul.2016.04.023

Logan, B. E., Hamelers, B., Rozendal, R., Schröder, U., Keller, J., Freguia, S., Aelterman, P., Verstraete, W., & Rabaey, K. (2006). Microbial fuel cells: Methodology and technology. In *Environmental Science and Technology* (Vol. 40, Issue 17, pp. 5181–5192). https://doi.org/10.1021/es0605016

Lu, L., Yazdi, H., Jin, S., Zuo, Y., Fallgren, P. H., & Ren, Z. J. (2014). Enhanced bioremediation of hydrocarbon-contaminated soil using pilot-scale bioelectrochemical systems. *Journal of Hazardous Materials*, *274*, 8–15. https://doi.org/10.1016/j.jhazmat.2014.03.060

Mao, D., Lu, L., Revil, A., Zuo, Y., Hinton, J., & Ren, Z. J. (2016). Geophysical Monitoring of Hydrocarbon-Contaminated Soils Remediated with a Bioelectrochemical System. *Environmental Science and Technology*, *50*(15), 8205–8213. https://doi.org/10.1021/acs.est.6b00535

Marzocchi, U., Palma, E., Rossetti, S., Aulenta, F., & Scoma, A. (2020). Parallel artificial and biological electric circuits power petroleum decontamination: The case of snorkel and cable bacteria. *Water Research*, *173*, 115520. https://doi.org/10.1016/j.watres.2020.115520

Matturro, B., Viggi, C. C., Aulenta, F., & Rossetti, S. (2017). *Cable Bacteria and the Bioelectrochemical Snorkel: The Natural and Engineered Facets Playing a Role in*

Hydrocarbons Degradation in Marine Sediments. *8*(May), 1–13. https://doi.org/10.3389/fmicb.2017.00952

Mccauley, A. (2009). *Soil pH and Organic Matter*.

Nandy, A., Radović, J. R., Novotnik, B., Sharma, M., Larter, S. R., & Thangadurai, V. (2020). Investigation of crude oil degradation using metal oxide anode-based microbial fuel cell. *Bioresource Technology Reports*, *11*. https://doi.org/10.1016/j.biteb.2020.100449

Noori, M. T., Thatikayala, D., & Min, B. (2022). Bioelectrochemical Remediation for the Removal of Petroleum Hydrocarbon Contaminants in Soil. In *Energies* (Vol. 15, Issue 22). MDPI. https://doi.org/10.3390/en15228457

O'Brien, P. L., DeSutter, T. M., Casey, F. X. M., Wick, A. F., & Khan, E. (2017). Evaluation of Soil Function Following Remediation of Petroleum Hydrocarbons—a Review of Current Remediation Techniques. In *Current Pollution Reports* (Vol. 3, Issue 3, pp. 192–205). Springer. https://doi.org/10.1007/s40726-017-0063-7

Ossai, I. C., Ahmed, A., Hassan, A., & Hamid, F. S. (2020a). Remediation of soil and water contaminated with petroleum hydrocarbon: A review. In *Environmental Technology and Innovation* (Vol. 17). Elsevier B.V. https://doi.org/10.1016/j.eti.2019.100526

Ossai, I. C., Ahmed, A., Hassan, A., & Hamid, F. S. (2020b). Remediation of soil and water contaminated with petroleum hydrocarbon: A review. In *Environmental Technology and Innovation* (Vol. 17). Elsevier B.V. https://doi.org/10.1016/j.eti.2019.100526

Park, D. H., & Zeikus, J. G. (2003). Improved fuel cell and electrode designs for producing electricity from microbial degradation. *Biotechnology and Bioengineering*, *81*(3), 348–355. https://doi.org/10.1002/bit.10501

Patel, B. R., Noroozifar, M., & Kerman, K. (2022). Recent improvements of ceramic membranes in microbial fuel cells for bioelectricity generation and wastewater remediation: From fundamentals to scale-up applications. *Journal of Environmental Chemical Engineering*, *10*(6). https://doi.org/10.1016/j.jece.2022.108664

Pous, N., Puig, S., Coma, M., Balaguer, M. D., & Colprim, J. (2013). Bioremediation of nitrate-polluted groundwater in a microbial fuel cell. *Journal of Chemical Technology and Biotechnology*, *88*(9), 1690–1696. https://doi.org/10.1002/jctb.4020

Rahimnejad, M., Bakeri, G., Ghasemi, M., & Zirepour, A. (2014). A review on the role of proton exchange membrane on the performance of microbial fuel cell. *Polymers for Advanced Technologies*, *25*(12), 1426–1432. https://doi.org/10.1002/pat.3383

Rogińska, J., Perdicakis, M., Midoux, C., Bouchez, T., Despas, C., Liu, L., Tian, J.-H., Chaumont, C., P. A. Jorand, F., Tournebize, J., & Etienne, M. (2021). Electrochemical analysis of a microbial electrochemical snorkel in laboratory and constructed wetlands. *Bioelectrochemistry*, *142*, 107895. https://doi.org/10.1016/j.bioelechem.2021.107895

Rusli, S. F. N., Abu Bakar, M. H., Loh, K. S., & Mastar, M. S. (2019). Review of high-performance biocathode using stainless steel and carbon-based materials in Microbial Fuel Cell for electricity and water treatment. *International Journal of Hydrogen Energy*, *44*(58), 30772–30787. https://doi.org/10.1016/j.ijhydene.2018.11.145

Sammarco, P. W., Kolian, S. R., Warby, R. A. F., Bouldin, J. L., Subra, W. A., & Porter, S. A. (2016). Concentrations in human blood of petroleum hydrocarbons associated with the BP/Deepwater Horizon oil spill, Gulf of Mexico. *Archives of Toxicology*, *90*(4), 829–837. https://doi.org/10.1007/s00204-015-1526-5

Saponaro, S. (2022a). *Contaminants of concern - soil remediation*.

Saponaro, S. (2022b). *Remediation technologies - soil remediation*.

Saponaro S. (2022). *Remediation technologies 2 - soil remediation*.

Schröder, U., Harnisch, F., & Angenent, L. T. (2015). Microbial electrochemistry and technology: Terminology and classification. In *Energy and Environmental Science* (Vol. 8, Issue 2, pp. 513–519). Royal Society of Chemistry. https://doi.org/10.1039/c4ee03359k

Solomon, G. M., & Janssen, S. (2010). Health effects of the gulf oil spill. In *JAMA* (Vol. 304, Issue 10, pp. 1118–1119). American Medical Association. https://doi.org/10.1001/jama.2010.1254

Stein, L. Y., & Klotz, M. G. (2016). The nitrogen cycle. In *Current Biology* (Vol. 26, Issue 3, pp. R94–R98). Cell Press. https://doi.org/10.1016/j.cub.2015.12.021

Tatzber, M., Stemmer, M., Spiegel, H., Katzlberger, C., Haberhauer, G., & Gerzabek, M. H. (2007). An alternative method to measure carbonate in soils

by FT-IR spectroscopy. *Environmental Chemistry Letters*, *5*(1), 9–12. https://doi.org/10.1007/s10311-006-0079-5

Thiruvenkatachari, R., Vigneswaran, S., & Naidu, R. (2008). Permeable reactive barrier for groundwater remediation. In *Journal of Industrial and Engineering Chemistry* (Vol. 14, Issue 2, pp. 145–156). Korean Society of Industrial Engineering Chemistry. https://doi.org/10.1016/j.jiec.2007.10.001

Tiquia-Arashiro, S. M., & Pant, Deepak. (2019). *Microbial Electrochemical Technologies*. CRC Press LLC.

Tong, Y., & He, Z. (2013). Nitrate removal from groundwater driven by electricity generation and heterotrophic denitrification in a bioelectrochemical system. *Journal of Hazardous Materials*, *262*, 614–619. https://doi.org/10.1016/j.jhazmat.2013.09.008

Tucci, M., Cruz Viggi, C., Esteve Núñez, A., Schievano, A., Rabaey, K., & Aulenta, F. (2021). Empowering electroactive microorganisms for soil remediation: Challenges in the bioelectrochemical removal of petroleum hydrocarbons. In *Chemical Engineering Journal* (Vol. 419). Elsevier B.V. https://doi.org/10.1016/j.cej.2021.130008

Varjani, S. J., Kumar, A., Gnansounou, A. E., & Gurunathan, B. (n.d.). *Bioremediation: Applications for Environmental Protection and Management Energy, Environment, and Sustainability*. http://www.springer.com/series/15901

Varjani, S. J., & Upasani, V. N. (2017). A new look on factors affecting microbial degradation of petroleum hydrocarbon pollutants. In *International Biodeterioration and Biodegradation* (Vol. 120, pp. 71–83). Elsevier Ltd. https://doi.org/10.1016/j.ibiod.2017.02.006

Vidotto, M. M., Liduino, V. S., Andrade, T., Faria, J. K., & Bueno, R. de F. (2020). Remediation of nitrate-contaminated groundwater in a denitrifying bioelectrochemical system. *Desalination and Water Treatment*, *205*, 131–138. https://doi.org/10.5004/dwt.2020.26383

Viggi, C. C., Matturro, B., Frascadore, E., Insogna, S., Mezzi, A., Kaciulis, S., Sherry, A., Mejeha, O. K., Head, I. M., Vaiopoulou, E., Rabaey, K., Rossetti, S., & Aulenta, F. (2017). Bridging spatially segregated redox zones with a microbial electrochemical snorkel triggers biogeochemical cycles in oil-contaminated River Tyne (UK) sediments. *Water Research*, *127*, 11–21. https://doi.org/10.1016/j.watres.2017.10.002

Viggi, C. C., Presta, E., Bellagamba, M., Kaciulis, S., Balijepalli, S. K., Zanaroli, G., Papini, M. P., Rossetti, S., & Aulenta, F. (2015). The "Oil-Spill Snorkel": An innovative bioelectrochemical approach to accelerate hydrocarbons biodegradation in marine sediments. *Frontiers in Microbiology*, *6*(SEP). https://doi.org/10.3389/fmicb.2015.00881

Viggi, C. C., Tucci, M., Resitano, M., Matturro, B., Crognale, S., Feigl, V., Molnár, M., Rossetti, S., & Aulenta, F. (2022). Passive electrobioremediation approaches for enhancing hydrocarbons biodegradation in contaminated soils. *Science of the Total Environment*, *845*. https://doi.org/10.1016/j.scitotenv.2022.157325

Vijay, A., Khandelwal, A., Chhabra, M., & Vincent, T. (2020). Microbial fuel cell for simultaneous removal of uranium (VI) and nitrate. *Chemical Engineering Journal*, *388*. https://doi.org/10.1016/j.cej.2020.124157

Wang, C., Dong, J., Hu, W., & Li, Y. (2021). Enhanced simultaneous removal of nitrate and perchlorate from groundwater by bioelectrochemical systems (BESs) with cathodic potential regulation. *Biochemical Engineering Journal*, *173*. https://doi.org/10.1016/j.bej.2021.108068

Wang, H., Lu, L., Mao, D., Huang, Z., Cui, Y., Jin, S., Zuo, Y., & Ren, Z. J. (2019). Dominance of electroactive microbiomes in bioelectrochemical remediation of hydrocarbon-contaminated soils with different textures. *Chemosphere*, *235*, 776–784. https://doi.org/10.1016/j.chemosphere.2019.06.229

Wang, X., Cai, Z., Zhou, Q., Zhang, Z., & Chen, C. (2012). Bioelectrochemical stimulation of petroleum hydrocarbon degradation in saline soil using U-tube microbial fuel cells. *Biotechnology and Bioengineering*, *109*(2), 426–433. https://doi.org/10.1002/bit.23351

Wang, X., Cheng, S., Feng, Y., Merrill, M. D., Saito, T., & Logan, B. E. (2009). Use of carbon mesh anodes and the effect of different pretreatment methods on power production in microbial fuel cells. *Environmental Science and Technology*, *43*(17), 6870–6874. https://doi.org/10.1021/es900997w

Weber, K., & Quicker, P. (2018). Properties of biochar. In *Fuel* (Vol. 217, pp. 240–261). Elsevier Ltd. https://doi.org/10.1016/j.fuel.2017.12.054

Wu, Q., Jiao, S., Ma, M., & Peng, S. (2020). Microbial fuel cell system: a promising technology for pollutant removal and environmental remediation. In *Environmental Science and Pollution Research* (Vol. 27, Issue 7, pp. 6749–6764). Springer. https://doi.org/10.1007/s11356-020-07745-0

Yang, Q., Zhao, H., & Liang, H. H. (2015). Denitrification of overlying water by microbial electrochemical snorkel. *Bioresource Technology*, *197*, 512–514. https://doi.org/10.1016/j.biortech.2015.08.127

Yee, M. O., Deutzmann, J., Spormann, A., & Rotaru, A. E. (2020). Cultivating electroactive microbes-from field to bench. *Nanotechnology*, *31*(17). https://doi.org/10.1088/1361-6528/ab6ab5

Yu, B., Feng, L., He, Y., Yang, L., & Xun, Y. (2021). Effects of anode materials on the performance and anode microbial community of soil microbial fuel cell. *Journal of Hazardous Materials*, *401*. https://doi.org/10.1016/j.jhazmat.2020.123394

Zhang, F., Cheng, S., Pant, D., Bogaert, G. Van, & Logan, B. E. (2009). Power generation using an activated carbon and metal mesh cathode in a microbial fuel cell. *Electrochemistry Communications*, *11*(11), 2177–2179. https://doi.org/10.1016/j.elecom.2009.09.024

Zhang, Y., Wang, X., Li, X., Cheng, L., Wan, L., & Zhou, Q. (2015). Horizontal arrangement of anodes of microbial fuel cells enhances remediation of petroleum hydrocarbon-contaminated soil. *Environmental Science and Pollution Research*, *22*(3), 2335–2341. https://doi.org/10.1007/s11356-014-3539-7

List of Figures

List of Tables

List of symbols

Variable	Description	SI unit
$CDI_{j,i}$	chronic daily intake of chemical j through the exposure pathways	$\frac{mg_{pollutant}}{kg_{bodyweight} \cdot d}$
$C_{j,i}$	chemical j concentration at point of exposure in the environmental medium of concern for the exposure pathways i	$\frac{mg_{pollutant}}{d}$
CR_i	contact rate	$\frac{m^3_{air}}{d}; \frac{kg_{soil}}{d}$
EF	exposure frequency	$\frac{d}{ye}$
ED	exposure duration	ye
BW	body weight	$kg_{bodyweight}$
AT	average time	d
pH	solution acidity or alkaline indication	-
$CaCO_3eq$	equivalent calcite content	%
EC	electrical conductivity	$\mu S/cm$
COD	chemical oxygen demand	mgO_2/L
V	voltage	mV
I	current	mA
R	external load	Ω
p	power	mW
P	Power density	mW/m^2
CE	coulombic efficiency	%
DO	dissolved oxygen	mgO_2/L
r_{COD}	COD removal efficiency	%
$r_{nitrate}$	nitrate removal efficiency	%

Acknowledgments

I would like to thank first my mum and my dad for giving me the opportunity to live in Milan and to attend the Politecnico di Milano.
I thank Professor Sabrina Saponaro for introducing me to this project and Elena Sezenna for guiding me in my thesis work. I'm grateful for the support of Gabriele Beretta and for giving me the possibility, together with Marta Puddu, to compete this thesis.